Department of Experimental and Health Sciences
Faculty of Health and Life Sciences
Universitat Pompeu Fabra
Doctoral Thesis
2013

Ubiquitin ligases involved in the regulation of Snail1

Dissertation presented by
Rosa Viñas Castells
for the degree of Doctor of Philosophy

Work carried out under the supervision of Drs. Víctor Manuel Díaz Cortés and Antonio García de Herreros in the Epithelial to Mesenchymal Transition and Tumor Progression Group in the Cancer Research Program in the Institut Hospital del Mar d'Investigacions Mèdiques (IMIM)

Barcelona, 2013

Dr. Víctor M. Díaz Cortés,
(thesis co-director)

Dr. Antonio García de Herreros,
(thesis co-director)

Rosa Viñas Castells,
(PhD student)

ABSTRACT

Epithelial to mesenchymal transition (EMT) is a process by which epithelial cells acquire a mesenchymal phenotype. It is characterized by the down-regulation of the adherens junction protein E-cadherin, and it is important during embryonic development. Snail1 expression is sufficient to trigger EMT in cultured cells and is found up-regulated in some cancers. Snail1 is stabilized both at mRNA and protein levels and in this project we analyzed the action of ubiquitin ligases affecting protein half-life. Apart from the already described β-Trcp1, that degrades Snail1 in a GSK-3β phosphorylation-dependent manner, we found the F-box proteins FBXL14 and FBXL5 as novel E3 ubiquitin ligases for Snail1. FBXL14 is a cytoplasmic ubiquitin ligase that is down-regulated in hypoxia through a transcriptional mechanism. FBXL5 is nuclear and modulates Snail1 binding to the DNA and nuclear ubiquitination. FBXL5 protein is destabilized after γ-irradiation, inducing high levels of Snail1. Together, these ligases keep a tight control of Snail1 cellular levels, maintaining them low in normal conditions.

La transició epiteli-mesènquima (EMT, per l'acrònim en anglès de: "epithelial to mesenchymal transition") és un procés durant el qual cèl·lules epitelials adquireixen un fenotip mesenquimal. Està caracteritzat per la baixada de l'E-caderina, una proteïna de les unions adherents, i és important en el desenvolupament embrionari. L'expressió de Snail1 és suficient per desencadenar la EMT en cèl·lules en cultiu i s'ha trobat sobre-expressada en alguns càncers. Snail1 s'estabilitza tant a nivell de mRNA com de proteïna i en aquest projecte hem analitzat l'acció de les lligases d'ubiquitina que afecten els nivells de la proteïna. Apart de la ja descrita β-Trcp1, que degrada Snail1 de manera depenent a la fosforilació per GSK-3β, hem trobat les proteïnes F-box FBXL14 i FBXL5 con a noves lligases d'ubiquitina E3 que degraden Snail1. La FBXL14 és citoplasmàtica i els seus nivells disminueixen en hipòxia a través d'un mecanisme transcripcional. La FBXL5 és nuclear i modula tant la unió de Snail1 al DNA com la seva ubiquitinació nuclear. La proteïna FBXL5 es desestabilitza degut a la radiació gamma (γ) induint els nivells de Snail1. Juntes, aquestes lligases controlen de forma molt ajustada els nivells cel·lulars de Snail1, mantenint-los baixos en condicions normals.

TABLE OF CONTENTS

FIGURE INDEX

Introduction

Results

TABLE INDEX

Introduction

Materials & Methods

NOTES TO THE READER

Unless otherwise stated, all exogenous Snail1 used throughout this study is the murine homolog.

GENES appear in upper italic case.

Proteins appear in lower case.

ACRONYMS AND ABBREVIATIONS

aa: amino acids
AMF: Autocrine motility factor
APC: anaphase promoting complex
ATM: Ataxia telangiectasia mutated
ATP: adenosine triphosphate
bHLH: basic helix-loop-helix
BID: BcI-interacting death agonist
BMPs: Bone morphogenic proteins
β-**Trcp1:** β-transducin repeat containing protein 1
CA9: Carbonic Anhydrase 9
CAR: Coxsackie and adenovirus receptor
CBC: Cullin2/elongin B/elongin C
CDK4: cyclin-dependent kinase 4
ChIP-Seq: Chromatin immunoprecipitation sequencing
CHK1: Checkpoint kinase-1
CHX: cycloheximide
CIP: calf intestinal phosphatase
CK1/2: Casein kinase 1/2
CoREST: repressor element-1 silencing transcription factor co-repressor
CRM1: Exportin-1 (XPO1)
CSC: Cancer stem cells
CT: C-terminal
CSN2: COP9 signalosome 2
CtBP1: carboxyl terminal binding protein 1
DFF40: DNA fragmentation factor 40
DTT: dithiothreitol
DUBs: de-ubiquitinating enzymes
E1: Enzyme 1
ECM: Extracellular membrane
EGF: Epidermal growth factor
EMSA: electrophoretic mobility shift assay
EMT: Epithelial to mesenchymal transition
ER: Estrogen receptor
ERK: extracellular signal-regulated kinase
FANC: Fanconi anaemia
FBXL14: F-box leucine-rich-repeat protein 14
FBXL5: F-box leucine-rich-repeat protein 5
FGF: Fibroblast growth factor
GFP: Green fluorescent protein
GSK-3β: Glycogen synthase-3β
GST: Glutathione-S-Transferase
H: histone
HA: Hemagglutinin
HDAC1/2: histone deacetylase 1 and 2
HECT: Homologous to Human Papilloma Virus E6 Carboxyterminal domain
HIF: Hypoxia inducible factor
HPRT: Hypoxanthine phosphoribosyltransferase
HRE: HIF-responsive element
HRP: Horseradish peroxidase
IF: immunofluorescence
IGF: Insulin-like growth factor
IgG: Immunoglobulin G
IKK-β: inhibitor of κB kinase-β
IL-6: Interleukin 6
ILEI: Interleukin-related protein
IP: immunoprecipitation
IRP: Iron regulatory protein
LB: Luria-Beltrani
LMB: Leptomycin B
LOX: Lysyl oxidase
LOXL2/3: Lysyl-oxidase-like 2/3
LRR: leucine-rich repeats
LSD1: lysine-specific demethylase 1
mAb: monoclonal antibody
Mdm2: Murine double minute 2
MET: Mesenchymal to epithelial transition

miRNA: micro RNA
Mkp3: MAP kinase phosphatase-3
MMPs: matrix metalloproteases
mRNA: messenger RNA
MS: Mass Spectrometry
mut: mutated
NAT: natural antisense transcript
NCoR: nuclear receptor co-repressor 1
NES: Nuclear export sequence
NF-κB: Nuclear factor kappa-light-chain-enhancer of activated B cells
Ni-NTA: Nickel nitrilotriacetic acid
NT: N-terminal
O-GlcAc: O-linked β-N-acetylglucosamine
OGT: O-GlcNAc transferase
pAb: polyclonal antibody
PARP1: poly(ADP-ribose) polymerase 1
PD: pulldown
PDGF: Platelet-derived growth factor
PEI: polyethylenimine
PI3K: phosphoinositide 3 kinase
PK: Pyruvate kinase
PKA: Protein kinase A
PKD1: Protein kinase D1
Ppa: Partner of paired
PRC2: polycomb repressive complex 2
Prd: Pax transcription factor Paired
PRMT5: protein arginine methyltransferase 5
P-S rich: phospho-serine rich
p21: cyclin-dependent kinase inhibitor 1
Rb: retinoblastoma
RING: Really Interesting New Gene
RLD: RCC1-like domain
ROS: reactive oxygen species
RTKs: Receptor tyrosine kinases
SBE: SMAD-binding element
SCF: Skp1-Cullin-F-box
SCP: Small C-terminal domain phosphatase
s.d.: standard deviation
SDHA: Succinate dehydrogenase complex subunit A
SDS: sodium dodecyl sulfate
shRNA: short hairpin RNA
TGF-β: Transforming growth factor-β
TNF-α: Tumor necrosis factor-α
UV: ultraviolet
VEGF: Vascular endothelial growth factor
VHL: von Hippel-Lindau
WD40: tryptophan repeats
wt: wild type
XR11: *Xenopus* Bcl-xL homologue
ZO-1: Zonula Occludens-1
ZnF: Zinc finger

INTRODUCTION

I.1. Cancer: a general overview

The careful regulation of cell multiplication and division is what ensures a correct response to the body needs. When growth is required cell multiplication exceeds cell death in order to increase the size of the animal. In contrast, when growth is stopped, the equilibrium between cell multiplication and death is finely tuned [1]. The problem arises when mutations in somatic cells affecting critical genes that regulate cell proliferation and survival appear, causing fatal cancers [2].

A lot of work has been put in the definition of what cancer is and which are its hallmarks or common characteristics. Tumors are more than insular masses of proliferating cancer cells with mutations or alterations that directly promote malignancy. It is proposed that they are complex tissues with distinct cell types capable of interacting. Moreover there is further interaction of the tumor mass with the surrounding tissue, the tumor-associated stroma, which actively participates in the tumorigenesis. Therefore cancer is not the tumor *per se* but the tumor and its microenvironment [3, 4].

The first proposition of the hallmarks of cancer in which six characteristics were described has been refined in the past years, with a remarkable progress in the area of the biology of cancer. These characteristics were initially defined as self-sufficiency in growth signals, insensitivity to anti-growth signals, limitless replicative potential, sustained angiogenesis, evading apoptosis and tissue invasion and metastasis [5-7]. The refinement of these hallmarks allows for better interpretation of the disease (*Figure I.1*).

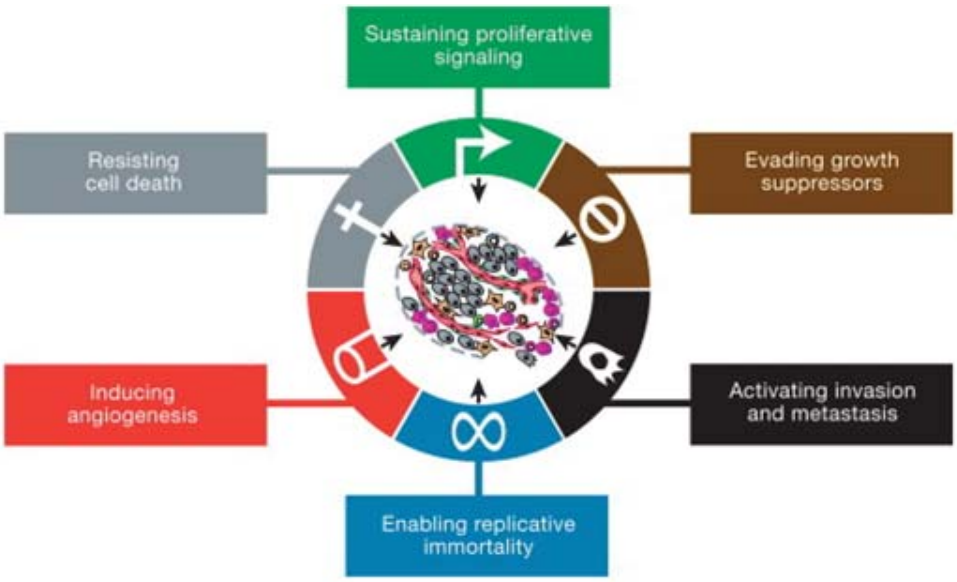

Figure I.1. The hallmarks of cancer. Schematic illustration of the six hallmarks of cancer proposed by Hanahan & Weinberg (2011) [4].

Shortly, the first characteristic that is now considered a hallmark is the sustained proliferative signaling which allows chronic proliferation of cells by somatic mutations that activate downstream pathways, disruptions in the feedback mechanisms that provide the control of proliferative signaling and low signaling that allows for maintained proliferation by bypassing the process of senescence. The second trait is evading growth suppressors by mechanisms of contact inhibition between adjacent cells and their subsequent evasion. The Transforming growth factor-β (TGF-β) is one such suppressor and has been seen to activate an alternative cellular program termed epithelial to mesenchymal transition (EMT) that will be further described in this section. Resisting cell death is the third hallmark characterized by cellular evasion of apoptosis, and it has been seen that the necrosis (dying) of cells has pro-inflammatory and tumor-promoting potential that can be under genetic control [4].

Enabling cells to have replicative immortality is another characteristic that empowers the disease, and it has been described that both telomere lengthening and bypassing senescence can have fatal consequences. The induction of angiogenesis and the activation of invasion and metastasis are the last proposed hallmarks. Tumor angiogenesis is a complex process and cells such as pericytes and a range of bone marrow-derived cells have been shown to contribute towards it. The actions of metastasis and cell invasion are again greatly supported by the process of EMT, as well as the plasticity and molecular characteristics of the stroma and the metastatic colonizers and the recipient organs [4].

A better interpretation of cancer should allow for an improved model in targeting the disease. A series of stress phenotypes have been recently described, and there are functional interplays between these hallmarks that promote the tumorigenic state and suppress what is termed as oncogenic stress. These are DNA damage stress, oxidative stress, mitotic stress, proteotoxic stress and metabolic stress, a large class of non-oncogenes that have been demonstrated to be essential for cancer survival and are now being used as targets for different drugs in anti-cancer therapy [3].

I.2. EMT

EMT is a reversible process by which epithelial cells acquire a mesenchymal phenotype. During the transition the cell-cell adhesion junctions of cells, including adherens junctions, desmosomes and cytokeratins, change their polarity and cause a rearrangement of their cytoskeleton in which intermediate filaments are reverted to vimentin from keratins. The resulting cells are spindle-shaped, motile and more resistant to apoptosis. Although EMT was identified in the context of development decades ago, its molecular mechanisms are being unraveled more recently, since the discovery of its role in tumor invasiveness was made.

I.2.1. Physiological EMT

I.2.1.i. EMT in embryonic development

Constructing a whole organism is a complex process that needs co-ordination in order to build from the zygote, a single cell, all the tissues that conform an organism. This occurs through several rounds of EMT and mesenchymal to epithelial transition (MET). There are three rounds of this process that are called primary, secondary and tertiary EMT (*Figure I.2*) [8].

There are four main stages in the process of embryonic development which are cleavage, patterning, differentiation and growth. First, the zygote undergoes many rounds of mitosis and cytokinesis to generate a large number of cells with its exact genetic material. The genes and proteins expressed at this time are still the maternal ones that promote the cleavage which results in the formation of the blastula. Cells are then organized in this primary cellular mass through patterning, a process that would not occur without gastrulation. Gastrulation is where primary EMT happens and it results in the formation of the three germ layers: ectoderm, mesoderm and endoderm. The zygotic genes are activated and cause invagination of epithelial cells through an axis. These cells undergo changes in the phenotype, from the narrowing of the apical compartment and the re-distribution of the organelles to the bulging of the basal compartments. Migration of these cells along the extracellular space under the ectoderm completes the primary EMT, when the endoderm is produced. It is only then that cells will start to differentiate or specialize in their structure and function and then grow to form a bigger-sized organism [9]. Neural crest delamination is another example of primary EMT in vertebrates. As shown in *Figure I.2A* there is a group of cells termed neural crest cells characterized by their high motility that allows them to populate distant tissues. These cells, which have rounded and pleiomorphic shapes contrasting the polarized cells that are nearby in the neural tube, lose their cell-cell adhesion and invade in an active manner through the basal lamina,

migrating away from the neural tube. This results in the differentiation into bone, smooth muscle, peripheral neurons, glia and melanocytes [10].

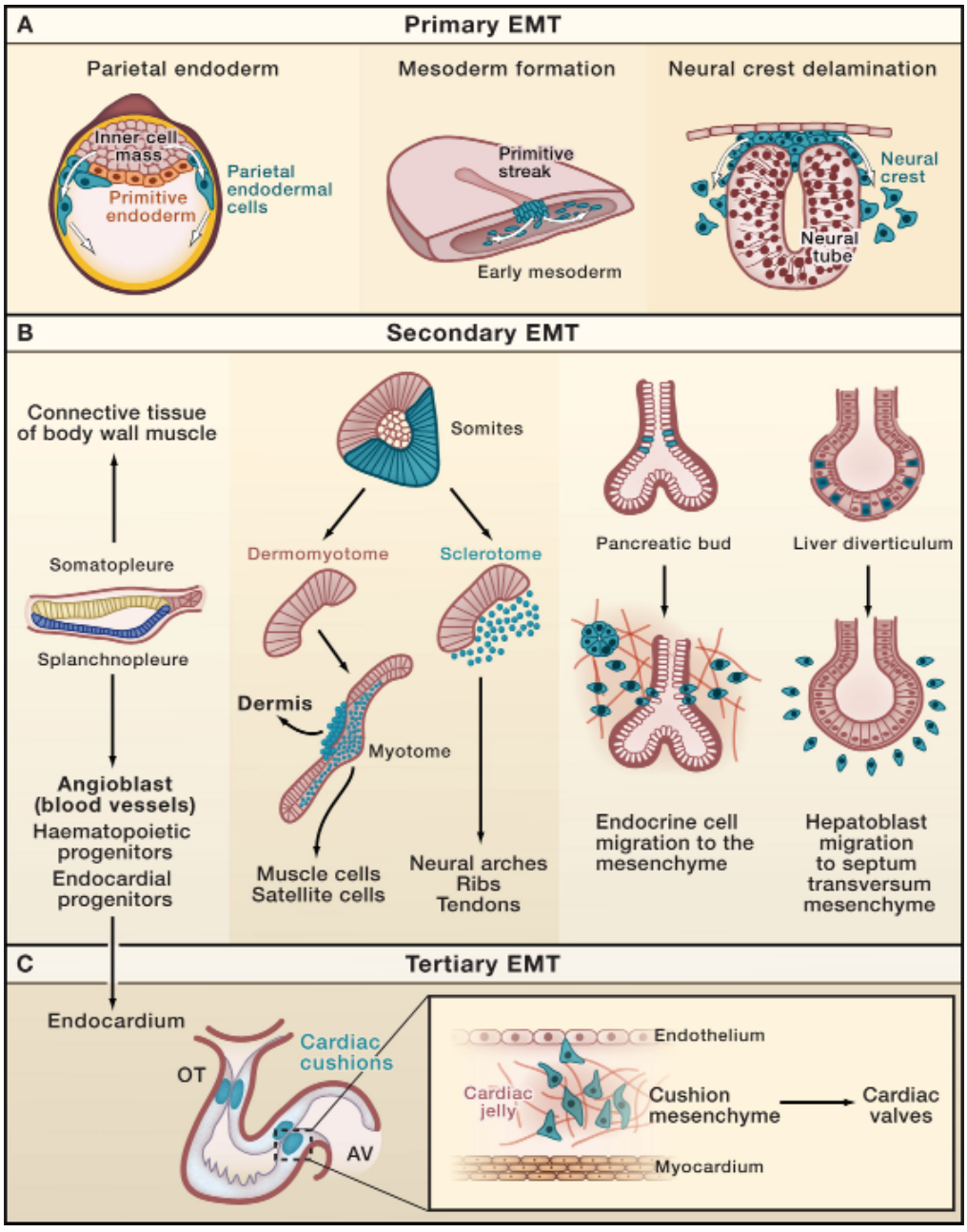

Figure I.2. EMT during embryonic development. (**A**) Primary EMT in early embryonic development when, before implantation, there is formation of the parietal endoderm. After implantation the first EMT is by the mesendodermal progenitors during gastrulation. (**B**) Early mesodermal cells are subdivided into axial, pariaxial, intermediate and later plate mesodermal cells that will condense into the transient epithelial features called notochord, somites, somatopleure and splanchnopleure. These will give rise to mesenchymal cells that will differentiate into specific cell types through secondary EMT. (**C**) Tertiary EMT occurs in many tissues, an example of which is the formation of the cushion mesenchyme in the heart, the precursor of cardiac valves, from the atrioventricular canal (AV) or the outflow tract (OT) [8].

Secondary EMT occurs after the resulting primary EMT through which cells have condensed into transient epithelial structures by the MET process, forming the notochord, the somites, the somatopleure, the splanchnopleure and the precursor urogenital system. All but the notochord will undergo secondary EMT [8]. As shown in *Figure I.2B* the epithelial cells from the lateral plate mesoderm, which is condensed into the ventral and dorsal epithelia, separated by a cavity termed coelom, undergo EMT to give rise to different tissues. From the somatopleure (dorsal epithelium) most cells conserve their epithelial characteristics except some that will undergo EMT and give rise to connective tissue. Cells from the splanchnopleure will generate endocardial progenitors, angioblasts and hematopoietic stem cells after secondary EMT [8].

The somites are primary tissues that also undergo two differentiated secondary EMTs to give rise to a range of tissues. The dorsal part converts into dermal mesenchyme and the myoblasts that delaminate from the myotome will become progenitors of muscle and satellite cells. The ventral part of the somites will transform into sclerotomal mesenchyme cells that will form the vertebrae [11, 12]. In hepatic and pancreatic tissues secondary EMT gives rise to the transversal mesenchyme and the surrounding mesenchyme, respectively. In the pancreas, pancreatic endocrine cells specified in the bud having first undergone EMT and then migrated to the mesenchyme will revert their phenotype through MET to form the islets of Langerhans (*Figure I.2B*) [13].

A well-studied tertiary EMT process during embryonic development is cardiac valve formation. The heart forms through three successive cycles of EMT and MET. During gastrulation the cardiac mesodermal cells are specified and in the secondary EMT the cardiac progenitors develop from the splanchnopleure. The primitive foregut that arises from the secondary EMT allows mesenchymal cells forming it to delaminate and give rise to the endothelial cell lining of the heart through another MET. The result is an endocardial tube lined with myocardial epithelium that will, in time, develop to be the heart primordium. Tertiary EMT happens when the endothelial cells from the atrioventricular canal invade the cardiac jelly and give rise to the endocardial cushion. These cushions will become the cardiac valves (*Figure I.2C*) [8, 14].

I.2.1.ii. EMT in wound healing

A physiological role for EMT that persists throughout the life of an individual is the response to injury or wound healing. Keratinocytes at the border of the wound partially recapitulate the EMT process. The repair of the broken dermis requires the recruitment of fibroblasts to the site and the

hyper-proliferation of keratinocytes at the wound edge. Keratinocytes move between the injured dermis and the fibrin clot by rearranging their actin cytoskeleton and extending lamellipodia but, differently to total EMT, they maintain loose contacts rather than migrating as individual cells. However, they detach from the basement membrane and are able to degrade connective tissue facilitating migration in the area though the alteration of expression of integrin receptors [15]. In the menstrual cycle it has also been described that wound healing of the ovarian surface epithelium after ovulation follows a similar process to that described for skin or keratinocyte-mediated wound healing [16].

I.2.2. Pathological EMT

I.2.2.i. EMT in organ fibrosis

In organ fibrosis the process of EMT is very similar to that of physiological EMT. In fibrosis it has been described that myofibroblasts, which are usually recruited at sites of tissue damage, secrete an excessive amount of collagen and other extracellular membrane (ECM) proteins in the form of fibers (*Figure I.3*, left). The deposited fibers greatly compromise the tissue and organ function leading to its eventual failure. The importance of EMT in this condition was described in 2002 when, by lineage tracing studies, Iwano and coworkers found that the myofibroblasts that give rise to the fibrotic collagen network in renal tubes result from the EMT of epithelial cells in the organ [17]. A large number of studies have also demonstrated that a similar chain of events leads to fibrosis in lens epithelium, endothelium, hepatocytes, cardiomyocytes and alveolar epithelial cells of the lung [18-20].

I.2.2.ii. EMT in tumor progression

It has not been until recently that the significance EMT has during cancer progression been accepted. EMT has been greatly studied in many *in vitro* cancer models; however, it is quite difficult to obtain convincing data using clinical samples. The reason for this is that lineage tracing cannot be used in human tumors and thus it is quite difficult to determine if a mesenchymal cell among epithelial tissue is derived from this same tissue or has migrated from other tissues. Moreover, the phenotype of the metastasis is similar to that of the primary tumor which can be interpreted as a detachment of a bulk of cells that implants in the tissue or as a reversion of the EMT (MET process) before cells colonize distal tissues [21, 22].

Having mentioned that it is difficult to track the EMT process in clinical samples, there is a lot of evidence that this process is occurring *in vivo*. The expression of EMT markers in primary tumors is correlated with

enhanced invasiveness and poorer clinical prognosis. Cancer cells at the tumor edge having undergone EMT secrete cytokines and proteases that promote angiogenesis, remodel the peritumoral ECM and activate non-neoplastic cells. At the same time stromal cells release factors that increase EMT in cancer cells and foster survival, growth, and invasiveness of the tumor, thus generating a reciprocal influence between the tumor and its microenvironment [23, 24]. Moreover, cells having undergone EMT present more resistance to cell death and senescence as well as resistance to chemotherapy and immunotherapy since they escape immune surveillance (*Figure I.3*, right) [8].

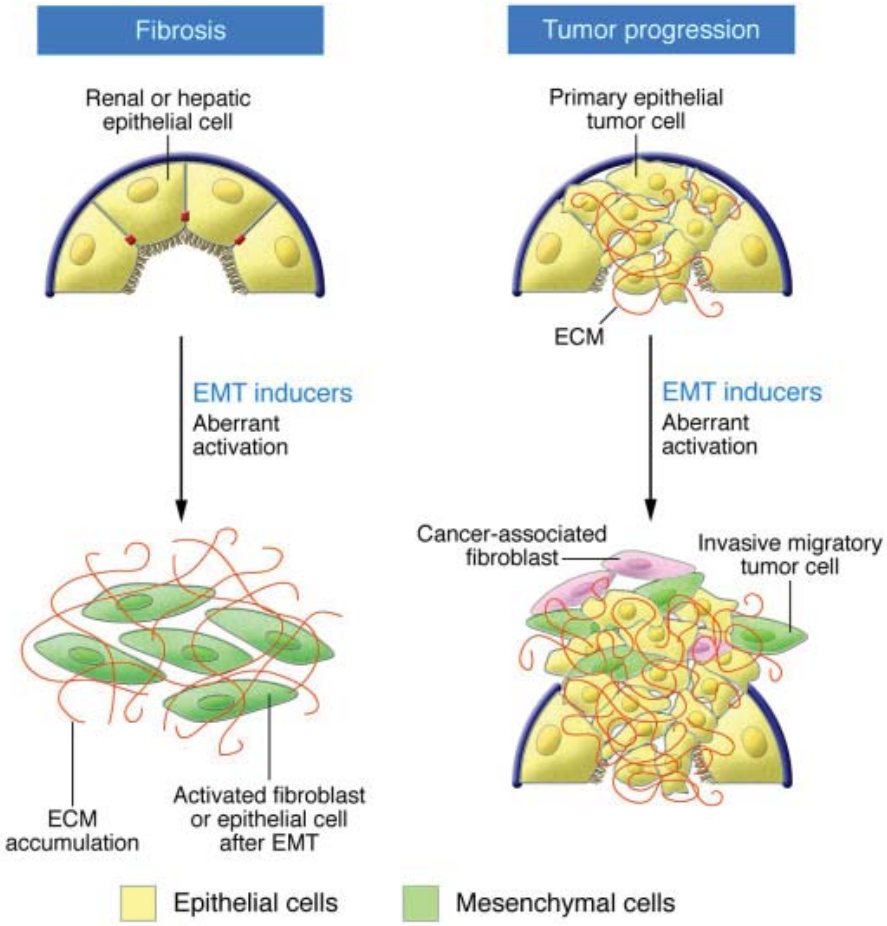

Figure I.3. Pathological EMT models. Fibrosis and the invasive front in tumor progression are two situations during which silent EMT inducers are reactivated. Adapted from [20].

The current *in vivo* model for EMT-mediated metastasis is depicted in *Figure I.4*, where the primary tumor mass, formed by tumor cells surrounded by epithelial cells, contains a group of cells that become mesenchymal through EMT and are able to migrate out of the tumor walls. Due to its newly acquired motility and loss of cell-cell junctions the invasive front can intravasate and become a circulating cancer cell in the bloodstream. Cells that secrete

factors such as fibroblasts and immune cells aid the cancer cells to maintain their mesenchymal phenotype. From the bloodstream it is possible for the cancer cells disseminated from the primary tumor to reach organs with a microenvironment similar to that of the tumor where MET will allow cells to start the growth of a metastasis [25, 26].

Stem-like characteristics are attributed to cancer cells having undergone EMT since many of the signals that control normal stem cell homeostasis are inducers of EMT and contribute to the generation and maintenance of cancer stem cells (CSCs). The self-renewal and migratory capacities of CSCs is important both for the genesis of new tumor masses and metastasis from primary tumors. It is thought that since current treatments focus on the characteristics and properties of the tumor bulk CSCs remain unaffected and cause recurrence and resistance to treatment in many cases [27]. Recent studies show that CSCs can be detected very early in the tumor and disseminated throughout other organs, giving a plausible explanation to why early surgical removal of a tumor mass is frequently not enough to avoid metastasis in distal organs [28, 29].

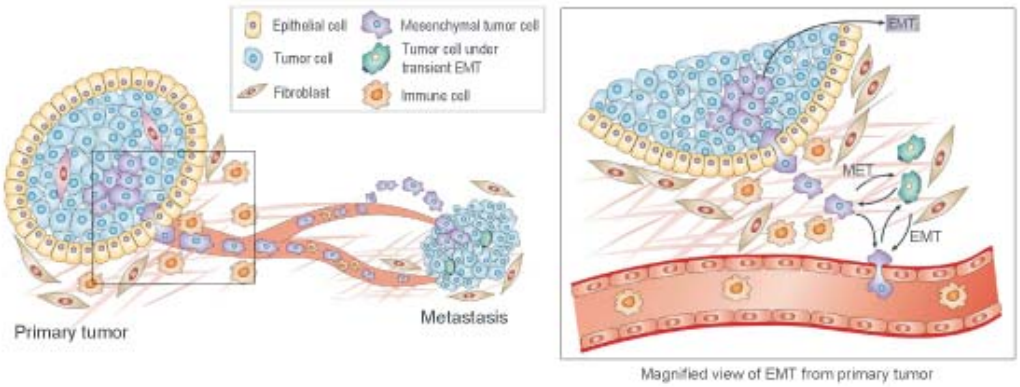

Figure I.4. EMT and MET in tumor progression and metastasis. Cells in the primary tumor undergo EMT and migrate from the epithelial tissue and intravasate into the blood stream where they can migrate to distal organs. In order to form a secondary tumor or metastasis cells undergo MET and attach to other organs where they can grow. Adapted from [25].

The shared characteristics of stem cells and CSCs are: (a) extensive proliferative potential and ability to give rise to new tissues; (b) the tissues they give rise to (either tumors or normal tissues) are composed of heterogeneous combinations of cells at various differentiation stages; and (c) due to the clonal capacity of the cells [30, 31]. It is thought that CSCs can be the result of either the transformation of normal stem cells or the induction of EMT in more differentiated cells [32]. Moreover, the characterization of an intermediate phenotype of cancer cells, termed 'partial EMT' or

'metastable phenotype', must be kept in mind since it gives consistency to the CSC theory. In this case cells undergoing EMT retain some characteristics of epithelial cells but also show features of mesenchymal cells. The features of these cells allow them to migrate as a 'cohort' since they have the ability to migrate in groups of cells that partially maintain cell-cell contacts. Also, the fact that they express factors of both phenotypes, enables cells to have better adaptability and fast transcriptional reprogramming [10, 33]. More recently the involvement of the transcription factor Twist1 has been related to CSCs and their need to undergo MET to be able to metastasize. The dissemination of the invasive cells has been shown to be dependent on EMT transcription factors and the reverse process is only allowed when these factors are down-regulated [34]. Due to the stemness properties provided by the EMT process CSCs are non-proliferative, and colonization and macrometastasis require to bypass this problem. It has been suggested that the EMT activator Prrx1 suppresses these EMT stemness properties, making this homeobox factor unique as it uncouples EMT and stemness and is associated to patient survival and lack of metastasis [35, 36].

I.3. Biomarkers for EMT

The aim of this section is to describe the main molecules regulating EMT, the transition of epithelial cells into a mesenchymal phenotype. *Figure I.5* is a schematic representation of this process in which the well-organized apical-basolateral structure of epithelial tissue cells and the reorganization of the cytoskeleton in mesenchymal cells is shown. In the field the hallmark recognized to be key is the down-regulation of E-cadherin, a molecule that forms part of the adherens junctions of epithelial cells.

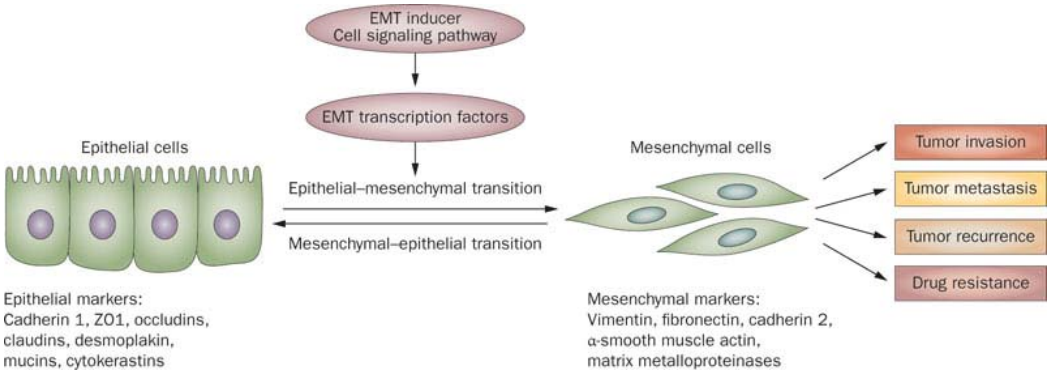

Figure I.5. Loss of cell polarity during EMT. EMT occurs when epithelial, well-organized cells lose their epithelial characteristics and become mesenchymal, more motile cells. In this process the apical-basolateral cell polarity is lost and there is reorganization of the actin cytoskeleton. Epithelial markers such as E-cadherin, occludins and claudins are no longer expressed due to a stimulus that induces EMT and mesenchymal markers such as vimentin, fibronectin or N-cadherin are up-regulated. An increase in tumor malignancy is achieved due to invasion, metastasis, recurrence and drug resistance of the tumor [34].

Epithelial cells are typically arranged forming sheets, tubes or vesicles where the apical polarity between cells is established. In tubular structures the apical side is exposed to the lumen and the basolateral surface rests on a basement membrane. The intimate association of epithelial cells is through specialized cell-cell contact structures, the tight junctions, the adherens junctions and the desmosomes [38]. Tight junctions are membrane fusions at the lateral side close to the apical surface providing intercellular sealing. Occludins and claudins are the main intercellular components, and Zonula Occludens-1 (ZO-1) and p120 are undercoating the structure. ZO-1 cytoplasmic tails attach to actin filaments, giving strength and integrity to the junctions [39]. Adherens junctions are also in the basolateral surface compartments of cells, next to tight junctions. They connect the cytoskeletal microfilaments surrounding the lateral interface of cells [40]. E-cadherin, the down-regulation of which is considered to be the hallmark of EMT, is an essential homotypic adherens junction protein [41]. This adherens junction protein is the prototypic type I cadherin that mediates homophilic

intercellular interactions by forming adhesive bonds between one or several immunoglobulin domains in their extracellular region, connecting to the cell's cytoskeletal protein actin indirectly through α- and β-catenin in the cytoplasm [42]. The anchoring to the actin cytoskeleton is directly through α-catenin or indirectly through α-actinin and vinculin [43]. Desmosomes are similar to adherens junctions in structure with transmembrane cadherins and linker proteins connecting cadherins to intermediate filaments. Their organization is as individual units and not as a structure that surrounds the cell and associate to desmoplakins, providing a link to keratin intermediate filaments [44].

In early EMT there is dissociation of tight junctions with the loss of polarity due to the redistribution of ZO-1, occludins and claudins. This induces a change in the organization of the cell's cytoskeleton [38]. In EMT the adherens junction complexes disassemble and the actin cytoskeleton reorganizes from an epithelial cortical alignment associated with cell-cell junctions into actin stress fibers anchored to focal adhesion complexes. Desmosome components are down-regulated during EMT but the order in which this process occurs remains to be elucidated [45, 46].

The direct down-regulation of the E-cadherin (*CDH1*) gene has been described to be though its promoter, which has four E-box sequences (CACCTG or CAGGTG) that are directly bound by several transcription factors and cause the transcriptional down-regulation of the gene [47]. Among these factors are Snail1 and 2, Zeb1 and 2, E47 and KLF8. There are also indirect repressors such as Twist1, Goosecoid, E2.2 and FoxC2 [8, 33]. The main focus of this thesis will be on Snail1 and, to a lesser extent, Twist1. Each gene and gene family will be described in the required detail, according to their importance in this study.

I.3.1. The Snail family

The Snail family of repressors is comprised of three members: Snail1 (formally known as Snail), Snail2 (Slug) and Snail3 (Smuc). These transcription factors have similar domains which are also highly conserved. Snail1 is the most widely studied protein and is considered to play a role in triggering EMT. In the N-terminal part of the protein there is a SNAG (Sna/Gfi) domain (amino acids (aa) 1–9) which is required for transcriptional repression and a phospho-serine rich domain (P-S rich, aa 90–120) that contains various phosphorylation motifs (*Figure I.6*). Where and how posttranslational modifications affect Snail1 will be discussed in a later section. Snail1 also has a nuclear export sequence (NES) that binds to CRM1 (Exportin-1, XPO1; aa 139–148). At the most C-terminal part we find four zinc fingers (ZnF) of the C_2H_2 type which are important for DNA binding though E-boxes,

the consensus sequence of the fourth finger is however atypical and thus different to that of the first three Zn fingers [48, 49]. It must be taken into account that Snail1 is, when compared to Snail2, a more efficient repressor since it has better affinity for E-box sequences [50].

The SNAG domain (*Figure I.6*) is important in repression and is finely controlled. It has been shown that Snail1 overexpression is correlated to a global deacetylation of histones 3 and 4 (H3 and H4) due to the recruitment of histone deacetylase 1 and 2 (HDAC1/2) through the Sin3A co-repressor [52]. This step is required for the posterior binding of polycomb repressive complex 2 (PRC2) to the E-cadherin promoter and trimethylation of lysine 27 on H3 [53]. The manner by which Snail1 represses genes and may serve as a chromatin remodeling factor is through its interaction through the SNAG domain with Ajuba which functions as a platform for the recruitment of the protein arginine methyltransferase 5 (PRMT5) on the E-cadherin promoter [54].

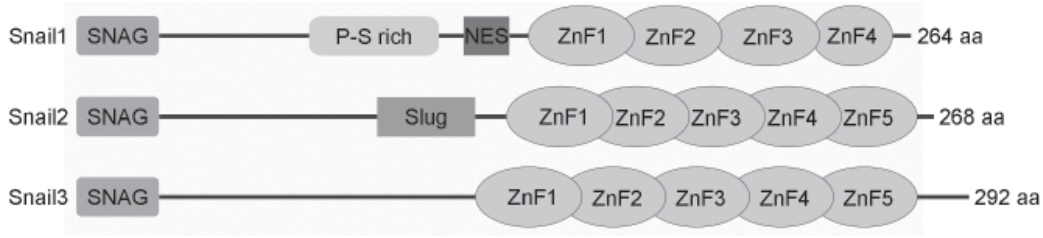

Figure I.6. The Snail family of transcription factors. Domain structure of the proteins of the Snail family. The three members have a SNAG domain and multiple zinc fingers (ZnF), important for DNA binding. Snail1 also has a phospho-serine rich (P-S rich) domain and a nuclear export sequence (NES). Snail2 has a Slug domain. Adapted from [48].

Snail1 also interacts with the histone demethylase LSD1 (lysine-specific demethylase 1) and CoREST (repressor element-1 silencing transcription factor co-repressor) forming a ternary complex (Snail1-LSD1-CoREST) that represses epithelial gene promoters. LSD1 removes dimethylation of lysine 4 on histone H3 (H3K4me2), a covalent modification associated with active chromatin. This protein is essential for the transcriptional repression mediated by Snail1 [55-57]. As mentioned in the EMT signaling section above, Snail1 can also bind to SMAD3/4 through a SMAD-binding element (SBE) located close to one of the E-boxes in the E-cadherin promoter when the gene is silenced by TGF-β-induced EMT. The Snail1-SMAD3/4 complex has also been detected in the promoters of CAR (Coxsackie and adenovirus receptor, a tight junction associated protein) and occludin. [58]. Lysyl-oxidase-like 2 and 3 (LOXL2 and LOXL3) are also cooperating

through the direct interaction with Snail1 in the repression of the *CHD1* gene, a mechanism that may require oxidation of some lysines [59, 60]. In *Drosophila*, Snail1 binds to the carboxyl terminal binding protein-1 (CtBP1) for repression, a known transcriptional co-repressor; however, this interaction is not conserved in humans [61, 62]. A more recent study also shows that Snail1 interacts with Akt2 to repress the E-cadherin gene promoting threonine 45 phosphorylation on histone H3, a mark that is now related to Snail1 action [63]. Moreover, Snail1 binds to and represses its own promoter to control its expression through a feed-back mechanism [64].

The NES present in the Snail1 sequence (*Figure I.6*) is capable of binding CRM1 and control the nuclear export of the protein. Different deletion mutants of Snail1 allowed seeing the part of the protein responsible for its nuclear localization. While the N-terminal part of the protein is exclusively cytosolic (aa 1–151), the C-terminus is nuclear (aa 152–264). Moreover, it is known that the protein responsible for the export is CRM1 since a series of experiment using Leptomycin B (LMB), an antifungal molecule capable of binding CRM1 blocking its function, showed that Snail1 is retained in the nucleus. Mutation of the leucines in the NES inhibited the export of Snail1, confirming the proposed sequence to be an NES. To conclude this study is was seen that phosphorylation of the P-S rich domain, which is in close proximity to the NES, helps in the export of Snail1 from the nucleus, probably due to a conformational change in the protein and a better accessibility of CRM1 to the NES [65]. Finally, a unique nuclear localization signal (NLS) that mediates the nuclear import of Snail family proteins has been identified, composed by non-consecutive basic residues at defined positions in at least three sequential ZnFs [66, 67].

Snail1 has not only been described to down-regulate E-cadherin but also other epithelial markers such as desmoplakin, Muc-1, cytokeratin 18, occludin, claudins, Vitamin D receptor and others [41, 46, 68-70]. It is also important in ECM modification. Both Snail1 and Zeb1 are able to induce the expression of matrix metalloproteases (MMPs) that can degrade the basement membrane, favoring invasion. It has also been shown that some proteases can induce EMT, probably by a feedback loop that stabilizes the EMT process. For example, MMP3 triggers EMT since it increases ROS cellular levels and induces Snail1 expression [71]. In colon carcinoma cell lines the transmembrane serine protease TMPRSS4 is overexpressed, inducing EMT due to E-cadherin down-regulation and promoting metastasis in nude mice [72]. Other MMPs such as MMP13 and Periostin have also been determined to promote EMT, invasion and metastasis [73, 74].

Snail1 is of great importance during EMT, especially to trigger it and to allow for a complete transition. This was confirmed with the Snail1 knockout mouse strain which showed great defects in the formation of the mesoderm germ layer, with many cells retaining their epithelial phenotype. These embryos died during the process of gastrulation because they could not undergo a full EMT [75]. Analysis of tumor samples and their surrounding stroma has confirmed that Snail1 protein is at the tumor-stroma interface, probably aiding in the communication between tumor and stroma and converting carcinoma cells to stromal cells [76]. A later study using colorectal tumors correlates Snail1 nuclear levels in the stroma to the bad prognosis of patients [77]. Snail1 has also been detected in many other tumor types, these being breast, ovarian, colon, squamous cell, synovial and hepatocarcinoma [25].

Snail2 has been less studied than Snail1; however, it is a transcription factor that can also induce EMT through the repression of E-cadherin [78]. Snail2 can be imported into the nucleus through a similar sequence as Snail1 but lacks a P-S rich region (*Figure I.6*) [66]. Snail2 has a central Slug domain with unknown function that binds CtBP1 for repression, also recruiting proteins such as HDAC1 in the promoters of genes. The site of interaction with HDAC1 has not been described [79, 80]. A recent study shows that the co-repressors CtBP1 and nuclear receptor co-repressor 1 (NCoR) need both the Slug and SNAG domains to be recruited, and that phosphorylation on serine 4 contributes to the functionality of the protein [81]. Contrary to what happens with the Snail1 knockout, Snail2 mutant mice are viable, showing that Snail2 is not essential for mesoderm formation [82].

I.3.1.i. Snail posttranslational modifications

Snail1/2 are regulated both at transcriptional and translational levels. The focus of this thesis is on the posttranslational modifications of Snail1, particularly on the ubiquitination. This will be the topic that will be described in this section; however, the transcriptional modulators of the transcription factors that induce EMT must not be disregarded. Snail1 protein is very short-lived, with an approximate half-life of 25 minutes. Many Snail1 posttranslational modifications have been described to be important for both its localization and stability. These modification can be grouped into phosphorylations, mainly on serine residues, ubiquitination and others such as poly(ADP-ribosyl)ation or O-GlcNAc modification (*Table I.1*).

Phosphorylation

Glycogen synthase-3β (GSK-3β) was the first kinase described to phosphorylate Snail1. After analysis of the stability of Snail1 in the presence of the proteasome inhibitor MG132 or lithium, the inhibitor of GSK-3β, it

was found that both molecules potently stabilized Snail1 in many cancer cell lines [83]. Snail1 has several putative GSK-3β phosphorylation motifs which are characterized by an SxxxSxxxS consensus sequence, important for nuclear export and degradation. Regarding nuclear export, Yook *et al.* (2005) showed that phosphorylation of S104 and possibly that of S107 (the second GSK-3β motif) are necessary to localize Snail1 in the cytoplasm [84]. However, Zhou and collaborators (2004) had stated that the phosphorylation of the four serines from S107 to S119 influence nuclear export [83]. Importantly, both studies were coincident in that these phosphorylations are acting as priming site for the second round of phosphorylation of S96 and S100 (the first GSK-3β motif) that gives rise to a consensus destruction motif or degron DSGxxS sequence for β-transducing repeat containing protein 1 (Trcp1) binding and degradation (further described in a later section) [83].

More recently it has been found that there is regulation of GSK-3β localization through the nucleocytoplasmic chaperone Axin2 which is regulated by the Wnt canonical pathway through a β-catenin-TCF-dependent EMT program [85]. Another kinase that is involved in the phosphorylation of these serines and that seems to be priming the phosphorylation by GSK-3β is Casein kinase 1 epsilon (CK1-ε) that phosphorylates S104 and S107. This kinase interacts with the ZnF domain of Snail1 and regulates its stability together with GSK-3β [86].

Other kinases affecting the phosphorylation of Snail1 that positively regulate its stability are Casein kinase 2 (CK2) and Protein kinase A (PKA). CK2α phosphorylates Snail1 on S92 and is seen to interact with it *in vivo*. PKA strongly phosphorylates Snail1 on S11 *in vitro*. A series of experiments determined that the phosphorylation of both serines is necessary for Snail1 stability and repression of E-cadherin [87]. Supporting the evidence that CK2α regulates the stability of Snail1 a report linking aberrant expression of this protein and EMT in breast tumors was recently published by Deshiere and coworkers [88]. Protein kinase D1 (PKD1) also phosphorylates Snail1 on S11, in this case the authors described this modification to have an inhibitory effect on EMT, causing the up-regulation of E-cadherin in a prostate cancer model. The proposed mechanism is that upon S11 phosphorylation nuclear export of Snail1 is triggered via 14-3-14σ binding [89]. However, the effects of phosphorylation on S11 by PKD1 are controversial in the field: in another prostate cancer model PKD1-induced phosphorylation of Snail1 was found to suppress EMT [89] and in a study of the role of Snail1 in breast invasive ductal carcinoma PKD1 is observed to induce a DNA-bound inactive Snail1 transcriptional repressor complex that cannot repress E-cadherin levels [90].

Another recent publication supports the idea that PKD1 phosphorylation enhances nuclear Snail1 transcriptional repression activity [91].

Phosphorylation of residues in the C-terminal part of Snail1 has been described to happen through two different kinases: p21 activated kinase 1 (PAK1) and Lats2. PAK1 phosphorylates Snail1 on S246 and this causes the transcription factor to be retained in the nucleus, increasing its repressive potential [92]. Similarly, Lats2 phosphorylation on T203 also induces nuclear retention of Snail1, potentiating its activity [93]. PAK1γ has been described to be up-regulated due to DNA damage after γ-irradiation [94]. Another study showing that this insult causes Snail1 phosphorylation on S246 also fits in the idea that this phosphorylation is important in the positive regulation of the stability of the protein [95], although they point out that it may be the Checkpoint kinase-1 (CHK1) that is causing this phosphorylation [96]. DNA damage through camptothecin, a topoisomerase I poison, induces a hyper-phosphorylation of the kinase Ataxia telangiectasia mutated (ATM) on S1981. The modification of the kinase causes Snail1 phosphorylation on S100 which stabilizes the protein, inhibits its interaction to GSK-3β and thus prevents degradation [97].

aa	Modification	Effector	Description
S11	P	PKA	Increased stability
	P	PKD1	Controversial effect
S92	P	CK2α	Increased stability
S96	P	GSK-3β	Degron (with S100) for degradation by β-Trcp1
		CK1ε	Priming P to allow GSK-3β-mediated P
S100	P	GSK-3β	Degron (with S96) for degradation by β-Trcp1
	P	ATM	Increased stability, prevents GSK-3β binding
S107	P	GSK-3β	Export to cytoplasm
S109	P	GSK-3β	Export to cytoplasm
S111	P	GSK-3β	Export to cytoplasm
S112	O-P	GSK-3β	Export to cytoplasm
	O-GlcNAc	OGT	Increased stability
S115	P	GSK-3β	Export to cytoplasm
T203	P	Lats2	Increased stability
S246	P	PAK1	Increased stability
	P	CHK1	Increased stability
R	ribosylation	PARP1	Increased stability
K	Ubi	β-Trcp1	Degradation
K	Ubi	Mdm2	Degradation
S	de-P	SCP	Increased stability by de-P of GSK-3β motifs

Table I.1. Snail1 posttranslational modifications. Compilation of the modifications on Snail1 protein by different effector molecules and their biological significance. P: phosphorylation; O-P: O-phosphorylation; O-GlcNAc: O-linked β-N-acetyl-glucosamine; Ubi: ubiquitination; de-P: de-phosphorylation.

Ubiquitination

As mentioned in the previous section, phosphorylation of GSK-3β on S96 and S100 generates a consensus destruction motif for β-Trcp1-mediated degradation similar to the previously described for IκBα, β-catenin and Emi [83]. Another ligase that has been found to be able to degrade a Snail family member, Snail2, is Murine double minute 2 (Mdm2). Mdm2 is known to degrade the tumor suppressor p53, which prevents cancer progression by inhibition of proliferation and induction of apoptosis. p53 can modulate the action of the EMT transcription factor Snail2 by forming a p53-Snail2-Mdm2 complex that facilitates the degradation of Snail2 [98]. Due to the structural similarities between Snail2 and Snail1 it is possible that the same ligase targets both proteins. In fact, a preliminary study shows that Mdm2 can also degrade Snail1 in a p53-dependent manner [99].

Another ubiquitin ligase controlling Snail2 stability has been described in *Xenopus*. It is during neural crest development that the F-box protein Partner of paired (Ppa; the human homologue is the F-box leucine-rich-repeat protein 14 or FBXL14) regulates ubiquitin-mediated degradation of Snail2, showing a transcriptional expression pattern that is contrary to that shown for Snail2 [100].

Other modifications

Snail1 can be poly(ADP-ribosyl)ated by poly(ADP-ribose) polymerase 1 (PARP1), which interacts with the protein and modifies it, causing its stabilization [101]. Another very dynamic modification that occurs on S112 of Snail1 is O-linked β-N-acetylglucosamine (O-GlcNAc). This modification happens as a balance of protein O-phosphorylation by GSK-3β in hyperglycemic conditions by the O-GlcNAc transferase (OGT). When OGT adds the O-GlcNAc modification on Snail1, which will substitute the O-phosphorylation modification on the same amino acid, Snail1 action is enhanced. This modification provides a link between cellular glucose metabolism and the control of EMT [102]. So far, the removal of phosphorylation marks has only been attributed to a Snail1-specific phosphatase called small C-terminal domain phosphatase (SCP). This phosphatase stabilizes Snail1 expression while dephosphorylating it through its binding to the C-terminal part of Snail1. However, the effect of the SCP is allocated to the N-terminal part of the transcription factor, where it de-phosphorylates Snail1 at the GSK-3β motif [103].

I.3.2. The ZFH family

The ZHF family of transcription factors is highly conserved across species and is constituted by two members: Zeb1 and Zeb2 [104]. It consists of two groups of ZnFs of the C_2H_2 and C_3H type at the N- and C-terminal part of the protein with an internal homeodomain. Zeb proteins bind to CtBP co-repressors recruiting histone deacetylases and methyltransferases, PRC1/2 and CoREST among other factors [29].

Zeb1 and Zeb2 can repress epithelial markers and activate mesenchymal ones thus triggering EMT [105]. Similarly to the Snail family, TGF-β activates these mesenchymal genes [106], and Zeb1 is also overexpressed by the aberrant activation of the canonical Wnt pathway [107]. Moreover, Snail1 is able to induce Zeb1 in many ways: through the inhibition of micro RNA (miRNA) 200, induction of ETS1 and by achieving the stabilization of the Zeb1 protein [68, 108]. Zeb1 also binds to the E-boxes in the E-cadherin promoter and can thus directly cause a down-regulation of this protein. However, Zeb1 induces a latter but more sustained down-regulation of E-cadherin [109]. Zeb2 protein can also be induced by Snail1 in an indirect manner through the alternative processing of the *ZEB2* mRNA [110].

I.3.3. The bHLH family of transcription factors

The basic helix-loop-helix (bHLH) family of transcription factors has a common structure among the different members with two parallel amphipatic α-helices joined by a loop that is required for dimerization. bHLH proteins can bind DNA as homo- or heterodimers using consensus E-boxes and can act both as transcriptional activators or repressors [111]. The E2A gene products such as E47, the Id proteins and Twist proteins are transcription factors of this subfamily.

Twist1 and Twist2 are the most widely described bHLH proteins involved in EMT. Apart from sharing the common bHLH domain they have, at the C-terminal end of the protein, a Twist box important both for transcriptional activation and repression [112]. E-cadherin repression by Twist1 needs to be accompanied by the recruitment of chromatin remodeling complexes to the E-cadherin promoter. Among these complexes PRC1 and PRC2 have been described to be important for Twist1 action, as well as for its interaction with the NuRD complex [113]. SET8, a H4K20 methyltransferase, can also be found together with Twist1 repressing the E-cadherin promoter, inducing the activation of N-cadherin [114].

Similarly to Snail1, the subcellular localization of Twist1 regulates its function and the dimerization partner. This is modulated by integrin-

mediated adhesion to the ECM and posttranslational modifications [115]. Twist factors predominantly heterodimerize with E12 and their function can thus be determined by the availability of this protein as well as by the phosphorylation status of the bHLH domain [116]. As described for Snail and Zeb family members, Twist proteins are up-regulated by TGF-β, Wnt signaling, RTKs and hypoxia among others. Twist1 is directly modulated in hypoxia since it has a Hypoxia inducible factor (HIF)-responsive element (HRE) that is bound by HIF-1α in low oxygen conditions and causes its stabilization [117].

I.4. EMT signaling pathways

Many signaling pathways have been associated to the induction of EMT, resulting in a down-regulation of the E-cadherin (*CDH1*) gene. Most of the pathways that have been studied up to now are associated to a stabilization of Snail1 and not to other EMT biomarkers. These signaling pathways do not act in a linear manner but interact with each other. A schematic representation of the pathways affecting Snail family gene expression is seen in *Figure I.7*. Tumors are found in microenvironments with many inputs from the bloodstream, surrounding tissues, cells that migrate to the site such as fibroblasts and immune cells and external stress factors such as hypoxia and reactive oxygen species (ROS). Therefore, although this section is divided in short parts describing the signaling pathways known to be important for the induction of EMT, an interrelation between all the activation cascades must be kept in mind. In fact, it has been described that TGF-β, one of the major EMT inducers, cross-talks with stem cell pathways like Wnt, Ras, Hedgehog and Notch in order to promote EMT; and that this promotes SMAD complexes which are involved in the repression of epithelial genes and the activation of mesenchymal ones [118].

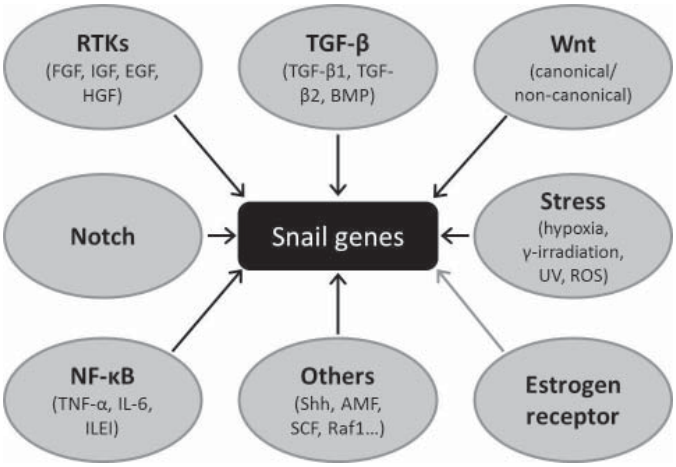

Figure I.7. EMT signaling pathways. The main signaling pathways for EMT are RTKs, TGF-β, Wnt, Notch, NF-κB and others such as the Shh, AMF, stem cell factor (SCF) c-kit and Raf1. Stress in cells can also cause and up-regulation of Snail genes. Hypoxia, γ-irradiation, UV light and ROS are among these stress factors. The activation of the Estrogen Receptor causes a down-regulation of Snail1. Black arrows indicate activation of the genes, the gray arrow silencing. Adapted from [117].

I.4.1. RTKs signaling

The induction of EMT during development was first described to happen through receptor tyrosine kinases (RTKs). Several RTKs play critical roles in the regulation of EMT, including the family members of Met, Fibroblast growth factor (FGF), Insulin-like growth factor (IGF), Epidermal growth

factor (EGF) and Platelet-derived growth factor (PDGF) [9]. For example, it has been described that FGF is important in neural crest formation, gastrulation, limb development and in the maintenance of tumor cells [119]. The Hepatocyte growth factor (HGF)/Met pathway promotes partial EMT. It is through multiple downstream signaling pathways with Ras as a main effector and MAP kinase, phosphoinositide 3 kinase (PI3K) and Rac/Cdc42 being activated what orchestrates the changes in cell adhesion and motility needed for partial EMT to occur [120, 121]. Moreover, fibroblasts in the stroma of tumors can become activated and secrete factors that trigger RTK-mediated signaling, inducing further EMT and increasing the invasive potential of epithelial tumor cells [122, 123].

I.4.2. TGF-β signaling

Members of the TGF-β superfamily are considered to be the major EMT inducers both in development and in pathological processes. Although the signaling pathways activated by different TGF-β family members varies, it is clear by all the evidence that has been provided over the years that this pathway is a primary inducer of EMT. For example, Bone morphogenic proteins (BMPs) are required for the induction and migration of neural crest cells in the development of chick and mice [124]. It was also recently described that Snail1 forms a complex with SMAD3 and SMAD4 which targets to the gene promoters of E-cadherin and CAR, a tight-junction protein, during TGF-β-driven EMT [58]. This demonstrates that this superfamily does not only cooperate with the signaling pathways triggering EMT such as RTKs and Wnt but can achieve a direct activation of the transition [125]. Our lab has found that Snail1 also controls TGF-β responsiveness and differentiation of mesenchymal stem cells, demonstrating that there is a signaling loop between Snail1 and TGF-β in these cells [126].

I.4.3. Wnt signaling

The canonical Wnt signaling pathway is implicated in the initiation and maintenance of mesoderm formation. The canonical Wnt/β-catenin pathway is important for cell determination and has been linked to EMT due to the crucial role of β-catenin as a component of adherens junctions providing a scaffold for E-cadherin and α-cadherin, and modulating cell-cell adhesion, proliferation and migration [127]. It was recently described that the canonical Wnt signaling starts tumor cell dedifferentiation and activates the invasive capacity of cells though an Axin2-dependent pathway that stabilizes Snail1 by controlling the localization of GSK-3β in the cell, the dominant kinase modulating Snail1 protein turnover and activity [85]. Although the canonical Wnt pathway is the one mostly linked to EMT, the non-canonical pathway has also been described to be important in *Xenopus*,

where Wnt11/Frizzled7-mediated activation plays an essential and specific role in neural crest migration [128].

I.4.4. Notch signaling

Activation of the Notch pathway has also been associated to the induction of EMT. This pathway is involved in the regulation of cell fate specification, stem cell maintenance and initiation of differentiation in embryonic and post-natal tissues [130]. For instance, in frog and chick, Notch signaling has been seen to regulate cranial neural crest cells in an indirect manner through the effect it exerts on BMPs expression [131]. This pathway also promotes EMT during cardiac valve formation and in cultured epithelial cells derived from kidney tubules, mammary glands and epidermis [132]. However, differing to what happens with other signaling pathways such as Wnt and TGF-β, the Notch pathway is not conserved in all the EMT processes and thus it is thought that it alone is not sufficient to trigger EMT, requiring coordination with other signals. Some studies have focused on how the acquired resistance of tumor cells to different chemotherapeutic treatments allows them to undergo EMT due to the activation of the Notch pathway [133-135].

I.4.5. NF-κB signaling

Inflammation has been linked to cancer and metastasis in many studies. The Nuclear factor kappa-light-chain-enhancer of activated B cells (NF-κB) pathway emerged as a mediator of EMT in a mouse model of breast cancer progression [136]. In human mammary epithelial cells NF-κB was found to be the upstream regulator of Snail1 [137]. Moreover, Snail1 and the p65 subunit of NF-κB are known to interact in a complex together with PARP1 to activate the transcription of the mesenchymal gene *FN1* (Fibronectin1) [138]. A study shows that tumor necrosis factor-α (TNF-α), an inflammatory cytokine, activates NF-κB and is capable of directly stabilizing Snail1 through the induction of COP9 signalosome 2 (CSN2) which blocks the ubiquitination and degradation of Snail1 [139]. Other pro-inflammatory cytokines such as Interleukin 6 (IL-6) and Interleukin-related protein (ILEI) are also associated to EMT [140, 141].

I.4.6. Stress pathways

There is a link between EMT and resistance to apoptosis [95] that complicates the current approaches for treatment of cancer [142]. There are several insults that have been shown to trigger EMT in a tumor context. Hypoxia, which is described as a low oxygen condition, activates the EMT program and triggers angiogenesis [143, 144]. Snail1 and Zeb2 are induced

in hypoxia; however, Twist1 is the transcription factor that is directly affected by this stress condition. As described before, Twist1 contains a HRE in its proximal promoter and is directly induced by the stabilization of HIF-1α in hypoxia [117]. Notch also potentiates HIF-1α recruitment to the Lysyl oxidase (LOX) promoter, stabilizing Snail1 protein [145]. In the renal system the von Hippel-Lindau (VHL) tumor suppressor also negatively regulates HIF-1α and its loss is associated with decreased E-cadherin levels. Other insults that lead to EMT are those related to DNA damage such as exposure to ultraviolet (UV) light [146], γ-irradiation [95, 147] or reactive oxygen species (ROS), also linked to hypoxia [148, 149].

I.5. Ubiquitination

As mentioned in previous sections, the focus of this thesis will be on the study of Snail1 protein modifications, in particular on its ubiquitination and degradation. As described before, Snail1 has a very short half-life [83]. This means this gene has either a very labile mRNA or that the protein is targeted by the ubiquitin-proteasome system thereby causing its degradation. We have studied the second option and for this purpose we introduce the more basic yet necessary concepts of the process of ubiquitination.

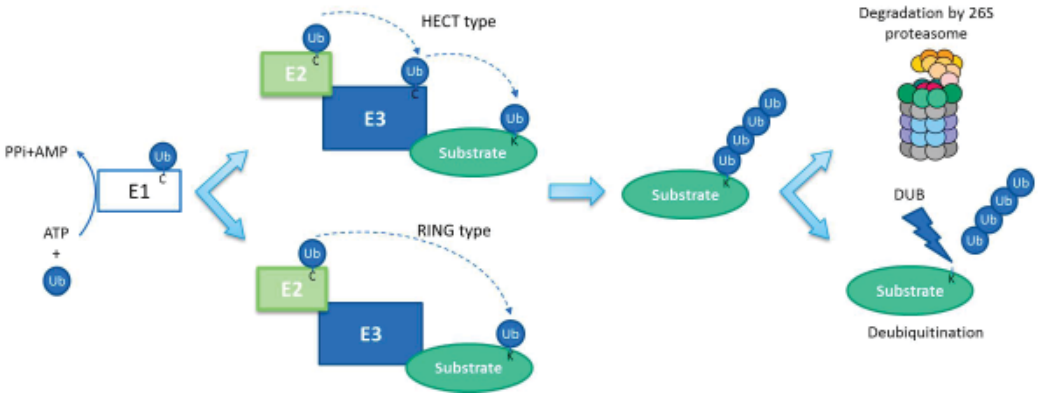

Figure I.8. General mechanism for the ubiquitination of substrates. Scheme showing actions of the ubiquitin-activating enzyme or E1, the ubiquitin-conjugating enzyme or E2 and the two types of E3 ubiquitin ligases: RING and HECT. Polyubiquitinated proteins are shuttled by other proteins to the 26S proteasome where they can be degraded or targeted by DUBs (de-ubiquitinating enzymes) which will remove ubiquitin chains. Adapted from [150, 151].

Ubiquitination is a process by which the 76-amino acid protein ubiquitin is attached to a target protein. An amide bond is formed between the carboxylic acid of the terminal glycine of an activated ubiquitin molecule and the ε-amine of a lysine residue in the target protein. Three types of enzymes are the ones responsible for the final ubiquitination of a substrate: first the Enzyme 1 (E1) or ubiquitin-activating enzyme that activates the ubiquitin molecule in an ATP (adenosine triphosphate)-dependent manner, with the formation of a thio-ester linkage between the E1 and the carboxyl terminus of ubiquitin; the second enzyme (E2) or ubiquitin-conjugating enzyme that transfers the activated ubiquitin moiety directly onto the substrate or to a third enzyme (E3) called ubiquitin ligase [150]. The way in which ubiquitin is loaded onto the substrate depends on the E3 that can be of the RING/RING-like (Really Interesting New Gene) or of the HECT (Homologous to Human Papilloma Virus E6 Carboxyterminal domain) types (*Figure I.8*) [152].

Proteins are recognized by the ubiquitin-ligase machinery through a degradation signal or degron, which is defined as a minimal element within a protein that is sufficient for recognition and degradation by the proteolytic apparatus [153]. For example, in the case of Snail1, as previously described in this report, phosphorylation by GSK-3β of S96 and S100 creates a degron of the type DSGxxS that is recognized by the E3 ubiquitin ligase β-Trcp1 (*Figure I.9*) [83].

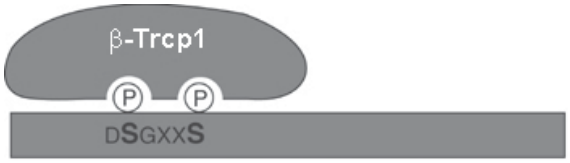

Figure I.9. The degron sequence for β-Trcp1. Two serine phoshorylations are needed for β-Trcp1 to recognize the substrate it must ubiquitinate. The first serine must be flanked by an aspartic acid (D) and a glycine (G), then two amino acids (XX) and the second serine placed at the end [154].

The specificity of the ubiquitination process is given by the combination of enzymes needed to ubiquitinate a substrate. The human genome encodes for only two E1 enzymes (UBA1 and UBA6), around 40 E2 enzymes and more than 600 ubiquitin ligases. The two families of E3 ubiquitin ligases differ in their catalytic modules but achieve the same end product. RING type E3 ubiquitin ligases account for the 95% of the human E3s and a total of 28 HECT type ligases have been found [155].

I.5.1. HECT type ligases

HECT type ligases have a C-terminal 350 amino acid HECT domain which was first characterized, as its name implies, in the E6-associated protein. It is responsible for the catalytic activity of the enzyme since it associates with the E2. The HECT domain also contains a conserved cysteine where activated ubiquitin is bound generating a thiol ester intermediate that is further transferred to the substrate [156]. Their substrate specificity is given by the protein interaction domain found in the N-terminal part, and gives further classification of these ligases into three subfamilies: HERC E3s containing RCC1-like domains (RLDs), C2-WW-HECT E3s with tryptophan-tryptophan (WW) domains, and SI(ngle)-HECT E3s lacking either RLDs or WW domains [157]. Among the best characterized HECT ligases are E6-AP which degrades p53, Nedd4-1 degrading PTEN, Nedd4-2 and Smurf1/2, which degrade TGF-β-receptor I and II as well as various members of the SMAD family [158].

I.5.2. RING type ligases

RING type ligases have a common RING finger domain that recruits E2s thioestered with ubiquitin to discharge the ubiquitin onto a substrate. RING finger proteins are divided into single and multi-subunit E3s. Single-subunit proteins have a substrate recognition and a RING domain in the same protein. An example of those is Mdm2, which ubiquitinates and degrades p53 [159]. Multi-subunit RING E3s are also called Cullin-RING E3s since all of them contain a Cullin scaffolding protein and include the anaphase promoting complex (APC), the von Hippel-Lindau-Cullin2/elongin B/elongin C (VHL-CBC), the Fanconi anaemia (FANC) E3 complex and the so called SCF (Skp1-Cullin-F-box) ubiquitin-ligase complexes. The SCF subfamily contains the adaptor protein Skp1, a Cullin scaffolding unit, the RING-H2 finger protein Rbx1 or Roc1 and an F-box protein. The F-box protein is the substrate-recognition subunit and contains, as its name implies, an F-box domain that is a common 50 amino acid motif used to bind Skp1 linking the N-terminal part of Cullin to the F-box protein. Rbx1 binds to the C-terminal part of the Cullin and acts as a docking site for the ubiquitin-activated E2 (*Figure I.10A*) [160]. Despite not forming part of the complex, Nedd8 has been determined a key player in the SCF complex enzymatic activity. Nedd8, which in humans is 60% homologous to ubiquitin, is needed to modify the Cullin subunit to enable it to recruit the E2 to the complex [161]. An important regulation mechanism is performed by the COP9 signalosome complex (CSN) that hydrolyses Cullin-Nedd8 conjugates (deneddylation) [162]. Interestingly, CAND1 sequesters Cullin complexes that are not neddylated and prevents their assembly into SCF complexes [163].

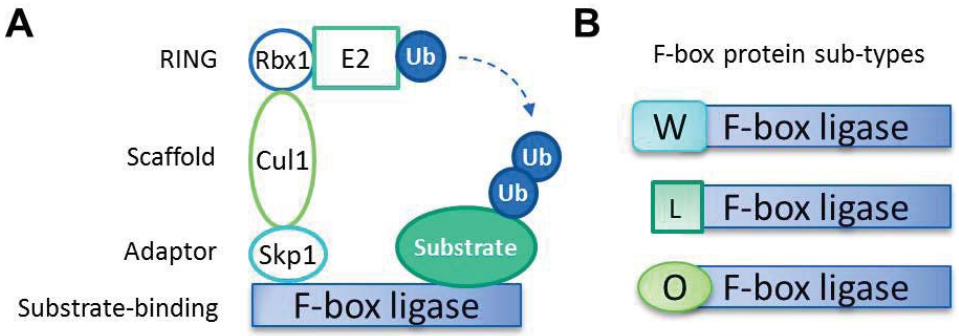

Figure I.10. Schematic representation of the SCF ligase complex. (**A**) The SCF complex is formed by different subunits. At the N-terminal part of the F-box ligase there is an F-box domain that allows the adaptor protein Skp1 to interact with it and link the ligase to Cullin1 which in turn binds to the RING protein Rbx1 and allows the ubiquitin-conjugating E2 to load ubiquitin onto the substrate. (**B**) F-box ligases can be of the W (WD-40, tryptophan rich repeats), L (LRRs, leucine rich repeats) or O (other types of domains).

There are three subtypes of F-box ubiquitin ligases, depending on their protein interaction motif. FBXL proteins are those that contain leucine-rich repeats (LRR) at their C-terminal part and FBXW proteins the ones with tryptophan repeats (WD40) at this same end. The F-box proteins that do not contain LRR or WD40 protein interaction motifs are termed FBXO (other) (*Figure I.10B*) [164, 165]. Cullin-RING E3 ligases can be assembled through Cullin1 (forming the described SCF complex), Cullin2, Cullin3, Cullin4A, Cullin4B, Cullin7 or the Cullin-like protein PARC. A summary of the formed complexes is listed in *Table I.2*.

Cullin-RING E3 ligase	RING-finger protein	Cullin	Adaptor protein	Substrate recognition protein
CRL1/SCF	Rbx1	CUL1	Skp1	F-box
CRL2	Rbx1	CUL2	Elongin C/B	VHL-box
CRL3	Rbx1	CUL3		BTB protein
CRL4A	Rbx1	CUL4A	DDB1	DCAF
CRL4B	Rbx1	CUL4B	DDB1	DCAF
CRL5	Rbx2	CUL5	Elongin C/B	SOCS-box
CRL7	Rbx1	CUL7	Skp1	FBW8
PARC	Unknown	PARC	Unknown	Unknown

Table I.2. Types of SCF ligases and their modules. The different subunits of the known Cullin-RING ligases are listed. Adapted from [166].

I.5.3. Types of modifications by ubiquitin

Ubiquitination is not always associated to the degradation of the target substrate [167]. There are many types of ubiquitin chains depending on the lysine used to elongate the chain. There are also chains that are mixed in the lysine linkages that form them (heterogeneous) and in the type of ubiquitin-like molecule that composes the chain (heterologous) [168]. In this report only the homotypic type of chains will be included. This type

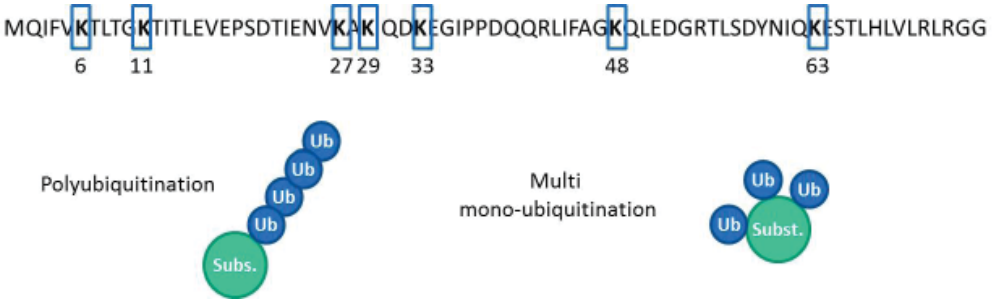

Figure I.11. Polyubiquitination and multi-ubiquitination. There are seven lysines through which ubiquitin may link itself to form chains. It can also attach to one or more lysines of a substrate and not elongate as a chain, mono-ubiquitinating or multi mono-ubiquitinating the substrate.

of polyubiquitination has been related to degradation of proteins in all but K63-linked chains (*Figure I.11*) [169].

K48-linked chains are the most abundantly found and were the first to be described as a destruction tag for proteosomal degradation. K11-linked chains are related to degradation of misfolded proteins by the endoplasmic reticulum and to the cell cycle control by the APC [170, 171]. K63-linked chains have been associated to signal transduction and protein internalization [172]. K27 and K29-linked chains have been associated to few proteins; however, it was found they have similar functions as they lead to the lysosomal degradation of Jun and Deltex, respectively [173, 174]. There is no information on the possible function of K6 and K33-linked chains in *in vivo* systems although they are found as homotypic chains in yeast [175] (*Table I.3*).

Ubiquitin chain	Function
K6/K33	Unknown function
K11	Cell cycle control and degradation of misfolded proteins by the endoplasmic reticulum
K27	Lysosomal degradation of Jun
K29	Lysosomal degradation of Deltex
K48	Proteosomal degradation
K63	Signal transduction and protein internalization

Table I.3. Homotypic lysine-linked chains and their function. All the lysines of ubiquitin are known to form homotypic chains. The functions of these lysine-linked chains are collected in this figure.

Apart from creating and elongating ubiquitin chains E3 ligases can mono-ubiquitinate a substrate by loading only one ubiquitin molecule onto the lysines. This can occur both as a mono-ubiquitination of one of the lysines or multi mono-ubiquitination, in which the posttranslational modification is present in more than one lysine (*Figure I.11*). Mono-ubiquitination has been associated to many types of signaling. For example, PTEN kinase has been described to be imported into the nucleus by mono-ubiquitination on lysine 289, and polyubiquitination of other lysines lead to its cytoplasmic degradation [176]. In addition, substrates can be ubiquitinated in different lysines with combinations of poly- and mono-ubiquitination. This versatility is due to the fact that despite being a small protein, ubiquitin has seven lysines that it may use to form ubiquitin chains [168].

I.5.4. Drugs and DUBs: inhibition of the Ubiquitin Proteasome System

The 26S proteasome is a large, multi-subunit, proteolytic complex that degrades proteins into small peptides. It consists of a 20S proteolytic core

and one or two regulatory 19S particles. These regulatory particles are able to recognize ubiquitinated proteins, unfold and translocate them inside the 20S core, where they are degraded [177]. The proteasome contains many enzymatic sites that allow for multiple drugs to target them in different ways. To date there are many inhibitors targeting this multi-subunit complex. They can be classified into drugs that form or not a covalent bond with the threonine amino acid of the active site. Peptide aldehydes are included in the group of inhibitors that covalently bind the threonine at the active sites and are characterized for being reversible and potent. An example of these is the widely used MG132 which, unless chemically modified, can only be used in *in vitro* studies since it is rapidly oxidized. Peptide boronates also belong to the first group and form a more stable bond with the threonines than peptide aldehydes, therefore they are more potent. Bortezomib is included in this type of inhibitors. This drug has been approved for clinical use for over a decade for the treatment of multiple myeloma due to its ability to cause apoptosis of cells that rapidly progress through the cell cycle. A dose of Bortezomib that causes partial inhibition of the proteasome *in vivo* has been seen to kill multiple myeloma cells while resulting non-toxic to normal cells. Different types of proteasome inhibitors targeting various catalytic sites of the complex have been developed and are being used in clinical trials [178].

Before some ubiquitinated proteins can reach the 26S proteasome de-ubiquitinating enzymes (DUBs) function on them by removing covalently attached ubiquitin molecules. Little is known about these proteins that control the abundance and activity of many substrates [179]. The human genome encodes for 98 DUBs which are grouped into six families based on their structural similarity and sequence: ubiquitin-specific proteases, ubiquitin carboxy-terminal hydrolases, ovarian-tumor proteases, Machado-Joseph disease protein domain proteases, JAMM/MPN domain-associated metallopeptidases and monocyte chemotactic protein-induced protein. All of these are cysteine proteases with the exception of JAMMs, which are metalloproteases [180]. DUBs can have three different roles and process ubiquitin precursors, de-conjugate ubiquitin from substrates and edit the ubiquitin conjugates [181]. Their roles are very diverse; however, most of the information known about them has been obtained from computational methods. It is a wide field of study that needs to be investigated. Their role in cancer progression is extended since they can regulate important proteins involved in many biological processes such as cell cycle control, DNA repair, chromatin remodeling and many transduction pathways [180].

OBJECTIVES

Snail1 has been described to be targeted for degradation in a phosphorylation-dependent manner by the E3 ubiquitin ligase β-Trcp1. However; we had data showing that a Snail1 phosphorylation-deficient mutant at the P-S rich region suffered proteolysis despite its inability to bind the ubiquitin ligase. For this reason we suspected there could be additional ubiquitin ligases directly targeting Snail1 for degradation.

The general objective of this thesis is thus to describe novel ubiquitin ligases that regulate Snail1 stability. To this aim we focused on:

i) The characterization of the effect of the SCF ubiquitin ligase FBXL14.

ii) Finding new SCF ubiquitin ligases that may target Snail1 through a knockdown screening of all the known SCF ubiquitin ligases.

RESULTS

R.1. FBXL14 is a ubiquitin ligase that targets Snail1 for degradation and is regulated during hypoxia

R.1.1. Snail1 levels are regulated by a mechanism alternative to the GSK-3β/β-Trcp1 pathway in some cells

Snail1 is degraded through serine phosphorylation by GSK-3β in the Snail1 phospho-serine rich (P-S rich) domain (*Figure R.1A*). This modification forms the degron sequence (*Figure I.9*) that the SCF ubiquitin ligase β-Trcp1 needs for recognition, polyubiquitination and degradation of the protein [83]. We wanted to verify if Snail1 degradation is only controlled in this manner and decided to inhibit GSK-3β or the proteasome in different cell lines with LiCl or MG132, respectively. All the cell lines used had detectable levels of endogenous Snail1 protein (see the cell line descriptions in *Table MM.1*). We compared their basal Snail1 levels to LiCl- or MG132-treated cells (*Figure R.1B*). The response to LiCl went from strong in SW620 and NIH3T3 cells to mild in RWP-1 cells, and MiaPaca-2 were characterized for being oblivious to the inhibition of GSK-3β. β-catenin, the control substrate of GSK-3β, was up-regulated after addition of LiCl in cell lines with non-saturated levels of the protein.

To further validate our hypothesis we decided to use two mutant constructs of Snail1 with the Hemagglutinin (HA) tag: Snail1SA-HA, which has the 14 serines comprised in the P-S rich domain (*Figure R.1A*) mutated to alanines, and the Snail1SD-HA mutant, which mimics the phosphorylation of all these serines though their replacement to aspartic acid [65]. We expected to see that these mutants would not be affected by the addition of LiCl since their regulation through GSK-3β is impaired. Indeed in *Figure R.1C* we saw there was no change in their levels after blocking this pathway but detected a notable stabilization of the protein after blocking the proteasome. Moreover, exogenous Snail1 was stabilized by both inhibitors, with MG132 exerting a stronger effect on the levels of the protein. This suggests there may be additional ligases targeting Snail1 regulated independently of GSK-3β.

An experiment to check if the mutant Snail1SA-HA, which cannot be targeted by the E3 ligase β-Trcp1, could be ubiquitinated would confirm that there is an alternative degradation pathway for Snail1. *Figure R.1D* shows how both Snail1-HA and Snail1SA-HA are ubiquitinated in the presence of MG132. HIS-tagged ubiquitin was co-transfected with Snail1-HA wild type (wt) or the SA mutant, MG132 was added prior to lysis and Nickel nitrilotriacetic acid (Ni-NTA) affinity beads were used to pull down all ubiquitinated proteins. Blotting against the HA tag showed the levels of ubiquitinated protein. As seen in *Figure R.1D* there was no difference

between the levels of ubiquitination of the Snail1-HA and Snail1SA-HA constructs.

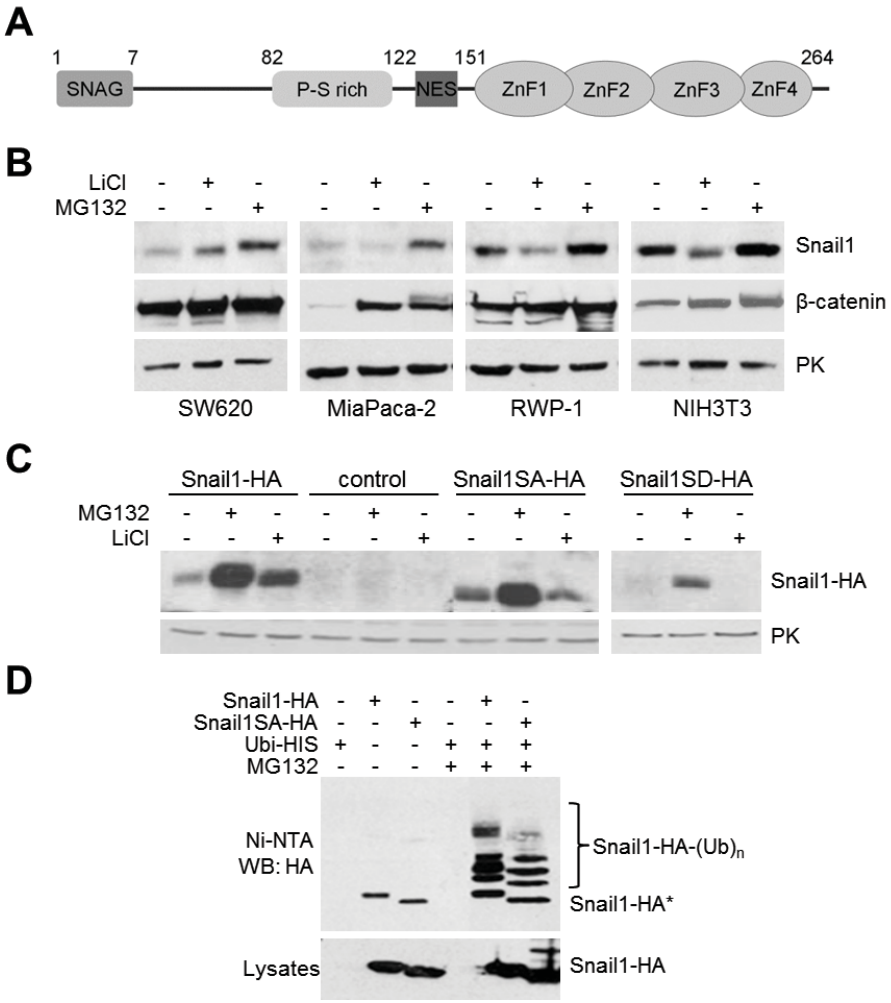

Figure R.1. Stabilization of Snail1 independent of phosphorylation by GSK-3β. (**A**) Schematic representation of Snail1 protein showing the different domains: SNAG, phospho-serine rich (P-S rich) domain, nuclear export sequence (NES) and the four Zinc fingers (ZnFs). The numbers show the amino acid location of each domain. (**B**) Cells were treated with 50 mM LiCl or 50 μM MG132 for 6h and Snail1 expression levels analyzed by Western blot using total cell extracts. β-catenin was analyzed as a positive control for LiCl stabilization. Analysis of pyruvate kinase (PK) was used as loading control. (**C**) HEK293T cells were transfected with the indicated Snail1-HA plasmids and treated for 6h with LiCl or MG132 and above. (**D**) HEK293T cells were transfected with Snail1-HA or Snail1SA-HA and a ubiquitin-HIS plasmid. After 24h cells were treated with MG132 where indicated to stabilize ubiquitinated proteins and purified using Ni-NTA affinity chromatography. Bound proteins were blotted against HA and ubiquitinated Snail1 was detected as a ladder of high molecular weight bands. Non-modified Snail1 was unspecifically bound to the beads and is marked as Snail1-HA*. The levels of the proteins in the lysate prior to purification are shown in the lower panel.

R.1.2. Snail1 interacts with the F-box protein FBXL14

It has been presented in the introduction that the F-box protein Ppa targets Snail2 for degradation in *Xenopus* [100]. The effect of Ppa on Snail2 is phosphorylation-independent and we thought that the homologue of

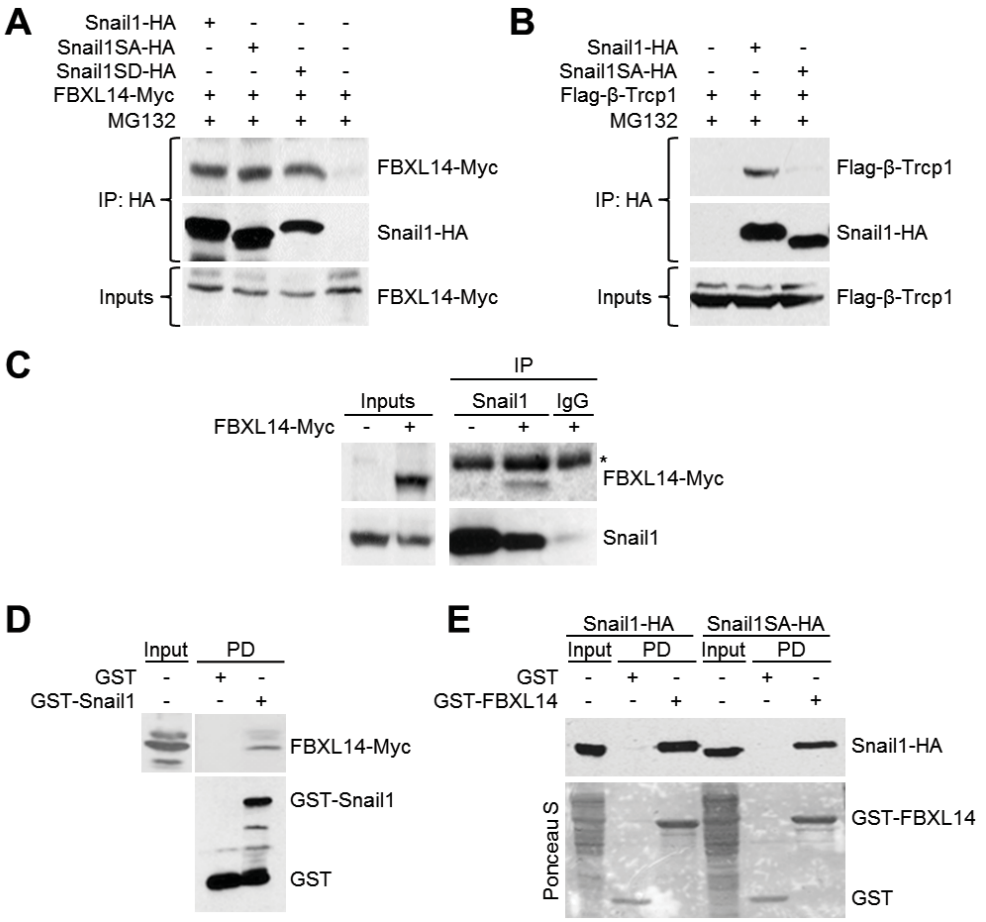

Figure R.2. Snail1 and FBXL14 interact. (**A**) HEK293T cells were transfected for 24h with pcDNA3-Snail1-HA, Snail1SA-HA, Snail1SD-HA or a control vector together with FBXL14-Myc and treated with 50 μM MG132 for 6h. Cell extracts were immunoprecipitated with rabbit anti-HA polyclonal antibody (pAb) and blotted against mouse anti-Myc monoclonal antibody (mAb) or rat anti-HA pAb. The expression levels of FBXL14-Myc are indicated in the lower panel (Inputs). (**B**) HEK293T cells were transfected with the indicated plasmids and immunoprecipitated as in (A). Immunocomplexes were analyzed with mouse anti-Flag mAb or rat anti-HA pAb. The expression levels of Flag-β-Trcp1 are indicated in the lower panel (Inputs). (**C**) NIH3T3 cells expressing high levels of Snail1 were transfected with FBXL14-Myc, treated with 50 μM MG132 for 4h and cell extracts immunoprecipitated with rabbit anti-Snail1 pAb or control Immunoglobulin G (IgGs) and analyzed with anti-Myc or anti-Snail1 mAb. (**D** and **E**) Pulldown (PD) assays were carried out using extracts from HEK293T cells transiently transfected with FBXL14-Myc (D), Snail1-HA or Snail1SA-HA (E). Proteins bound to Glutathione Sepharose beads were analyzed with Myc or HA antibodies. As a control recombinant fusion proteins were visualized with goat anti-GST pAb (D) or Ponceau S staining of the membrane (E).

Ppa, FBXL14, could be acting on Snail1 in mammalian cells. FBXL14 is an F-box protein that forms an SCF complex in order to ubiquitinate proteins. It contains six leucine-rich repeats (LRRs) in its C-terminal part, which is highly homologous to this same part of Ppa in *Xenopus*. The N-terminal part is almost identical structure and has no other described protein motifs apart from the F-box domain. We cloned the human FBXL14 and co-transfected it with Snail1-HA or the SA or SD mutants and performed immunoprecipitation (IP) experiments. When cells were pre-treated with MG132 and IP was performed against Snail1-HA using antibodies against the HA tag we saw FBXL14-Myc precipitated with all the Snail1-HA mutants (*Figure R.2A*). This suggests that the interaction of FBXL14 with Snail1 is independent on the phosphorylation status of the P-S rich domain. In contrast, when we checked the interaction of Flag-β-Trcp1 with the Snail1SA-HA mutant we could detect no interaction when compared to the wt construct (*Figure R.2B*). This is in agreement with the mechanism that has been described for the β-Trcp1-dependent degradation of Snail1, which needs phosphorylation of the serine residues that are mutated in the SA form [83].

The interaction of FBXL14-Myc with endogenous Snail1 was also achieved in MG132-treated NIH3T3 cells, which express high levels of the protein (*Figure R.2C*). To further verify the interaction with the two proteins we performed *in vitro* pulldown (PD) assays using Glutathione-S-Transferase (GST)-Snail1, GST-FBXL14 or GST protein produced in *E. coli*. In *Figure R.2D* cell extracts from HEK293T transfected with FBXL14-Myc were used and the protein was only observed in PD analysis with GST-Snail1 and not with the GST control. Similarly, GST-FBXL14 was able to pulldown Snail1-HA and Snail1SA-HA from cell extracts (*Figure R.2E*). These experiments demonstrate that FBXL14 and Snail1 interact.

R.1.3. Snail1 levels are regulated by FBXL14

After determining that FBXL14 binds Snail1 we wanted to examine if this E3 ubiquitin ligase can decrease Snail1 levels *in vivo*. For this we co-transfected Snail1-HA with increasing amounts of FBXL14-Myc and analyzed the remaining Snail1-HA levels in cells. Snail1 protein was decreased in an inversely proportional manner to FBXL14-Myc (*Figure R.3A*). Moreover, when we co-transfected the ΔF-FBXL14-Myc mutant, which is unable to bind Skp1 to form the SCF complex since it lacks the F-box domain, Snail1 protein levels were stabilized. Surprisingly, FBXL14-Myc levels were not corresponded to the amount transfected in lane 5, indicating that FBXL14 could be itself a target of its own degradation, as it happens for many E3 ubiquitin ligases (*Figure R.3A*). As expected, the degradation of Snail1-HA by FBXL14-Myc was impaired when the proteasome was blocked prior to

cell lysis (*Figure R.3B*), and also helped to recover FBXL14 levels in the cells. Treatment of cells co-transfected with Snail1-HA and FBXL14-Myc or the ΔF mutant with the protein synthesis inhibitor cycloheximide (CHX) also showed that the degradation of the Snail1-HA protein is accelerated in the presence of the E3 ubiquitin ligase (*Figure R.3C*).

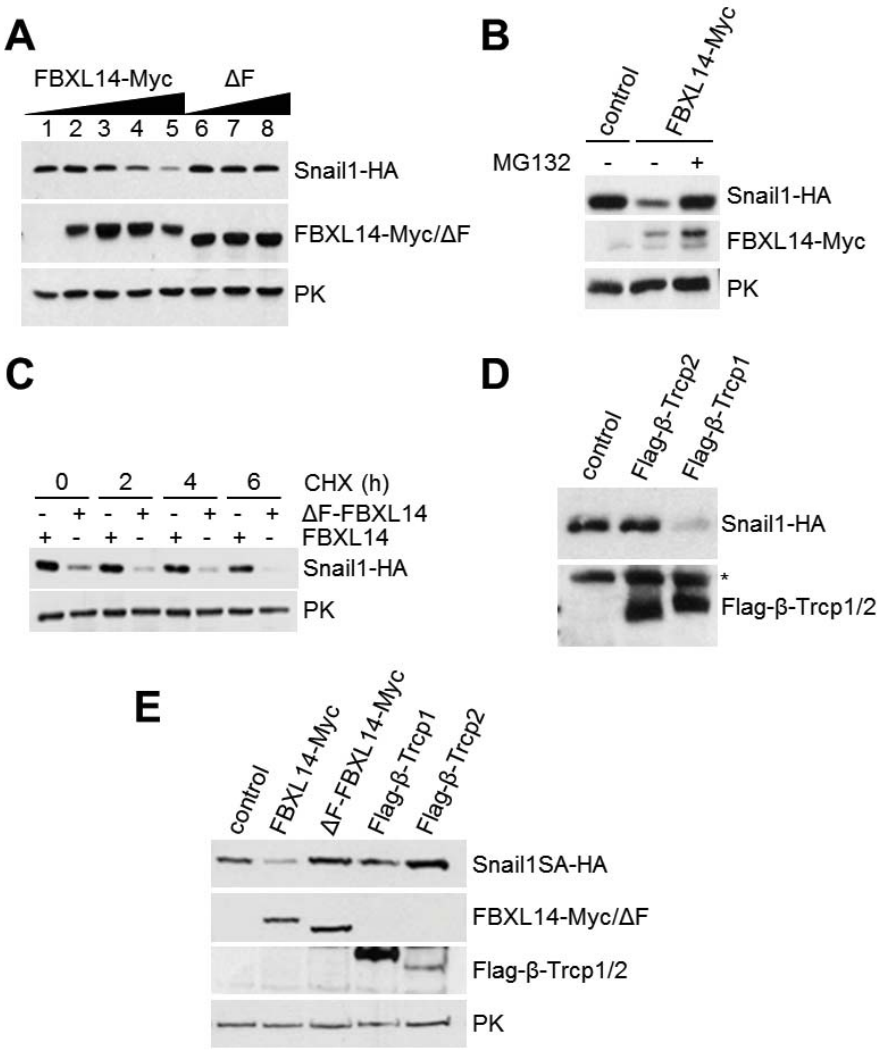

Figure R.3. Snail1 exogenous levels are regulated by FBXL14. (**A**) HEK293T cells were transfected with 0.2 μg Snail1-HA and increasing amounts of FBXL14-Myc (from 0.2 μg in lane 2 to 1.2 μg in lane 5) or the ΔF mutant (from 0.4 μg in lane 6 to 1.2 μg in lane 8). Snail1-HA protein was analyzed 24h after transfection by Western blot with anti-HA. FBXL14-Myc and PK levels were visualized as experimental and loading controls, respectively. (**B**) Cells were transfected as in (A) and treated or not for 6h with 50 μM MG132 prior to cell lysis. Results were analyzed by Western blot. (**C**) Similarly to (A) cells were transfected with 0.2 μg Snail1-HA and 1.2 μg FBXL14-Myc and the protein synthesis inhibitor cycloheximide (CHX) was added for the indicated time prior to lysis. Western blotting is shown as a result. (**D**) Degradation by Flag-β-Trcp1/2 was determined in an experiment similar to (B). Anti-Flag antibody was used to analyze β-Trcp1/2 levels. (**E**) The Snail1SA-HA mutant was co-transfected with the indicated plasmids and extracts were analyzed by Western blot.

We also determined the effect of other ubiquitin ligases. *Figure R.3D* shows how only Flag-β-Trcp1, and not Flag-β-Trcp2, degrades Snail1-HA. Moreover, to corroborate that FBXL14 acts on non-phosphorylated Snail1, we repeated the degradation assays using the Snail1SA-HA mutant and saw that only FBXL14-Myc, and not Flag-β-Trcp1, effectively down-regulates the levels of unphosphorylated Snail1 (*Figure R.3E*).

Having performed all the degradation assays using exogenous Snail1 (*Figure R.3*) we next wanted to determine if FBXL14 controls endogenous Snail1. For this purpose we used NIH3T3 cells that express high Snail1 levels. We transiently transfected the FBXL14-HA construct and observed a notable decrease in Snail1 protein levels. The effect was impaired when the transfected construct was the ΔF-FBXL14-HA mutant (*Figure R.4A*). Moreover, when we performed immunofluorescence (IF) experiments using the same cell line we detected that FBXL14-HA-transfected cells (marked with arrows) no longer expressed nuclear endogenous Snail1 (*Figure R.4B*, left panel). This contrasted with the transfection of the ΔF mutant which did not modify the levels of Snail1 (middle panel). When we checked the levels of CtBP1, another transcription factor expressed in the nucleus, it was not degraded by FBXL14-HA, indicating the specificity of the E3 ligase in the degradation of Snail1 (*Figure R.4B*, right panel).

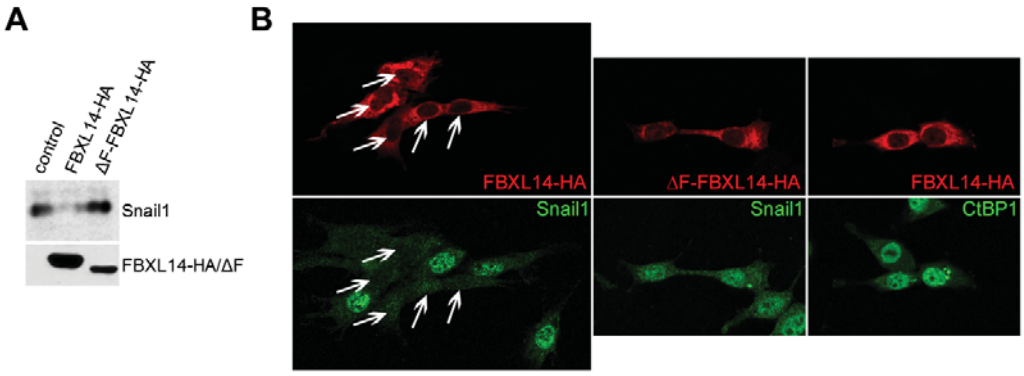

Figure R.4. Snail1 endogenous levels are regulated by FBXL14. (**A** and **B**) NIH3T3 cells were transiently transfected for 48h with FBXL14-HA/ΔF and endogenous Snail1 levels detected by Western blot (A) or immunofluorescence (IF; B). Confocal microscopy was used to visualize the results. A rabbit anti-HA pAb was used to detect FBXL14-HA/ΔF and mouse anti-Snail1 mAb to detect endogenous Snail1. CtBP1 was analyzed as control for specific degradation.

To determine the effect FBXL14 on EMT we transfected FBXL14 in a HT29-M6 clone stably expressing Snail1-HA that exhibits a strong mesenchymal phenotype (*Figure R.5A*, middle panel). We saw that upon stable transfection of the vector cells acquired a more compacted phenotype (right panel) similar to that of control epithelial cells (left panel). When we

tested the protein expression levels by Western blot we observed that Snail1-HA was depleted from cells transfected with FBXL14 and that E-cadherin was re-expressed (*Figure R.5B*). This set of experiments demonstrates that FBXL14 degrades Snail1 and reverses the Snail1-induced mesenchymal phenotype of cells.

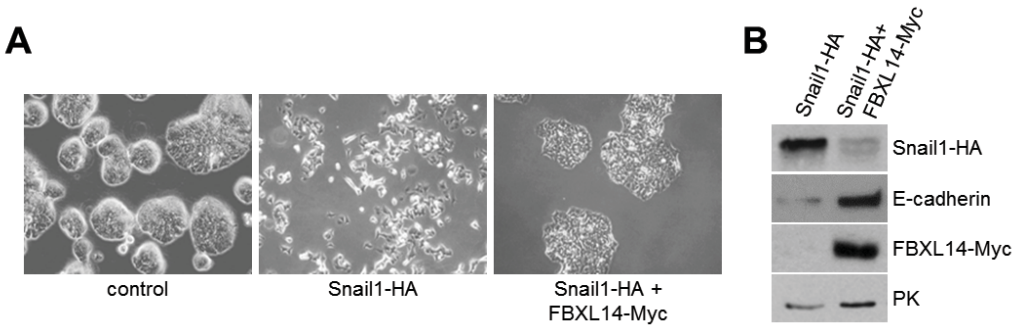

Figure R.5. The expression of FBXL14 can reverse the EMT process. (**A** and **B**) In order to check if FBXL14-Myc could reverse the phenotype of cells that had undergone EMT we used HT29-M6 cells with stable expression of pcDNA3-Snail1-HA (previously described in [41]) and transfected FBXL14-Myc. As seen in (A) cells went from a mesenchymal fibroblastic-like phenotype (middle panel) to a more epithelial compacted phenotype (right panel). Western blot analysis of these cells shows how Snail1-HA levels are completely depleted by the introduction of FBXL14-Myc in this stable clone. E-cadherin levels were analyzed as a control of the re-establishment of adherens junctions.

R.1.4. FBXL14 requires the N-terminal domain of Snail1 for degradation

To determine which domain of the Snail1 protein is sensitive to the degradation mediated by FBXL14 we co-transfected Green Fluorescent Protein (GFP) fusion proteins containing the Snail1 N-terminal (aa 1–151) or C-terminal (aa 152–264) domains together with FBXL14 (*Figure R.6A*). GFP-Snail1CT protein levels remained unaffected by co-transfection of FBXL14. However, a notable decrease in GFP-Snail1NT levels was detected in FBXL14 transfected cells, in the presence or absence of CHX (*Figure R.6A*). To further characterize the region needed for degradation by FBXL14 we co-transfected N-terminal deletion mutants with the ubiquitin ligase. *Figure R.6B* shows a schematic diagram of the constructs used. The construct lacking the P-S rich region (Δ90–120) was still very sensitive to degradation, reinforcing the idea that the β-Trcp1 destruction motif is not needed for the effect of FBXL14 upon Snail1. The effect was also strong on mutants lacking the first 82 or 90 aa; however, the partial removal of the NES (last 14 aa of the domain) reduced the effect of FBXL14 on Snail1 (*Figure R.6B*). This set of experiments suggests that aa 120–151 are important for the FBXL14-triggered degradation of Snail1 protein.

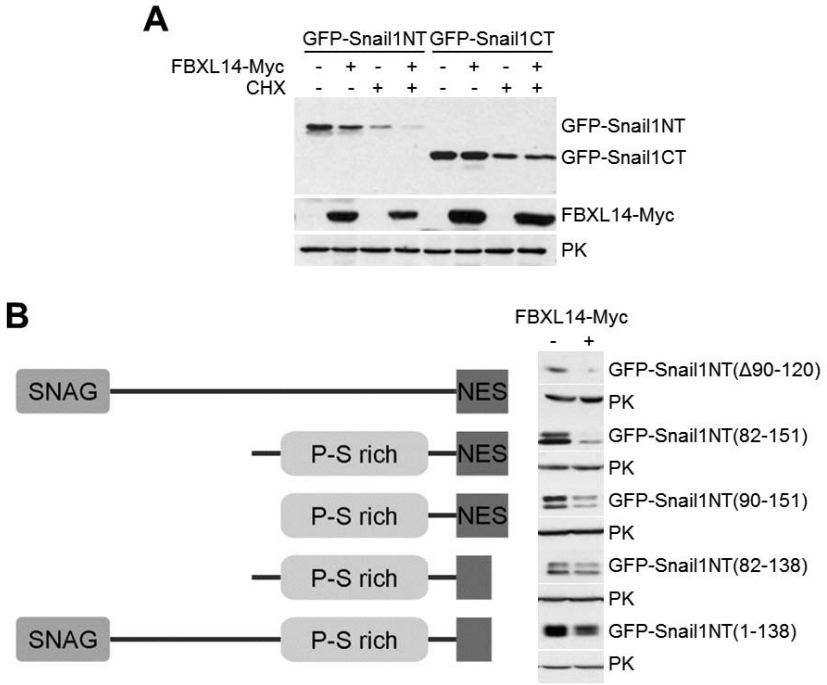

Figure R.6. The N-terminal domain of Snail1 is required for FBXL14-mediated degradation. (**A**) HEK293T cells were transfected with Snail1 constructs containing the N-terminal (NT) or C-terminal (CT) domain fused to GFP and FBXL14-Myc as shown. When indicated cells were treated with CHX for 6h prior to lysis. Western blot analysis was performed using rabbit anti-GFP pAb, anti-Myc and anti-PK as loading control. (**B**) HEK293T cells were transfected with Snail1 NT deletion mutants fused to GFP with or without FBXL14-Myc. The total levels of the Snail1 mutants were determined by analysis of GFP protein. The double band observed in all the mutants except the GFP-Snail1NT(Δ90–120) is due to the phosphorylation state of the P-S rich domain (phosphorylated or unphosphorylated). Both bands were similarly degraded by FBXL14.

R.1.5. Snail1 is ubiquitinated by FBXL14

To find out if FBXL14 stimulates the *in vivo* ubiquitination of Snail1 we performed ubiquitination experiments. *Figure R.7A* shows the IP of Snail1 protein after inhibition of the proteasome. The amount of ubiquitinated Snail1, labeled as Snail1-HA-$(Ub)_n$, is highly increased when FBXL14 is co-transfected, as would be expected for an E3 ubiquitin ligase targeting a protein. Despite the fact that Snail1 levels are equal in lysates of cells expressing or not FBXL14 due to the addition of MG132, the amount of posttranslationaly modified Snail1 was highly increased by the presence of FBXL14.

Similarly, when HIS-tagged ubiquitin was co-transfected with Snail1, FBXL14 or the ΔF mutant a similar result was observed (*Figure R.7B*). In this case all ubiquitinated proteins were purified through a Nickel column

(Ni-NTA), and only in the presence of FBXL14 and when the proteasome was blocked to preserve the ubiquitin chains, a ladder of ubiquitinated Snail1 was detected. The observed ubiquitin chains were a mix of mono- and polyubiquitinated forms. To corroborate the results obtained with wt ubiquitin we used the ubiquitin mutant UbiK7R, which bears mutations of all its lysines to arginines (*Figure R.7B*, right panel), and does not support

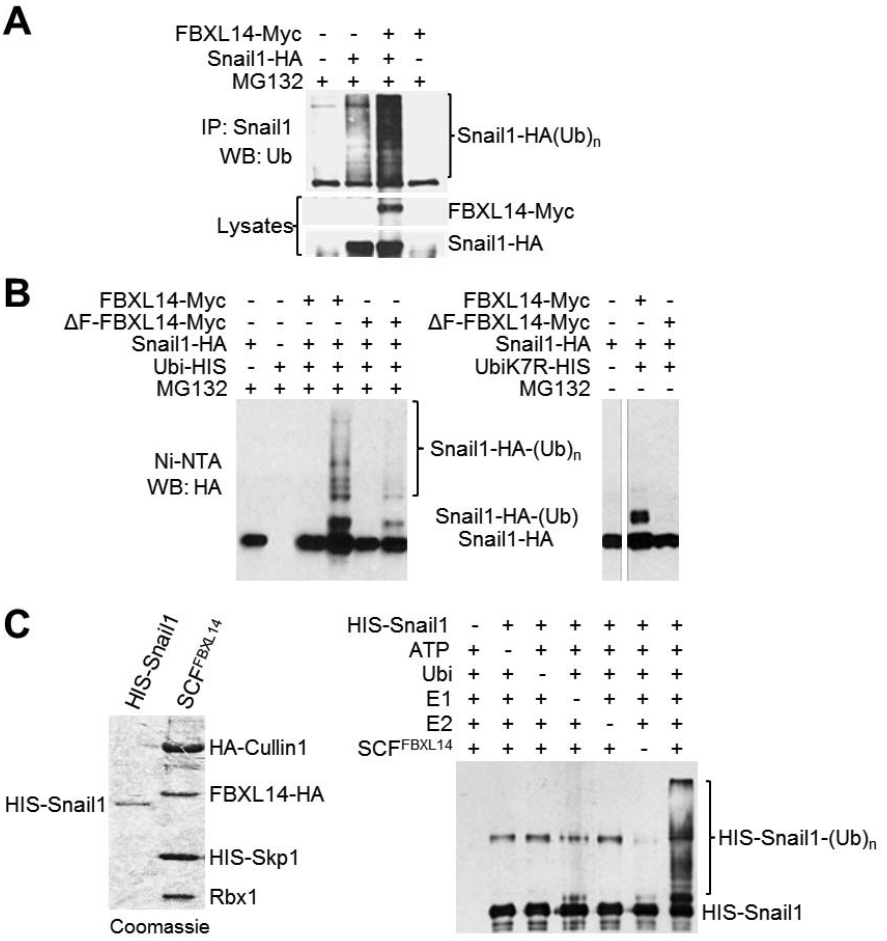

Figure R.7. Snail1 is ubiquitinated by FBXL14. (**A**) HEK293T cells were transfected with Snail1-HA and FBXL14-Myc for 24h and treated with 50 μM MG132 for 6h. Mouse anti-Snail1 mAb was used in denaturing conditions to IP all forms of Snail1 protein. Polyubiquitinated Snail1 (Snail1-HA-$(Ub)_n$) was detected using goat anti-ubiquitin pAb. The levels of Snail1-HA and FBXL14-Myc in the lysates was analyzed with anti-HA and anti-Myc antibodies, respectively. (**B**) HEK293T cells were transfected with the indicated plasmids and treated (left panel) or not (right panel) with MG132. Ni-NTA beads were used to pull down ubiquitinated proteins that were detected with anti-HA antibody. Note that in the right panel a ubiquitin construct bearing mutations in all the lysines (K7RUbi) was used and was unable to elongate ubiquitin chains showing only a discrete band over the non-modified form of Snail1. (**C**) Left panel: Coomassie staining of a polyacrylamide gel with the purified proteins obtained from infected Sf9 cells for *in vitro* ubiquitination assays (HIS-Snail1 and SCF^{FBXL14} complex, respectively). Right panel: Western blot analysis of *in vitro* ubiquitination reactions with the purified proteins of the left panel. E1, E2 and ubiquitin (Ubi) were commercial.

proteasome degradation as it is unable to elongate ubiquitin chains. This is due to the fact that modified proteins can only incorporate a single ubiquitin molecule in each lysine that is modified [182]. Again, the modification of Snail1, which was detected as a single band over the non-modified protein, was only observed in the presence of FBXL14 but not with the ΔF mutant (*Figure R.7B*, right panel).

In order to confirm that the ubiquitination of Snail1 mediated by FBXL14 is direct we set up an *in vitro* system in which we used baculovirus-infected Sf9 cells to produce recombinant protein and purified it using Ni-NTA affinity chromatography. HIS-Snail1 was purified alone and the SCF^{FBXL14} complex was isolated by infecting all the components (HA-Cullin1, FBXL14-HA, HIS-Skp1 and Rbx1; *Figure R.7C*, left panel) and purifying it through the binding of HIS-Skp1 to Ni-NTA agarose beads. To carry out *in vitro* ubiquitination reactions commercial E1 enzyme UBE1, E2 enzyme UbcH5c, ubiquitin and ATP were mixed with purified SCF^{FBXL14} and HIS-Snail1. The elongation of the Snail1 ubiquitination ladder was only achieved when all the components needed for the reaction were added (*Figure R.7C*).

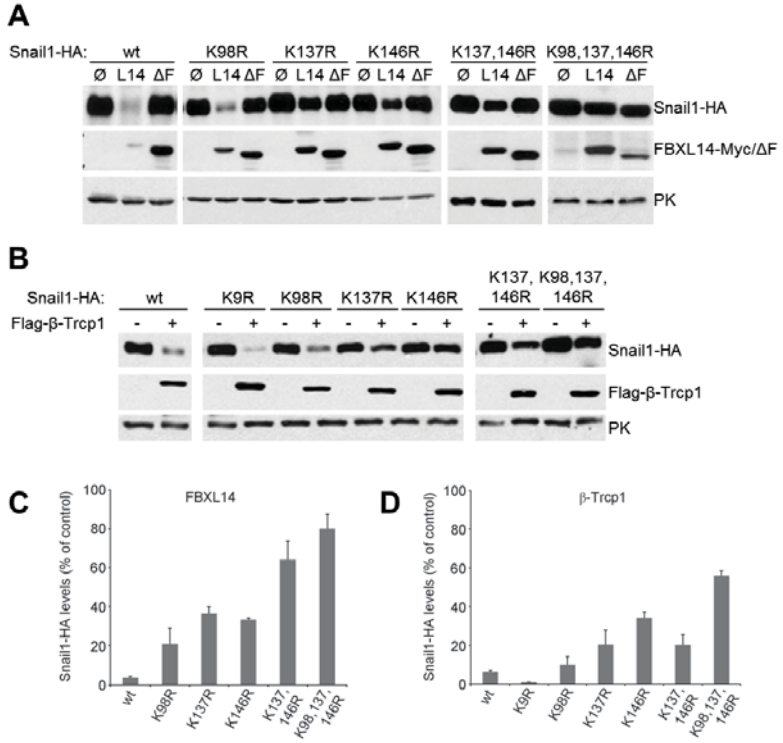

Figure R.8. The mutation of different lysines affects the degradation of Snail1 by FBXL14 and β-Trcp1. (**A** and **B**) The lysines that were found to be putatively ubiquitinated in Snail1 were mutated to arginines and the mutants were transfected for 24h together with FBXL14, the ΔF mutant (A) or β-Trcp1 (B), using 0.2 μg of the Snail1 plasmid and 1.2 μg of the control or ubiquitin ligase plasmid. (**C** and **D**) The quantification of Snail1-HA levels of three independent experiments ± the standard deviation (s.d.) are represented in panels (C) and (D), corresponding to (A) and (B), respectively.

R.1.6. Lysines K98, 137 and 148 are important for FBXL14 ubiquitination of Snail1

We wanted to analyze the lysines that participate in the ubiquitination of Snail1. We found that the N-terminal domain of Snail1, which is important for the FBXL14-mediated degradation of the protein (*Figure R.6*), contains five conserved lysines: K9, K16, K98, K137 and K146. Lysines 137 and 146 are contained in the sequence that was characterized by the N-terminal deletion mutants (aa 120–151) as being responsive to the action of FBXL14. Mutation of lysines K9 and K16 did not affect protein stability (data not shown). The mutation of lysine K98 to arginine (K98R) alone did not change the sensitivity of Snail1 to FBXL14 (*Figure R.8A* and *C*). The mutation of K137 or K146, or the double mutant, partially decreased the degradation rate of Snail1 when exposed to FBXL14. Nevertheless, the mutation of both lysines was not enough to abolish degradation by FBXL14. We only accomplished impaired down-regulation of Snail1 levels by FBXL14 by replacing lysines 98, 137 and 146 by arginines (*Figure R.8A* and *C*). This result suggests that the three lysines are participating in the degradation of Snail1 by FBXL14.

Since the lysines ubiquitinated by β-Trcp1 have not yet been described we decided to carry out a similar experiment as in *Figure R.8A* using β-Trcp1 to

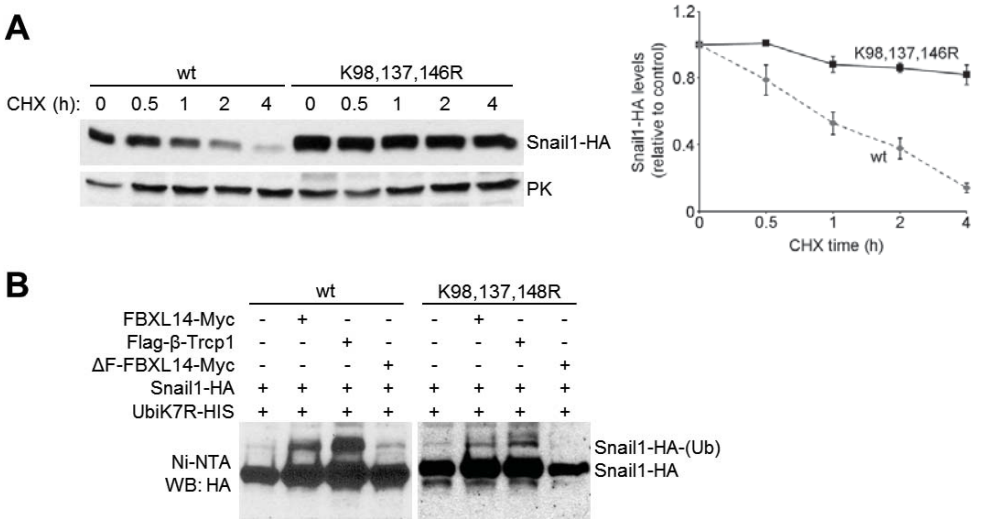

Figure R.9. The Snail1 mutant K98, 137, 146R is resistant to degradation and ubiquitination. (**A**) Determination of the degradation kinetics of the wt and K98, 137, 148R Snail1-HA constructs through the addition of CHX. The left panel shows a representative degradation assay and the right panel the densitometric analysis of three independent experiments ± the s.d. (**B**) Ubiquitination of the K98, 137, 146R Snail1 mutant was determined after the transfection of the indicated plasmids as in *Figure R.7B*. The ubiquitination of Snail1 was analyzed by Western blot after Ni-NTA affinity purification of the samples with anti-HA antibody.

degrade Snail1 and the lysine mutants. The lysines that conferred Snail1 with resistance against β-Trcp1 degradation were the same as for FBXL14 (*Figure R.8B* and *D*). To further confirm that the mutation of these lysines presents Snail1 with higher stability we submitted cells transfected with either the wt or K98, 137, 146R Snail1 constructs to a CHX time-course (*Figure R.9A*). In accordance to our previous results the stability of the mutant was higher than the wt with over 80% of the protein remaining after 4h of CHX. The study of the triple lysine mutant of Snail1 led us to also examine the ubiquitination capability of the triple mutant. *Figure R.9B* shows that this mutant presents lower ubiquitination efficacy by both FBXL14 and β-Trcp1, as expected due to its degradation resistance.

R.1.7. Knockdown of FBXL14 stabilizes Snail1 protein

Since the levels of *FBXL14* messenger RNA (mRNA) have not been studied in mammalian cell models we decided to analyze them in a range of cell lines. We found FBXL14 is expressed to a similar extent in all the cell lines analyzed (*Figure R.10*). We could not study the protein levels since no antibodies are available.

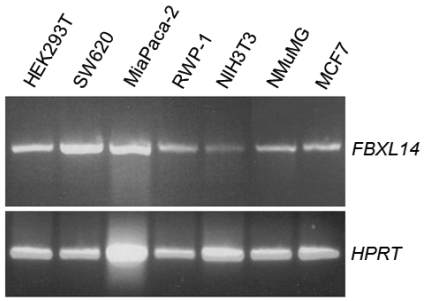

Figure R.10. *FBXL14* mRNA is expressed in all the cell lines studied. The levels of *FBXL14* mRNA were analyzed in the indicated cell lines by semi-quantitative RT-PCR. *HPRT* levels were determined as loading control.

To analyze if Snail1 levels were sensitive to the depletion of endogenous *FBXL14* we designed three different short hairpin RNAs (shRNAs) to specifically knock down the ubiquitin ligase. We tested these constructs using the co-transfection of FBXL14-Myc and the shRNAs in a transient manner, and obtained efficient down-regulation with sh FBXL14(1), sh FBXL14(2) and a combination of the two. sh FBXL14(3) did not affect FBXL14 protein levels (*Figure R.11A*). We next used the combination of the two shRNAs positive for knock down of FBXL14 in HEK293T cells transiently transfected with Snail1-HA and checked the stability of the target protein through a CHX time-course (*Figure R.11B*). When FBXL14 was depleted the stability of Snail1 was greatly increased. The quantification of the remaining protein indicates that Snail1-HA protein levels remained

stable for up to 2h after the addition of CHX in the absence of FBXL14 (*Figure R.11B*).

To check if this effect was also occurring at endogenous Snail1 levels we stably transfected SW620 and NMuMG cell lines with the shRNA against FBXL14 and obtained a clear accumulation in Snail1 protein. The mRNA levels of *FBXL14* were analyzed by semi-quantitative RT-PCR and were detected to be strongly down-regulated by the shRNA, as expected for a knock down condition (*Figure R.11C*). These results indicate that the absence of FBXL14 protein induces the stabilization of Snail1.

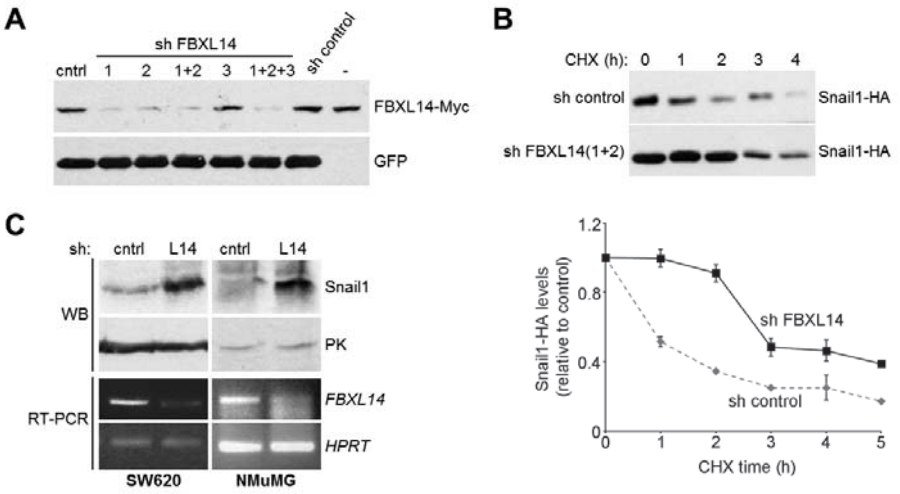

Figure R.11. FBXL14 inhibition increases Snail1 protein stability. (**A**) HEK293T cells were transfected with FBXL14-Myc and different combinations of short hairpin RNAs (shRNAs) cloned into pSUPER-Neo-IRES-GFP against FBXL14 or a scrambled control (sh control). Expression of exogenous FBXL14 protein was determined by Western blot with anti-Myc after 48h of transfection and GFP levels analyzed as transfection control. (**B**) The top panel shows a Western blot of HEK293T cells transfected for 48h with sh control or sh FBXL14(1+2), the combination which yielded the best results in (A). Cells were lysed after the addition of CHX at the indicated time points. A densitometric analysis of three independent experiments ± the s.d. was performed and the results are shown in the bottom panel. (**C**) SW620 and NMuMG cells were stably transfected with sh control or sh FBXL14 and Snail1 protein levels analyzed by Western blot. The down-regulation of *FBXL14* was verified by semi-quantitative RT-PCR. The levels of PK and *HPRT* were determined as loading controls for Western blot and RT-PCR, respectively.

R.1.8. *FBXL14* is down-regulated during hypoxia

In order to find a physiological role for FBXL14 we took advantage of two models of EMT widely used in our laboratory: hypoxia (1% oxygen atmosphere) and TGF-β_1 treatment. *Figure R.12A* shows the expression of various proteins after the two treatments in NMuMG and MCF7 cell lines. As expected, endogenous Snail1 protein levels were up-regulated with both treatments but only TGF-β_1 increased *SNAIL1* mRNA. E-cadherin was

down-regulated in both conditions although the effect was less drastic with hypoxia than by TGF-β_1 treatment. Nuclear HIF-1α protein was stabilized in hypoxia and this increase corresponded to a substantial decrease in *FBXL14* mRNA levels (*Figure R.12A*). The marked down-regulation of *FBXL14* in a 1% oxygen atmosphere led us to think that the regulation of this ligase may play a role in the protein stability of Snail1 under this particular stress condition.

To confirm that Snail1 protein stability was altered during hypoxia we co-transfected NMuMG and MCF7 cells with Snail1-HA and GFP as a transfection control, to ensure hypoxia was not affecting the transfection efficiency. Western blot analysis showed that Snail1 exogenous protein was expressed at least two-fold more in both cell lines under hypoxic conditions (*Figure R.12B* and *C*). This suggests that Snail1 protein gains stability

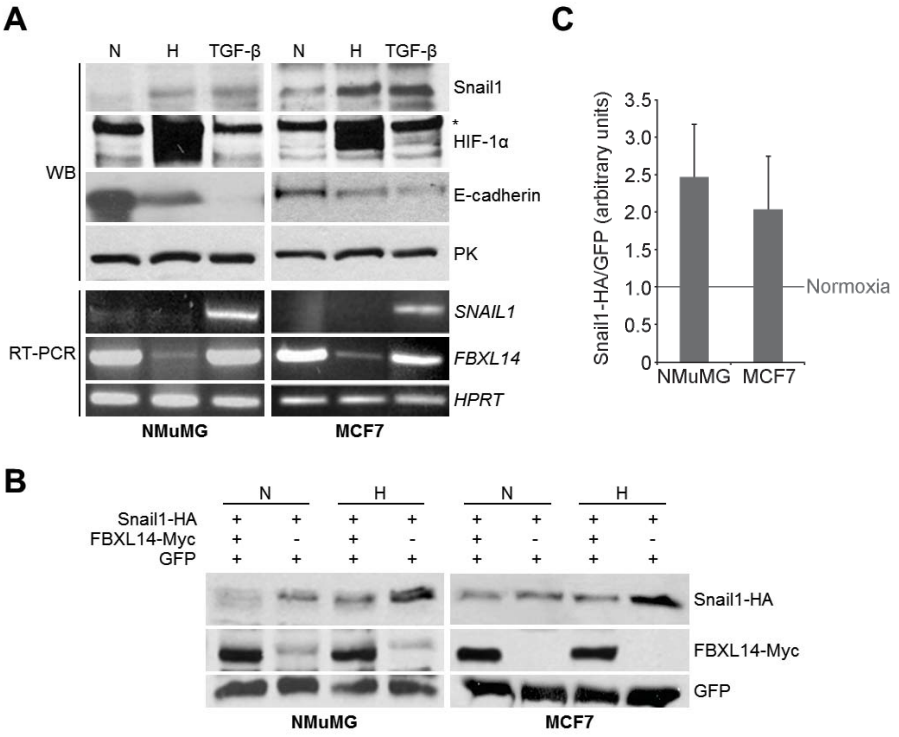

Figure R.12. *FBXL14* is down-regulated during hypoxia. (**A**) NMuMG (left) and MCF7 (right) cell lines were cultured in normoxia (N), hypoxia (H) or 5 ng/ml TGF-β_1 for 72h. Protein analysis was carried out by Western blot with anti-Snail1 and anti-E-cadherin antibodies. HIF-1α levels were analyzed in nuclear extracts as hypoxia control and PK as loading control. The mRNA levels of *SNAIL1* and *FBXL14* were analyzed by semi-quantitative RT-PCR. *HPRT* was used as loading control. (**B**) NMuMG (left) and MCF7 (right) cell lines were transfected where indicated with Snail1-HA, FBXL14-Myc and GFP as transfection control and cultured under N or H for 72h. Snail1-HA were determined by Western blot and compared to those of the normalization control GFP. (**C**) Three independent experiments carried out as in (B) were quantified and the relative Snail1-HA/GFP values calculated ± s.d. The bars show the hypoxic ratio of Snail1-HA/GFP when the normoxic ratio is brought to one.

in hypoxia. When FBXL14 was co-transfected in cells submitted to low oxygen conditions, Snail1 was not stabilized. This further indicates that the reinstatement of FBXL14 levels stimulates Snail1 degradation and suggests that the regulation of FBXL14 in hypoxia is mainly at the transcriptional level.

R.1.9. Hypoxia-induced down-regulation of *FBXL14* is associated with *TWIST1* expression

Twist1 is known to be directly regulated by HIF-1α through its HRE (described in more detail in the Introduction) [117] and therefore up-regulated in hypoxia. For this reason we checked the protein levels of Twist1 (*Figure R.13A*) in normoxia and hypoxia in NMuMG and SW620 cell lines, and detected an up-regulation of the protein concomitant with the increase in HIF-1α levels. Again, Snail1 protein levels were increased while the mRNA remained constant, and *FBXL14* was greatly down-regulated.

To evaluate if Twist1 is required for *FBXL14* down-regulation and Snail1 stabilization we knocked down Twist1 using shRNAs. In these conditions, Snail1 protein was no longer stabilized in hypoxia. The absence of Twist1 also inhibited the down-modulation of *FBXL14*. To check if this was the main pathway activated in hypoxia we determined the protein levels of GSK-3β/β-Trcp1 by Western blot and found that this pathway remained unchanged in NMuMG cells. However, in SW620, an increase in inactive GSK-3β (phosphorylated GSK-3β on serine 9; P-Ser9-GSK-3β) was detected in hypoxia, as well as an increase in β-Trcp1 levels in the same conditions, an up-regulation that was accentuated in the absence of Twist1 (*Figure R.13A*). Hence, the down-regulation of FBXL14 seems to be the preferred pathway to increase Snail1 protein stability in NMuMG cells while in SW620 there is evidence of a mixed mechanism since the two degradation pathways of Snail1 are inactivated in hypoxia.

To validate that Twist1 is directly acting on *FBXL14* levels we decided to transiently transfect Twist1 in three cell lines (RWP-1, MCF7 and NMuMG) as an alternative way of up-regulating the protein. We found that, in all the cases, *FBXL14* levels were greatly down-regulated (*Figure R.13B*). These results suggest there is a direct association between Twist1 expression in hypoxia and down-regulation of *FBXL14* levels.

We analyzed if *FBXL14* down-regulation was detected in pathological conditions of hypoxia in collaboration with Dr. Félix Bonilla in Hospital Puerta del Hierro (Madrid). To this aim, we determined the expression of *FBXL14* and *CA9* (Carbonic Anhydrase 9), a marker of hypoxia [183], in a set of 33 human colon adenocarcinomas. *CA9* was not detected in normal

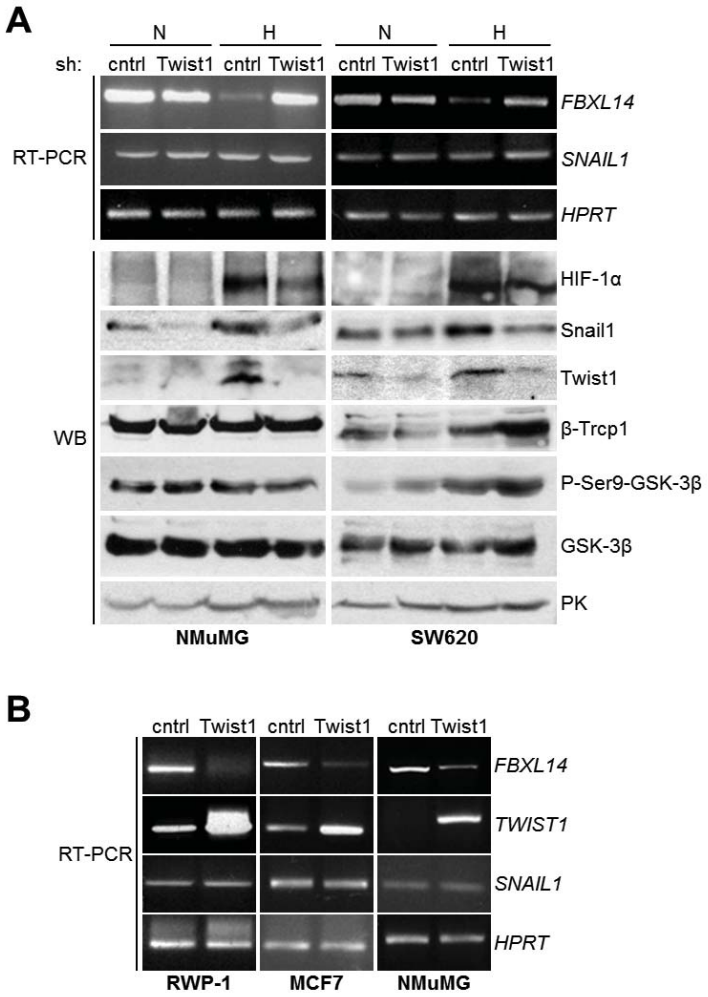

Figure R.13. Hypoxia down-regulates *FBXL14* levels which are directly controlled by Twist1. (A) Twist1 was stably down-regulated using shRNA infection in NMuMG (left) and SW620 (right) cells. These cells were cultured under normoxic (N) or hypoxic (H) conditions for 48h and mRNA levels of *FBXL14* and *SNAIL1* analyzed by semi-quantitative RT-PCR. The indicated proteins were detected by Western blot. *HPRT* and PK were the loading controls for RT-PCR and Western blot, respectively. (B) RWP-1, MCF7 and NMuMG cells were transiently transfected with Twist1 or a control vector (cntrl) for 48h and *FBXL14*, *TWIST1* and *SNAIL1* mRNA levels analyzed by RT-PCR. *HPRT* was used as loading control.

colon mucosa but was observed in 30 tumor samples. *FBXL14* was decreased in 25 tumor samples with respect to normal tissue. A statistical inverse correlation was observed between the expression of *FBXL14* and *CA9* (r=0.43, p=0.013; *Figure R.14A*). A correlation was also established between the presence and absence of *TWIST1* in these tumors. When *TWIST1* is present there is a down-regulation of *FBXL14* (geometric average 0.3 in *TWIST1*-positive cases *versus* 0.81 in negative *TWIST1* samples, p=0.046, analysis of variance). Expression of *TWIST1* also correlates with the up-regulation of *CA9* (geometric average 1.83 in cases with *TWIST1* presence *versus* 0.09 when *TWIST1* is not detected, p=0.012, analysis of variance;

Figure R.14B). Altogether these results indicate that hypoxia-induced down-regulation of *FBXL14* mRNA is associated with *TWIST1* expression both in cell lines and in human tumor samples.

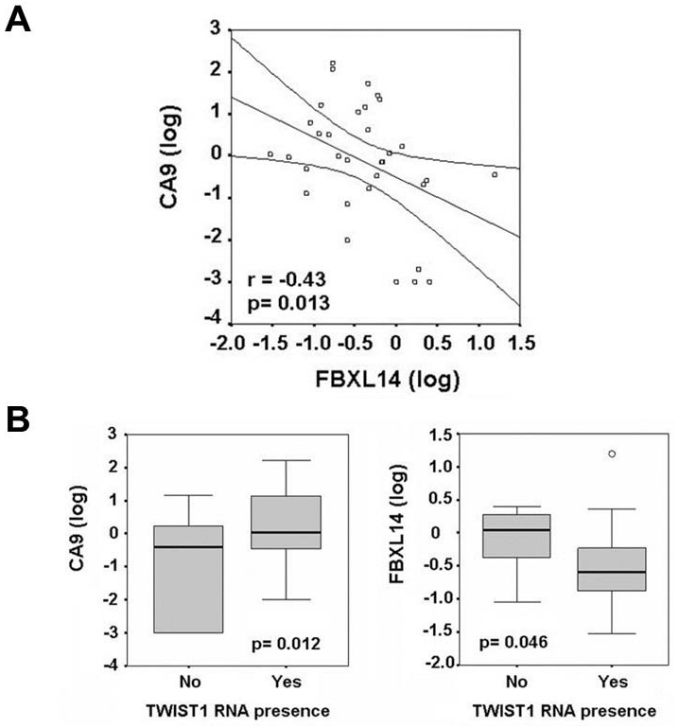

Figure R.14. *FBXL14* is down-regulated in hypoxic human tumors and is associated with *TWIST1* expression. (**A**) Expression of *CA9* (Carbonic Anhydrase 9), a marker of hypoxia, and *FBXL14* shows an inverse correlation in human tumors. The expression of the different transcripts was performed by quantitative RT-PCR. The result is the Pearson correlation coefficient between *CA9* (y-axis) and *FBXL14* (x-axis) expression. (**B**) Box plots depicting the relationship between the presence or absence of *TWIST1* in tumor tissues and *CA9* (left) or *FBXL14* (right) mRNA levels. Details of the statistical analysis are provided in the Materials & Methods section (*MM.7*).

R.1.10. *FBXL14* has a complex transcript regulation mechanism

To complete the work carried out with FBXL14 we decided to investigate the transcript regulation of this F-box ligase. The results presented in this section are preliminary. In the laboratory, a Chromatin immunoprecipitation sequencing (ChIP-Seq) analysis of the regions of endogenous Snail1 binding in SW620 cells suggested that the transcription factor binds to a region spanning nearly the whole first exon of the *FBXL14* transcript (*Figure R.15A*) (unpublished work by Alba Millanes). First we validated the high throughput results obtained for FBXL14 by repeating the experiment in the same cell line (not shown) and using cells expressing Snail1-HA. We observed there was significant enrichment of Snail1 protein in the putative

binding region, both in endogenous (not shown) and ectopic conditions (*Figure R.15B*). As negative control we used the promoter region of *FBXL14*, particularly a region containing a consensus E-box sequence like the three

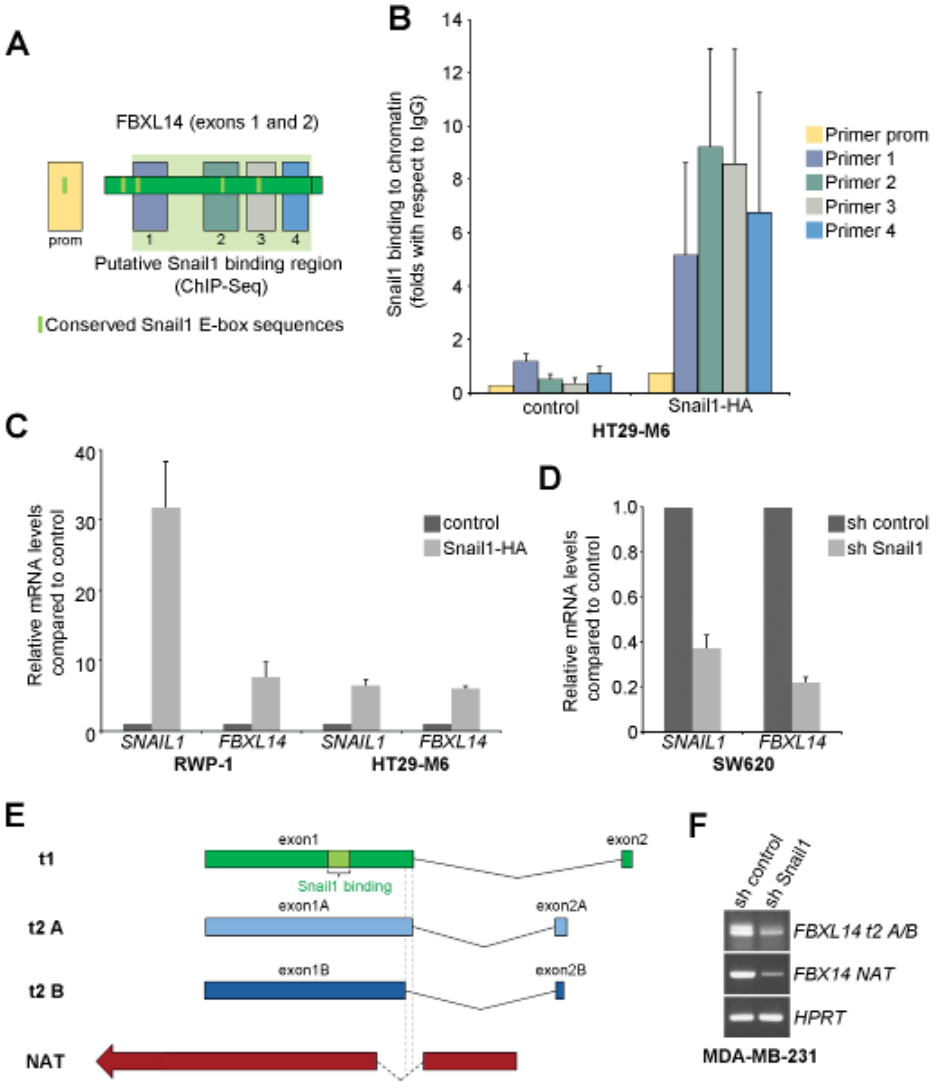

Figure R.15. Snail1 levels modulate *FBXL14* mRNA transcription. (**A**) Schematic representation of the putative Snail1 binding region from a Chromatin Immunoprecipitation Sequencing (ChIP-Seq) performed in the lab in SW620 cells (green region). The primers used for ChIP in (B) are labeled as prom, 1, 2, 3 and 4 and mapped against the *FBXL14* coding transcript (transcript 1). Small light-green rectangles show consensus E-box sequences for Snail1 binding. (**B**) ChIP was performed with Snail1 antibodies in HT29-M6 control or Snail1-HA clones. The result is the mean ± s.d. of three independent experiments. (**C** and **D**) Quantitative RT-PCR analysis of *FBXL14* in cells overexpressing (C) or with knocked down (D) Snail1 protein. Results are the mean ± s.d. of three independent experiments. (**E**) Schematic representation of *FBXL14* RNAs: *t1* is the protein-coding transcript, *t2 A/B* are two alternative transcripts and *NAT* is a long non-coding RNA mapped in the region. (**F**) Semi-quantitative RT-PCR analysis of *t2* and *NAT* of FBXL14 in MDA-MB-231 cells stably infected with sh control or Snail1.

found in the enriched region (2.5 kbp upstream of the transcription start site), and did not present any binding of Snail1.

To see if the levels of *FBXL14* mRNA were modulated by Snail1 we analyzed cells overexpressing or knocked down for Snail1 by RT-PCR. *Figure R.15C* shows that cells transfected with Snail1 had increased levels of *FBXL14* when the transcription factor was overexpressed in both RWP-1 and HT29-M6 cells. The opposite experiment confirmed that down-regulation of Snail1 leads to reduced *FBXL14* mRNA (*Figure R.15D*). The effect exerted by Snail1 on *FBXL14* was not due to Snail1 affecting the activity of the promoter region of *FBXL14* as confirmed by reporter assays (data not shown). These results open many questions. Transcription factors usually bind to the promoter region of genes. The fact that Snail1 is found immunoprecipitating with the chromatin of the coding region of *FBXL14* is, therefore, surprising. We decided to analyze the meaning of these results by looking at publicly available data of the transcripts that have been described to span the first exon of *FBXL14* (Ensembl Genome Browser and NATsDB).

As expected, we found that there is more than one transcript in the region found to be bound by Snail1. Apart from the protein coding transcript (transcript 1; t1) there are two alternative sense transcripts (transcripts 2 A/B; t2 A/B) that most probably code truncated forms of the FBXL14 protein as predicted by *in silico* analysis, although more work should be done in order to confirm this hypothesis. These have a similar first exon, although t2 B starts the splicing to the second exon a few bases (41 bp) before transcript t2A, with a first exon that is identical to that of the protein coding t1 (*Figure R.15E*). The fact that the start of the first exon coincides is what makes us think that t2 transcripts will be protein coding. The second exon, which is short in all the cases, starts a bit over 26 kbp from the last amino acid of exon 1 for t1, and over 5 kbp for both t2 transcripts. The protein sequence yields a truncated protein in both transcripts t2, with stop codons appearing very early in exon 2A and 2B sequences. Moreover, we found there is a long non-coding natural antisense transcript (NAT) that is described to start in the intronic region of all the transcripts and to span over the promoter region of the three *FBXL14* sense transcripts (*Figure R.15E*). We wanted to determine if Snail1 expression modulation also correlated to a differential expression of the other transcripts for *FBXL14*. We down-regulated the levels of the protein by shRNA and analyzed *FBXL14* t2 A/B and NAT levels (*Figure R.15F*). The synergy observed for t1 seemed to be maintained for the other transcripts, indicating that the Snail1 could indeed be directly regulating FBXL14 expression through the binding to the NAT promoter which may help stabilize the coding transcript t1 of *FBXL14*, the only FBXL14 protein we think is functional in cells. The intron length shown in the NAT needs

to be further characterized, hence the hashed lines indicating its length (*Figure R.15E*). These results suggest that there is complex regulation of *FBXL14* transcription and modulation, and indicate that there may be a positive feed-back loop between Snail1 protein levels and *FBXL14* mRNA expression that probably helps maintain Snail1 stability tightly controlled.

R.2. FBXL5 controls Snail1 DNA binding and function

R.2.1. FBXL5 is revealed as a new F-box ubiquitin ligase for Snail1 through a shRNA screening

Preliminary results showed that there are significant amounts of ubiquitinated Snail1 that resides in the nucleus, suggesting there could be additional ubiquitin ligases targeting Snail1. To this aim we carried out a shRNA screening of all the known F-box ubiquitin ligases. The screening was performed simultaneously in two cell lines: SW620, which express high basal Snail1 levels, and MCF7, with low Snail1 expression levels. *Figure R.16* shows the screening results for the SW620 cell line.

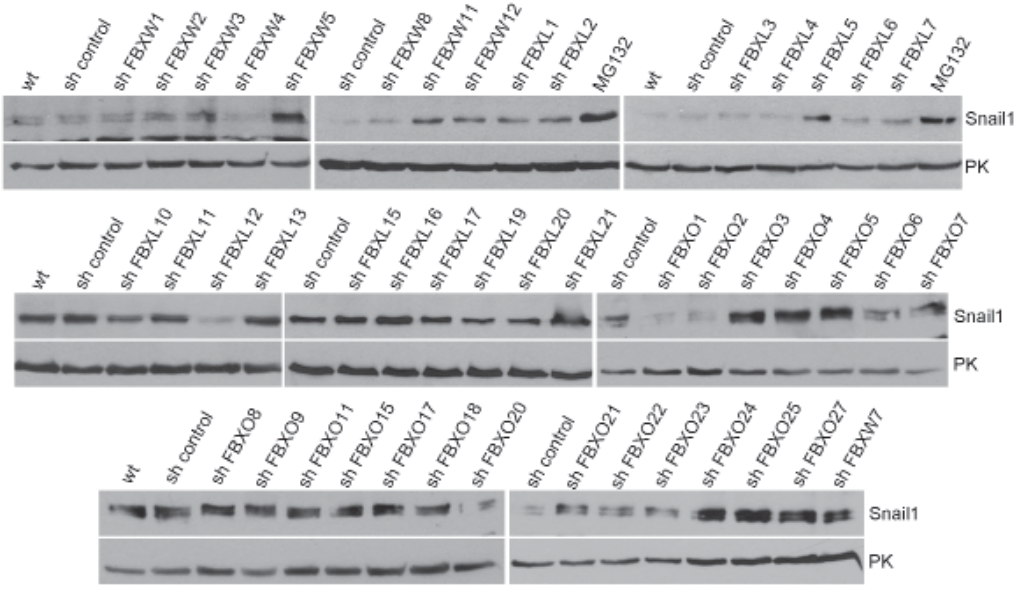

Figure R.16. Screening of F-box ligases targeting Snail1. SW620 cell line was stably infected with shRNAs targeting the indicated F-box ubiquitin ligases. Non-infected cells (wt) and a non-specific shRNA (sh control) were used as basal level controls, and MG132 was used as positive control for Snail1 stabilization. Protein levels for Snail1 were analyzed by Western blot. PK was used as loading control.

The shRNAs that passed the first round of screening were targeting the following F-box ubiquitin ligases: FBXW5, FBXL5, FBXO3, FBXO4, FBXO5, FBXO24, FBXO25 and FBXO27. The other ligases that seem to have an effect of Snail1 in *Figure R.16* were discarded by additional controls carried out in RWP-1 cells (data not shown). To confirm that the effect was directly affecting Snail1 protein stability we stably infected SW620 and MCF7 cells with pBabe-Snail1-HA, which is under the control of a weak promoter and thus expressed at low levels, and transiently transduced the indicated shRNAs before analysis (*Figure R.17*). In SW620 cells there only seemed to be an effect using shRNAs against FBXW5, FBXL5 and FBXO4

(*Figure R.17A*). The stabilization of Snail1-HA was especially strong in the conditions where FBXW5, FBXL5, FBXO24 and FBXO25 were knocked down in the MCF7 cell line (*Figure R.17B*).

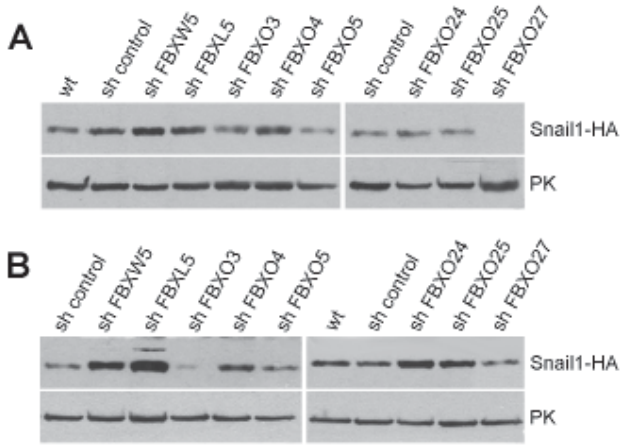

Figure R.17. Second round of shRNA screening. (**A** and **B**) Transient infection of the shRNAs that stabilized Snail1 in the first round of screening was carried out in SW620 (A) and MCF7 (B) cells stably expressing pBabe Snail1-HA. In this case wt is for cells only expressing Snail1-HA and sh control for cells expressing both a non-specific shRNA and Snail1-HA. Exogenous Snail1 levels were analyzed by Western blot.

Before going further into the study of one of the ubiquitin ligases with respect to Snail1 we decided to validate that the results observed in the screening were specific. For this we checked the mRNA levels of the ligases used in the second round of screening in knock down cells of the same ligase compared to sh control conditions (*Figure R.18*). We found that all the shRNAs were down-regulating their target gene by more than 50%, with exception of sh FBXO24 which was reducing this ligase's levels by less than 20%.

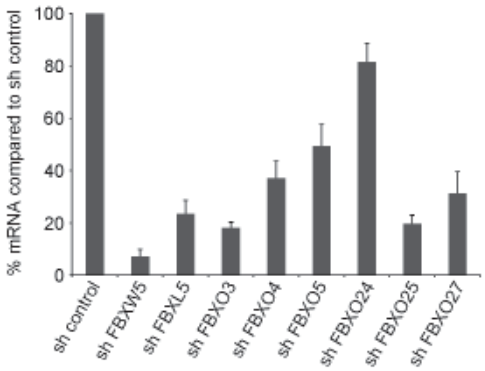

Figure R.18. mRNA levels of knocked down ubiquitin ligases. The mRNA levels of the E3 ligase with which SW620 cells were stably infected (indicated under each bar) were analyzed by quantitative RT-PCR. The results represent three independent experiments ± s.d.

The results obtained from the two rounds of screening pointed at FBXW5 and FBXL5 as putative novel ubiquitin ligases targeting Snail1 for degradation. We started working with both ligases but decided to develop the project with FBXL5 since we found out that it is a nuclear protein (shown later) while FBXW5 is located in the cytoplasm. FBXL5 protein has a hemerythrin domain in its N-terminal part, an F-box domain and six leucine-rich repeats (LRRs) at its C-terminal end. The two substrates that had been described for it were $p120^{Glued}$, a protein important to drive vesicular transport and mitotic spindle organization [184] and Iron regulatory proteins (IRP) 1 and 2, involved in cellular iron homeostasis [185, 186]. The hemerythrin domain of FBXL5 was the first of its kind found in mammals, making FBXL5 a very attractive protein to study since hemerythrin domains in other species have been described to bind iron through di-iron centers in a reversible manner, regulating protein stability in a very dynamic manner. The two studies about

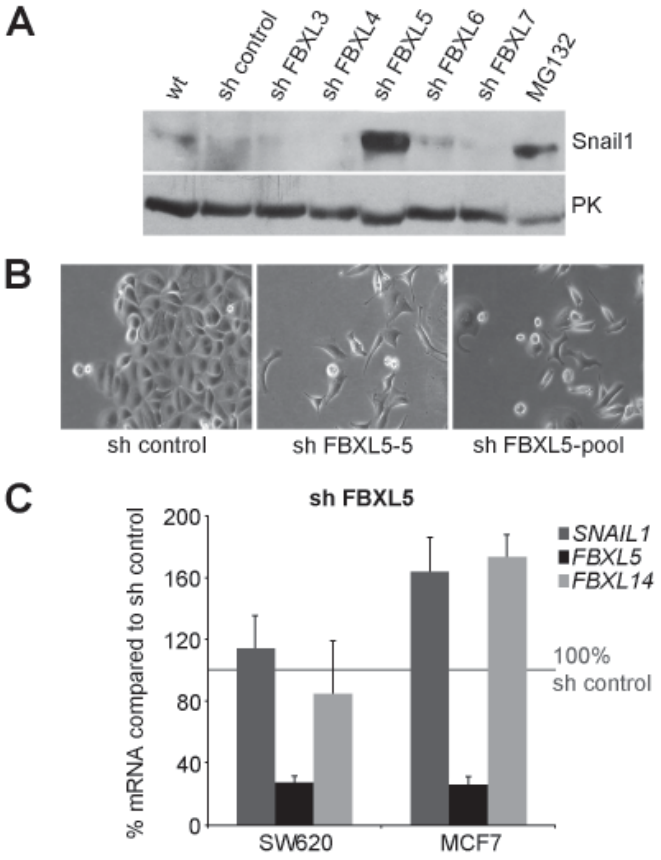

Figure R.19. FBXL5 is a candidate for the degradation of Snail1. (**A**) Part of the first round of shRNA screening in MCF7 cells in which the effect of sh FBXL5 is seen compared to non-infected cells (wt), sh control and MG132 as positive control for Snail1 stabilization. (**B**) Morphology of MCF7 cells under light microscopy after being stably infected with sh control, sh FBXL5-5 or a mix of all the plasmids targeting the FBXL5 sequence (sh FBXL5-pool). (**C**) The levels of *SNAIL1*, *FBXL5* and *FBXL14* mRNA were analyzed in cells stably expressing sh FBXL5 relative to sh control condition. The results are the average of three independent experiments ± s.d.

IRP1 and IRP2 report that FBXL5 is stabilized through the addition of iron and de-stabilized when the metal is removed from cells.

The effect of the shRNA of FBXL5 on Snail1 levels in MCF7 cells was very strong (compare *Figure R.16* and *R.19A*). We had seen during the first round of the screening with MCF7 cells that the levels of Snail1 were up-regulated even higher than those in which the proteasome inhibitor was blocked using MG132. Moreover, the phenotype of cells after infection of sh FBXL5 was switched from epithelial to mesenchymal, with cells presenting a fibroblast-like morphology (*Figure R.19B*). *Figure R.19C* shows the mRNA levels of *SNAIL1* when *FBXL5* levels were down-regulated by 70%. To discard a possible off-side effect due to down-regulation of *FBXL14* we determined its mRNA levels in sh FBXL5 conditions. A slight decrease of about 15% was noted in SW620 cell line whereas in MCF7 cells we detected an increase (*Figure R.19C*). Altogether, the localization and the results showing the notable increase in Snail1 levels obtained through down-regulating FBXL5 in different cell lines prompted us to focus our study on this ubiquitin ligase.

R.2.2. FBXL5 and Snail1 interact through the C-terminal end of Snail1

The action of F-box ubiquitin ligases on a substrate is through direct interaction of both proteins. To determine this interaction we first used the overexpression of tagged Snail1 and FBXL5 in cells in the presence of iron (addition of Ferric Ammonium Citrate; FAC) to stabilize FBXL5 and of the proteasome inhibitor MG132 to avoid Snail1 degradation. We found that Myc-FBXL5 co-immunoprecipitated with Snail1-HA in these cells (*Figure R.20A*). We verified the endogenous interaction in RWP-1 cells also treated with FAC and MG132, and detected association between Snail1 and FBXL5 (*Figure R.20B*).

To prove that the interaction between the two proteins was direct we carried out a pulldown assay with recombinant protein obtained from Sf9 cells and found that Flag-FBXL5 directly associated to GST-Snail1 and not to GST (*Figure R.20C*). To ensure the interaction of FBXL5 was specific for Snail1 and not a general mechanism of action of transcription factors involved in EMT, we performed pulldown analysis using GST and GST-FBXL5 purified from bacteria with cell extracts expressing Snail1, Snail2, Twist1 and Zeb1. Interestingly, both Snail1 and Snail2 were bound by FBXL5.

To map the binding region in Snail1 protein we used GFP-Snail1 deletion mutants comprising the C-terminal (CT) part of Snail1 (GFP-CT: aa 152–264) or the N-terminal (NT) Snail1 (GFP-NT: aa 1–151). Only the CT domain of Snail1 presented FBXL5 binding capacity (*Figure R.21A*), suggesting that the binding of FBXL5 to Snail1 is though the ZnF domain.

GST-FBXL5 also pulled down endogenous Skp1, as would be expected for a correctly folded and active F-box protein (*Figure R.21A*). The interaction with Skp1 was not competed by GFP-Snail1, suggesting that an SCF^{FBXL5}-Snail1 degradation complex may be assembled *in vitro*.

To further map the interaction of the C-terminal part of Snail1 with FBXL5 we determined the contribution of each of the ZnF to the binding by means of deletion mutants. Constructs lacking ZnF4 (aa 236–263) retained full

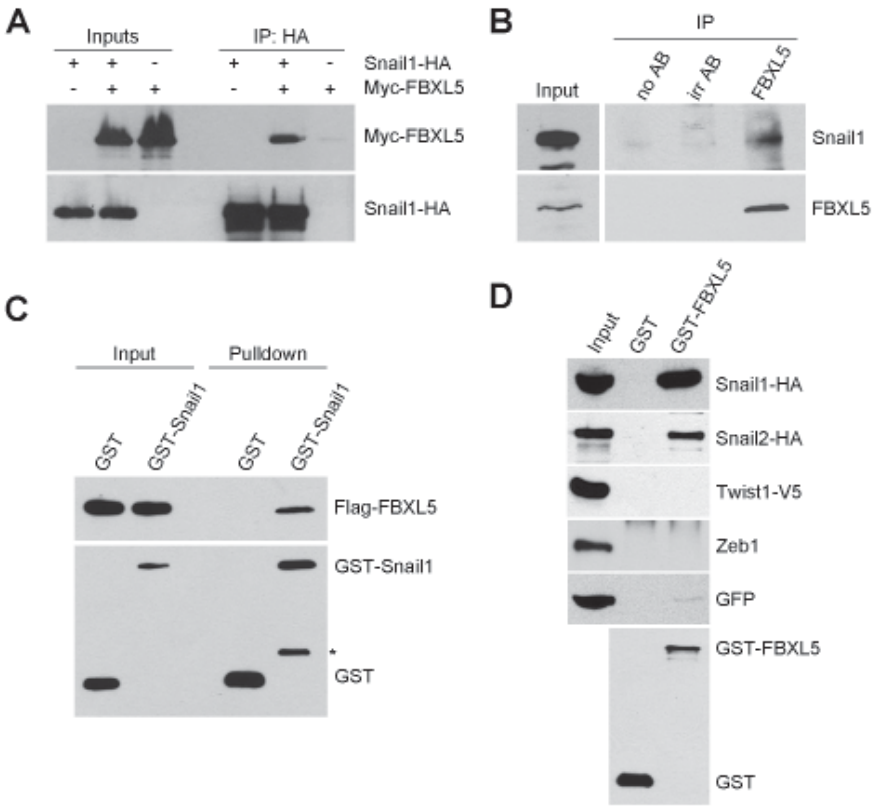

Figure R.20. Snail1 directly interacts with FBXL5. (**A**) HEK293T cells were transfected for 24h with Snail1-HA, Myc-FBXL5 and a control plasmid as indicated. They were treated with 100 μM FAC for 6h and 10 μM MG132 for 5h prior to lysis. Immunoprecipitation (IP) was carried out using rabbit anti-HA pAb and Myc-FBXL5 levels analyzed by Western blot. Snail1-HA levels are shown as IP control. (**B**) Endogenous IP of FBXL5 was carried out in RWP-1 cells treated with 100 μM FAC and 10 μM MG132 for 6h prior to lysis. IP was carried out using rabbit anti-FBXL5 pAb and detection with mouse anti-Snail1 mAb and goat anti-FBXL5 pAb as IP control. no AB means that no antibody was added to the IP, and irr AB stands for irrelevant antibody of the same species as the specific antibody used for IP. (**C**) Pulldown (PD) analysis of the interaction between GST-Snail1 and Flag-FBXL5 using purified proteins from Sf9 insect cells to verify the direct interaction of the two proteins. FBXL5 and Snail1 were detected with anti-Flag and anti-GST antibodies, respectively. The band marked with an asterisk (*) is a degradation band of GST-Snail1 that appears after periods of incubation at room temperature. (**D**) GST or GST-FBXL5 protein purified from bacteria was used to PD the indicated proteins from lysates of HEK293T cells transfected for 48h. GFP was used as a negative control.

binding capacity but when both ZnF4 and ZnF3 (aa 209–235) were deleted the binding was decreased by over 50% (*Figure R.21B* and *C*). When ZnF2 (aa 181–208) was also deleted the association of the two proteins was completely abolished. Other mutant constructs bearing deletions in ZnF1

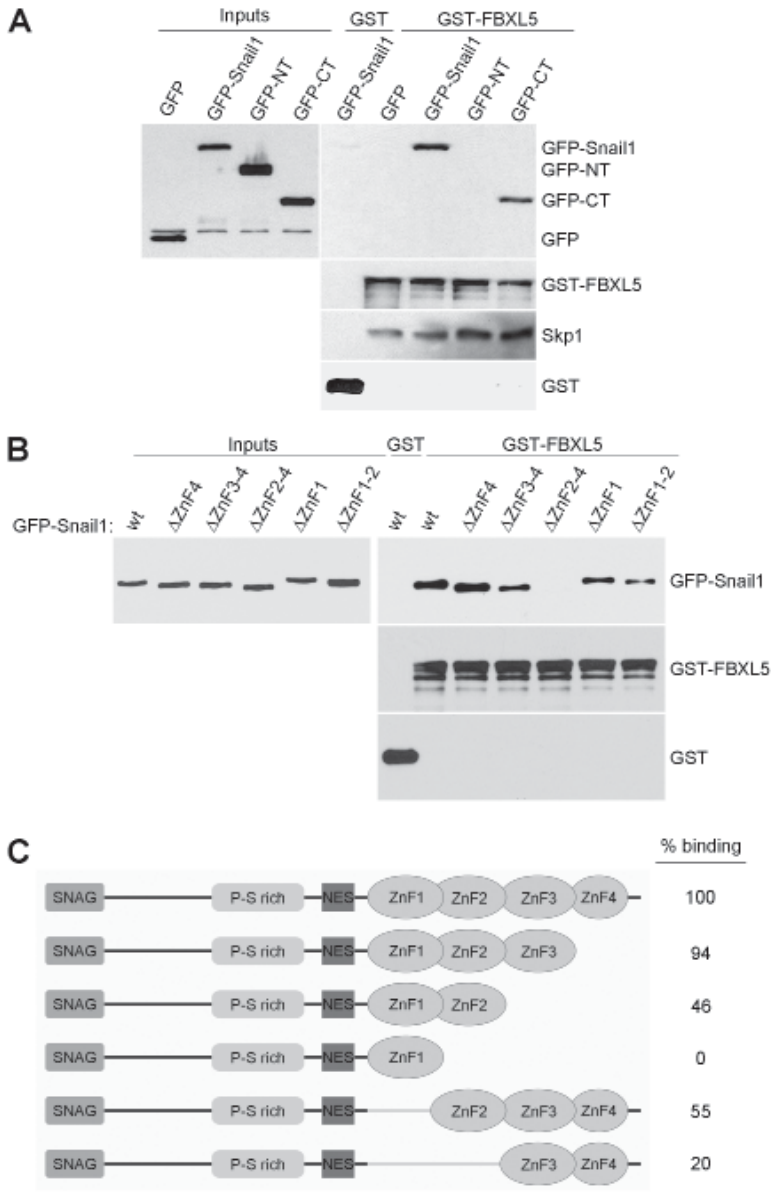

Figure R.21. The C-terminal part of Snail1 is needed for FBXL5 interaction. (**A**) PD analysis with GST or GST-FBXL5 protein purified from BL21 bacteria. Vectors encoding the GFP, GFP-Snail1, GFP-NT and GFP-CT proteins were transfected in HEK293T cells for 48h and extracts were used for PD. The result was analyzed by immunoblotting and Skp1 was a positive control of interaction with GST-FBXL5 to check the functionality of the protein. (**B**) PD analysis similar to (A) in which ZnF deletion mutants were used to map the site of interaction of FBXL5 with the C-terminal part of Snail1. (**C**) Schematic representation of the deletion mutants used for PD analysis to map the site of interaction of Snail1 to FBXL5 (B) and quantification of the percentage binding from three independent experiments.

(aa 150–180) or both ZnF1 and ZnF2 retained a binding of the 55 or 20% of the original full-length construct, respectively. These experiments suggest that the domain with a predominant role in FBXL5 binding is ZnF2 but that ZnF1 and ZnF3 also contribute to maintain this interaction (*Figure R.21B* and *C*).

R.2.3. FBXL5 is a nuclear ubiquitin ligase

Since little is known about the characteristics of FBXL5 we decided to determine its expression in different cells lines. We tested both the protein (*Figure R.22*) and mRNA levels (not shown) and did not find any striking differences between epithelial or mesenchymal cell expression nor a strong correlation between Snail1 and FBXL5 levels (*Figure R.22*).

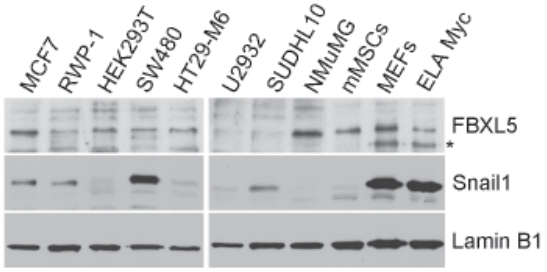

Figure R.22. Expression of FBXL5 in different cell lines. Testing of a series of cell lines to determine the expression of FBXL5 in enriched nuclear extracts using a validated antibody against FBXL5 (goat pAb, see *Figure MM.1* for further details) by Western blot. Snail1 levels were also determined, and Lamin1 was used as loading control. The asterisk (*) indicates an unspecific band detected with the FBXL5 antibody.

Analysis of the localization of FBXL5 by subcellular fractionation of cell lysates indicated that this ubiquitin ligase is mainly found in the nucleus (*Figure R.23A*). In this same analysis the localization of FBXW5, the other ligase found in the shRNA screening to be a potential candidate for Snail1 degradation, was also determined and was found to be cytoplasmic. The other two described Snail1 ubiquitin ligases, FBXL14 (*Figure R.4B*) and β-Trcp1 [83], are cytoplasmic. We also determined that there is strong interaction of Snail1-HA and Myc-FBXL5 in the nucleus of HEK293T cells in the presence of the proteasome inhibitor MG132 (*Figure R.23B*). Stable transfection with the shRNA against FBXL5 in MCF7 and RWP-1 cells (*Figure R.23C* and *D*) showed a down-regulation in nuclear FBXL5 levels. This demonstrated the specificity of the antibody against FBXL5. In the knockdown conditions Snail1 nuclear protein levels were greatly stabilized in both MCF7 and RWP-1 cell lines, further validating the screening performed to find new E3 ligases targeting Snail1 (*Figure R.23C* and *D*).

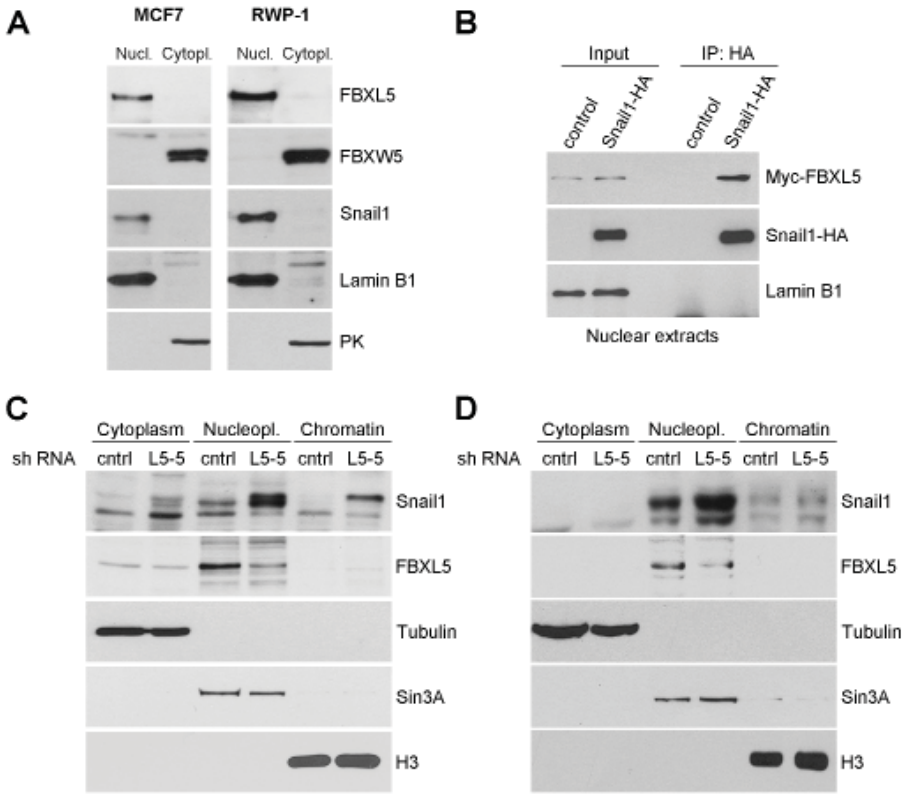

Figure R.23. Nuclear localization of FBXL5 by Western blot. (**A**) The indicated cell lines were sub-fractionated after a 4h treatment with 10 μM MG132. Western blot was used to determine the localization of the indicated proteins. Lamin B1 was used as nuclear fraction control and PK as cytoplasmic control. (**B**) HEK293T cells were transfected with the indicated plasmids for 24h and treated with 100 μM FAC for 6h and 10 μM MG132 for 4h prior to lysis. The cytoplasmic fraction of cells was washed off and the nuclear fraction used to immunoprecipitate Snail1-HA using rabbit anti-HA pAb. Myc-FBXL5 levels were analyzed by Western blot with mouse anti-Myc mAb and Snail1-HA levels with rat anti-HA pAb. Lamin B1 was used as loading control for nuclear extracts. (**C** and **D**) Stably transfected MCF7 (C) or RWP-1 (D) cells with pLKO-GFP sh control or FBXL5-5 vector were analyzed for endogenous FBXL5 (goat pAb) and Snail1 levels. Tubulin was used as cytoplasmic, Sin3A as nucleoplasmic and H3 as chromatin loading control, respectively. These antibodies were also used as controls of correct sub-fractionation of cell extracts.

We also performed immunofluorescence (IF) analysis in both RWP-1 and MCF7 cell lines with two pAb against FBXL5 (*Figure R.24A* and *B*). We found that the localization was mainly nuclear with some protein detected also in the cytosol. This was confirmed in RWP-1 cells (*Figure R.24A*) by the detection of the Myc-FBXL5 ectopic protein using antibodies against the Myc tag. Moreover, staining with the two different anti-FBXL5 pAb in MCF7 cells yielded the same results: there was strong, but not exclusive, nuclear localization of FBXL5 (*Figure R.24B*).

We further characterized the expression of ectopic Myc-FBXL5 and saw that untreated (control) cells expressed mostly nuclear FBXL5 with some cytoplasmic staining; when FAC was added the FBXL5 protein was stabilized, especially in the cytoplasmic compartment (*Figure R.24C*). As expected, when we inhibited nuclear export using Leptomycin B (LMB), FBXL5 was retained in the nucleus. When the proteasome inhibitor MG132 was used cells presented a strong nuclear signal with very little or no cytoplasmic staining.

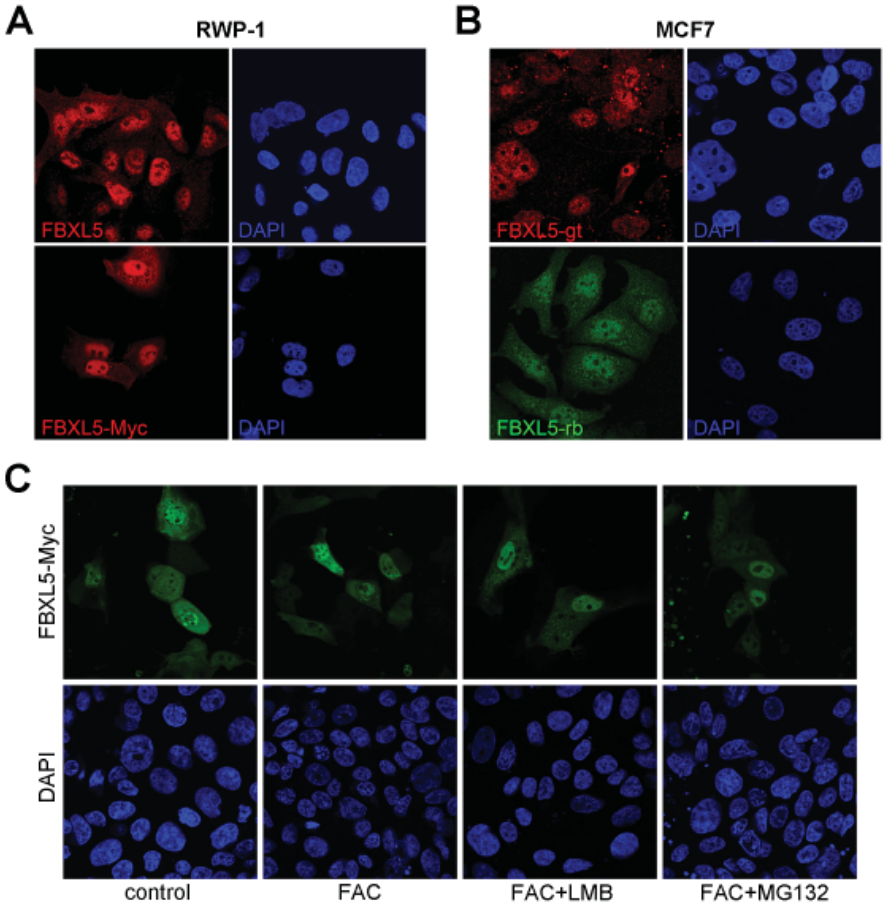

Figure R.24. IF analysis of FBXL5 localization. (**A**) Top panel: RWP-1 cells were stained with goat anti-FBXL5 pAb. Bottom panel: RWP-1 cells transiently transfected with Myc-FBXL5 were stained with mouse anti-Myc mAb. (**B**) MCF7 cells were stained with goat or rabbit anti-FBXL5 pAb. (**C**) MCF7 cells transiently transfected with Myc-FBXL5 (green) were treated with 100 μM FAC for 4h, 5 ng/ml LMB for 2h and 10 μM MG132 for 4h. DAPI (blue) staining was used to identify nuclei in all panels.

R.2.4. FBXL5 causes degradation of Snail1

To determine if FBXL5 can cause the degradation of Snail1 we co-expressed Snail1-HA and Myc-FBXL5 or a control vector and analyzed the stability of the protein by adding CHX. We found that Snail1 protein stability was

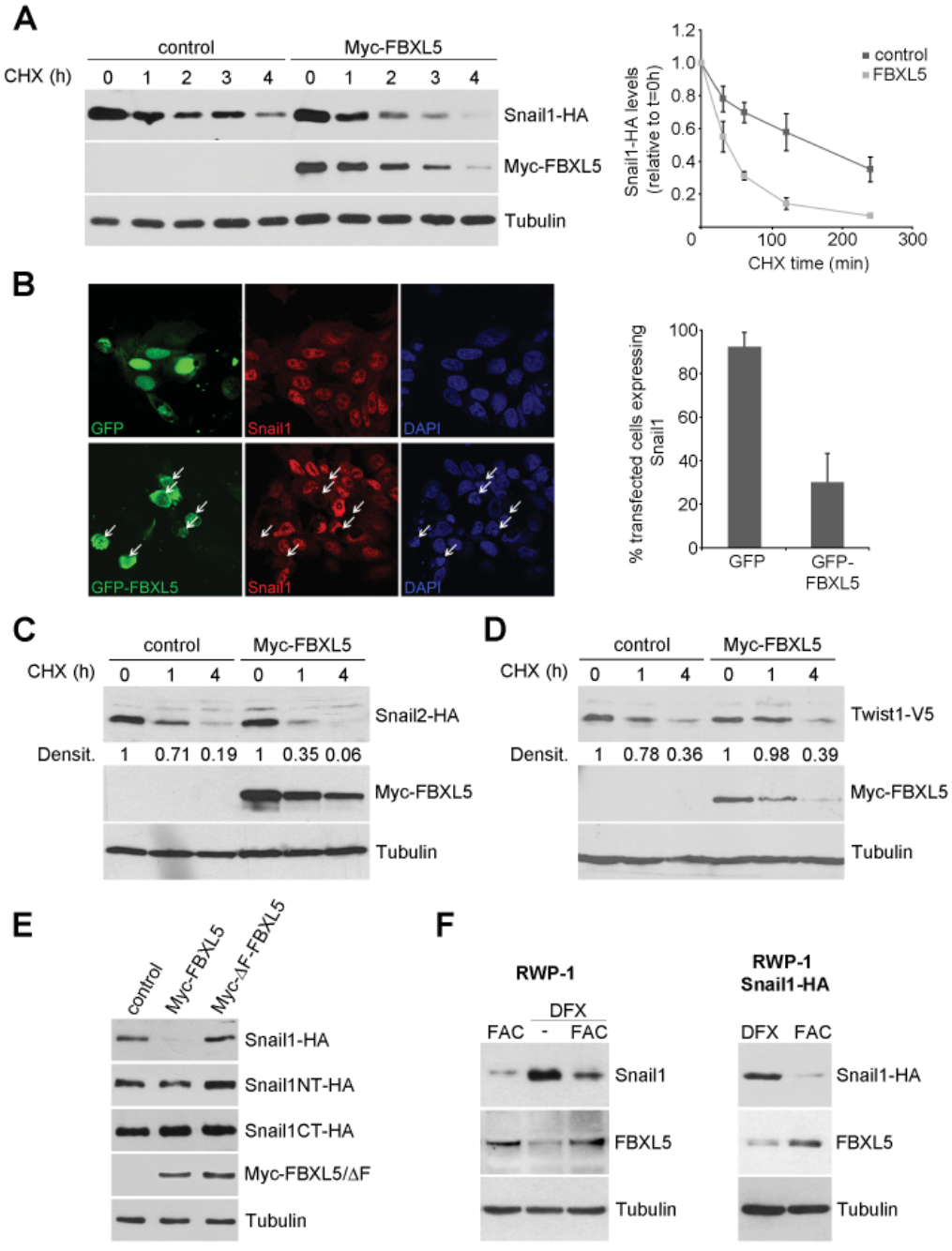

Figure R.25. Snail1 is degraded by FBXL5. (**A**) HEK293T cells were transfected for 24h and lysed after CHX addition. The graph shows the quantification of four independent experiments ± s.d. (**B**) RWP-1 cells were transfected with GFP or GFP-FBXL5 and Snail1 protein expression analyzed by IF. The graph shows the quantification of three independent experiments ± s.d. (**C** and **D**) Degradation experiments as in (A) but using Snail2-HA (C) and Twist1-V5 (D) instead of Snail1-HA. Densitometry of the bands relative to Tubulin levels was performed. (**E**) Different Snail1 constructs were analyzed for degradation with FBXL5 or the ΔF mutant using HEK293T cells transfected for 24h. (**F**) RWP-1 (left) or RWP-1 Snail1-HA (right) cells were treated for 6h with 100 μM FAC, overnight with 100 μM DFX or sequentially with both where indicated. Snail1 and endogenous FBXL5 levels were analyzed by Western blot.

decreased in the presence of FBXL5 (*Figure R.25A*). When we quantified Snail1 protein remaining in cells after 2h of CHX treatment only around 10% of Snail1-HA was present in cells transfected with FBXL5 compared to 60% in control cells (*Figure R.25A*, right panel). We could also detect the degradation of endogenous Snail1 when transfecting RWP-1 cells with GFP-FBXL5 fusion protein and analyzing Snail1 by IF. We found the GFP-FBXL5 protein localized both in the nucleus and the cytoplasm, and most cells expressing this construct were depleted of endogenous Snail1 compared to GFP-transfected cells (*Figure R.25B*). However, around 30% of the cells transfected with GFP-FBXL5 still expressed nuclear Snail1 that was resistant to FBXL5 degradation (*Figure R.25B*, right panel). We also analyzed if FBXL5 degrades Snail2-HA and found that that this is the case (*Figure R.25C*). In agreement with these results, the stability of Twist1 was not affected by FBXL5 overexpression (*Figure R.25D*).

Contrary to what happened with FBXL14, which was able to degrade the N-terminal deletion mutant of Snail1, FBXL5 was not capable of degrading either the Snail1-NT or -CT deletion mutants (*Figure R.25E*). This may indicate that the degron recognized by the ubiquitin ligase spans the two domains or that the domain required for binding and for ubiquitination is not found in the same half of the protein.

FBXL5 levels are modulated by iron, and we wanted to test if this metal also regulates Snail1 levels. To this aim we treated RWP-1 cells with FAC or the iron chelator deferoxamine (DFX) for the indicated times. Indeed we saw that upon iron addition and thus FBXL5 stabilization Snail1 levels were low; however, iron chelation caused Snail1 protein to be highly stabilized (*Figure R.25F*, left panel). When we depleted FBXL5 using DFX and then restored the iron levels with FAC we saw that FBXL5 endogenous levels recovered and Snail1 was degraded. This effect was also achieved when exogenous Snail1 protein was expressed (*Figure R.25F*, right panel). This set of experiments demonstrates that FBXL5 is capable of degrading Snail1, both through its overexpression and stabilization with iron.

R.2.5. FBXL5 ubiquitinates Snail1 *in vivo* and *in vitro*

The next step in determining the ubiquitin ligase activity of FBXL5 was to establish if it ubiquitinates Snail1, and more importantly if it does so in the nucleus. IP of ubiquitinated proteins using nuclear cell extracts clearly showed that FBXL5 ubiquitinates Snail1 in this compartment (*Figure R.26A*). Moreover, it also greatly increased polyubiquitinated Snail1 in total cell extracts (*Figure R.26B*). The use of HIS-tagged ubiquitin further demonstrated an augmented *in vivo* ubiquitination of Snail1 and of the C-terminal deletion mutant by FBXL5 (*Figure R.26C*).

We confirmed that the FBXL5-mediated ubiquitination of Snail1 was direct by setting up an *in vitro* system, similarly to what we did with the FBXL14 F-box protein. We isolated the SCF^{FBXL5} complex by infecting all

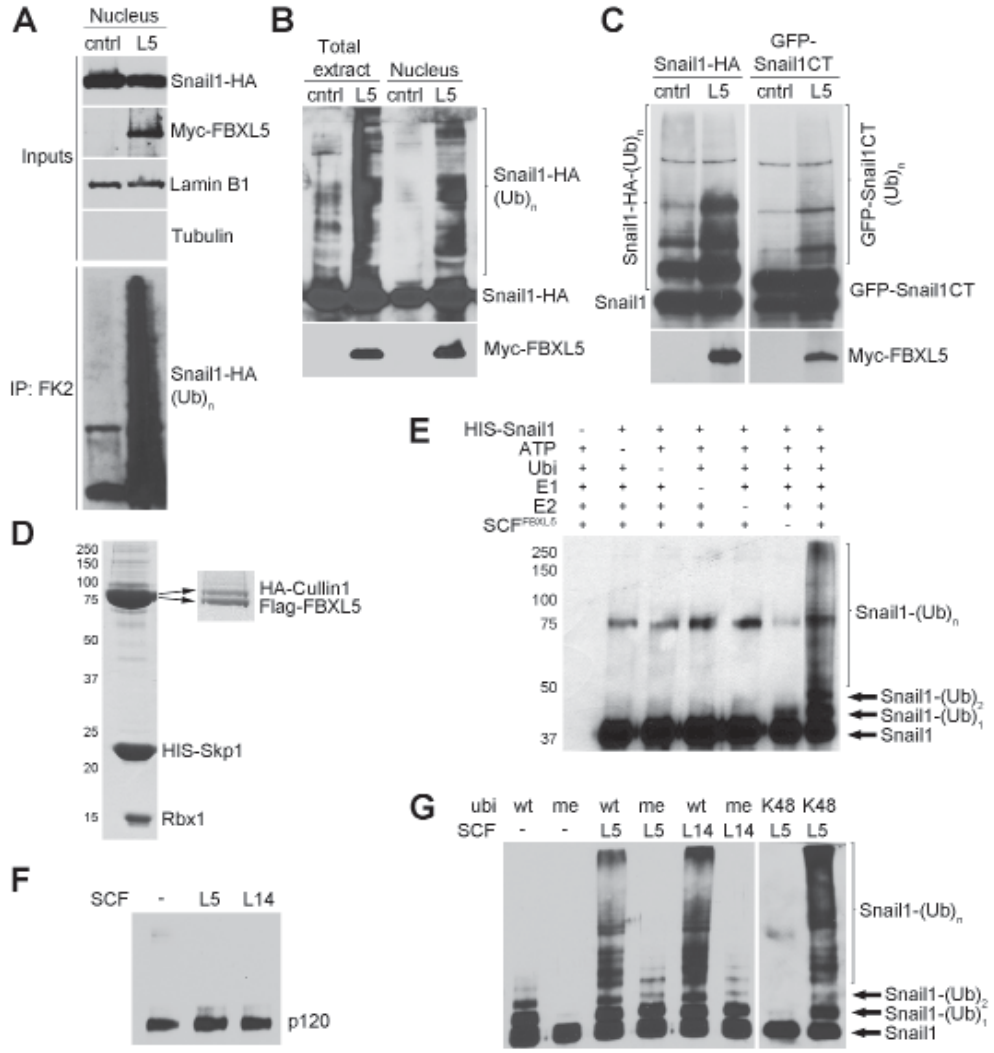

Figure R.26. Snail1 is ubiquitinated by FBXL5. (**A**) HEK293T were transfected with the indicated plasmids for 24h and treated with 10 μM MG132 for 3h. Denaturing IP of the nuclear extracts was carried out using mouse anti-FK2 mAb that recognizes ubiquitinated proteins. Immunoblotting was against the HA tag. (**B**) Total cell extracts or nuclear extracts were obtained from RWP-1 Snail1-HA cells transfected for 48h after a 4h treatment with 10 μM MG132. Lysis was in strong denaturing conditions with SDS buffer and immediate boiling of the samples to avoid the action of de-ubiquitinating enzymes. (**C**) RWP-1 cells were transfected with the indicated plasmids and HIS-tagged ubiquitin for 24h. 10 μM MG132 was added for 4h and Ni-NTA purification carried out in denaturing conditions. Anti-HA antibody. was used for immunoblotting. (**D**) The SCF^{FBXL5} complex was purified from Sf9 cells using Ni-NTA beads. Coomassie staining of a 12% polyacrylamide gel (left panel) and 7.5% gel (right panel) shows all the proteins forming the complex. (**E**) Western blot analysis of *in vitro* ubiquitination assays performed using SCF^{FBXL5}. (**F**) *In vitro* ubiquitination reactions using SCF^{FBXL5} or SCF^{FBXL14} and p120-catenin as substrate (specificity control). (**G**) Experiment similar to (F) in which different ubiquitin mutants are used.

the components (HA-Cullin1, Flag-FBXL5, HIS-Skp1 and Rbx1; *Figure R.26D*) in the Sf9 baculovirus system and used it to ubiquitinate HIS-Snail1, also obtained from baculovirus (see *Figure R.7C*, left panel). The purified complex could not modify an unspecific protein such as p120-catenin, and neither could the SCF^{FBXL14} complex (*Figure R.26E*). Only when all the components needed for ubiquitination were present the SCF^{FBXL5} complex was able to elongate ubiquitin chains on the Snail1 protein (*Figure R.26F*). When we used methyl-ubiquitin (me-Ubi) that cannot elongate ubiquitin chains instead of wt ubiquitin in the assays we detected a discrete pattern of bands corresponding to mono-, bi- and tri-ubiquitinated Snail1. The result was repeated for both SCF^{FBXL5} and SCF^{FBXL14} (*Figure R.26G*). This was indicative of the fact that three independent lysines can be ubiquitinated by the E3 ligases and that the ladder seen when using wt ubiquitin is due to the polyubiquitination of multiple lysines and not multi-mono-ubiquitination. We also found that SCF^{FBXL5} was able to elongate K48-Ubi chains (mark for proteosomal degradation), confirming that FBXL5 has a role in degradation since this mutant only allows the elongation of K48 ubiquitin chains as it has all the other lysines mutated to arginines (*Figure R.26G*).

Lysines 98, 137 and 146 are important for the degradation of Snail1 mediated by FBXL14 and β-Trcp1 (*Figure R.8A* and *B*). To figure out which are the important lysines for degradation by FBXL5 we performed Mass Spectrometry (MS) analysis of *in vitro* ubiquitinated Snail1. The three lysines we found to be significantly modified ($p<0.01$) were K85, K146 and K234 (*Figure R.27*). Lysines 85 and 146 are both located in the N-terminal part of Snail1; in fact K146 seems to be a highly targetable lysine for ubiquitination since it is modified by the three known ubiquitin ligases

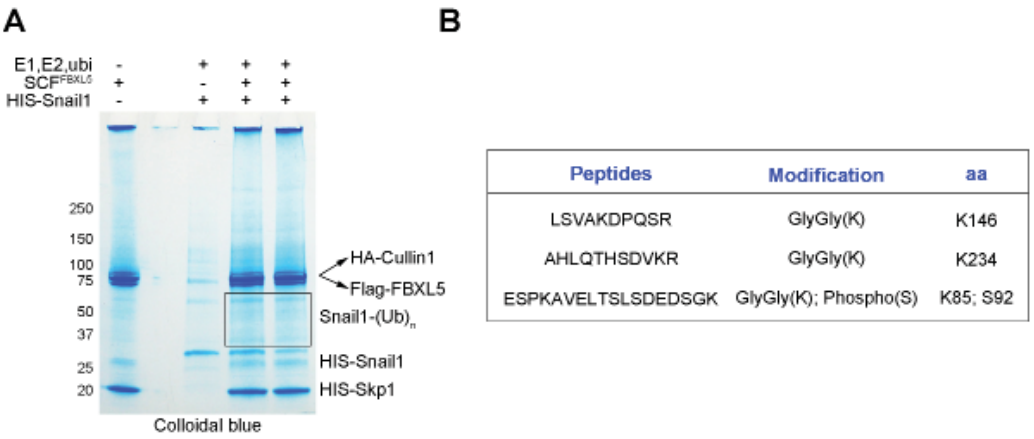

Figure R.27. MS analysis of Snail1 modified by SCF^{FBXL5}. (**A**) *In vitro* ubiquitination assays using the indicated components were carried out for 2h 30min at 30°C. The area marked with a black rectangle, which contains modified Snail1, was excised from the Colloida blue-stained polyacrylamide gel and analyzed by MS. (**B**) Output result of the MS analysis showing the statistically significant modifications ($p<0.01$) on Snail1.

for Snail1. Likewise, the peptide that was found ubiquitinated on K85 was simultaneously phosphorylated on S92, a modification described to be carried out by CK2α [87]. K234 is located in the C-terminal part of Snail1 between ZnF3 and ZnF4, in the region through which Snail1 mediates DNA binding and interacts with FBXL5.

We analyzed the MS results in detail and decided to study the phosphorylation by CK2 (S92, see *Figure R.27B*) to see if it is needed for FBXL5 action upon Snail1. Although not added to the results for the MS analysis due to the non-significant nature of the result ($p<0.01$), some of the Snail1 obtained from Sf9 cells also bared phosphorylation on the GSK-3β target serines. In *E. coli* purified proteins do not bear any posttranslational modifications. However, the Sf9 baculovirus system has been reported to yield proteins that can be phosphorylated [187]. We found this information very interesting since

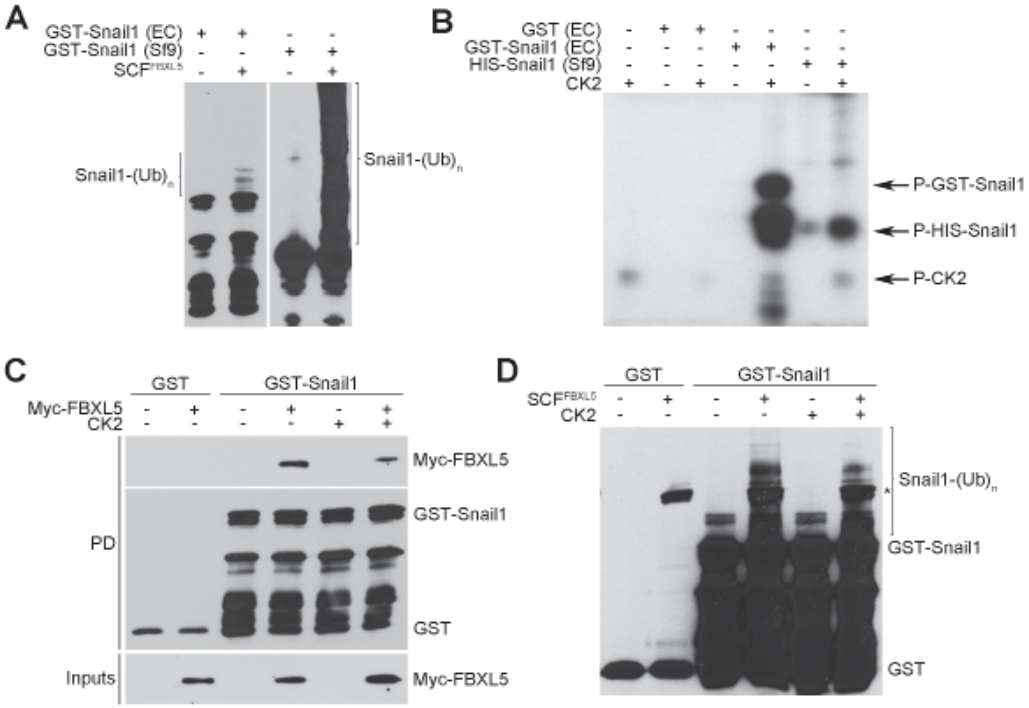

Figure R.28. Phosphorylation of Snail1 by CK2 does not modify its behavior towards FBXL5. (**A**) GST-Snail1 purified from bacteria (*E. coli*; EC) or from Sf9 infected cells (Sf9) was ubiquitinated *in vitro* by SCF^{FBXL5}. Note that the bands observed under the GST-Snail1 band (top band) are degradation fragments always detected in GST-Snail1 purified from bacteria and, to a smaller extent, in GST-Snail1 from baculovirus. (**B**) Autoradiography of GST-Snail1 or HIS-Snail1 phosphorylated by CK2 using radioactive ATP. GST was used as non-specific control. The arrows indicate the bands observed in the film, including the auto-phosphorylation of CK2. (**C**) GST-Snail1 phosphorylated or not by CK2 was used for PD analysis using HEK293T cells transfected for 48h with Myc-FBXL5. (**D**) GST-Snail1 phosphorylated or not by CK2 was used in *in vitro* ubiquitination assays. The asterisk (*) shows a band that is unspecifically recognized by the antibody when the SCF^{FBXL5} complex is added to the reaction.

previous assays in which we tried to ubiquitinate GST-Snail1 from bacteria had a very poor outcome when compared to Sf9-purified protein (*Figure R.28A*). To determine the importance of CK2-induced phosphorylation of Snail1 on FBXL5 binding and ubiquitination we phosphorylated the unmodified GST-Snail1 from bacteria (*Figure R.28B*) and used it for pulldown analysis and ubiquitination assays. We obtained high levels of phosphorylated Snail1 as shown by *in vitro* kinase assays using radioactive ATP (*Figure R.28B*). We performed parallel non-radioactive reactions and carried out pulldown assays (*Figure R.28C*) and *in vitro* ubiquitination

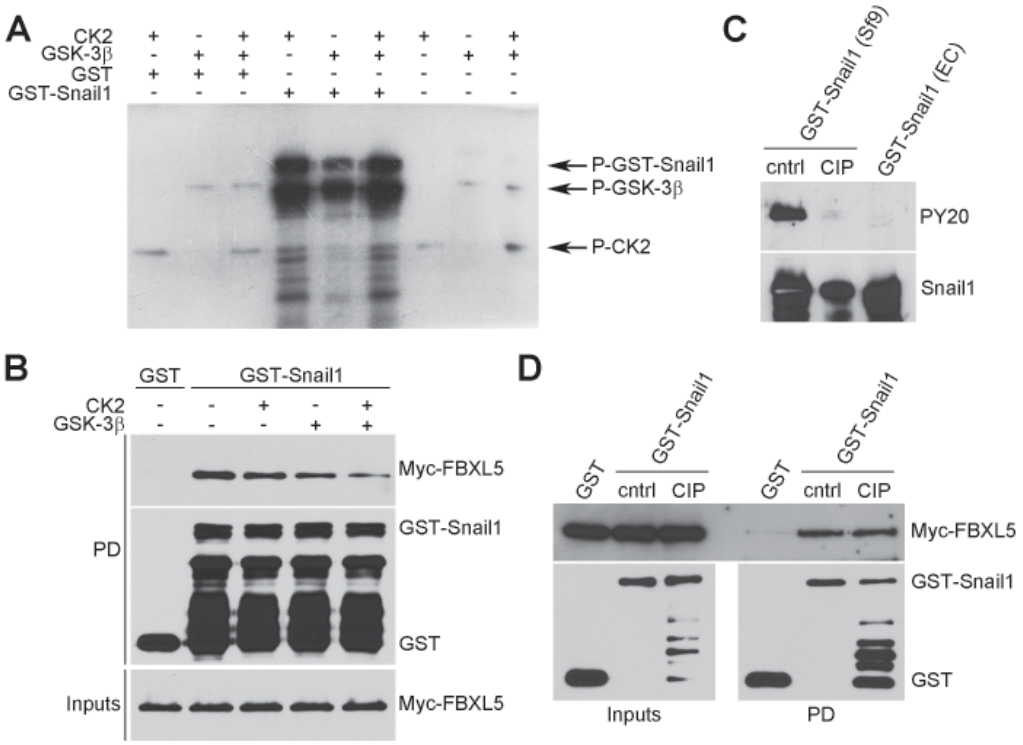

Figure R.29. Changing the phosphorylation status of Snail1 does not modify its interaction with FBXL5. (**A**) Autoradiography of GST-Snail1 purified from bacteria and phosphorylated by CK2, GSK-3β or a combination of the two kinases using radioactive ATP. GST was used as non-specific control. The arrows indicate phosphorylated GST-Snail1 and the auto-phosphorylation of both CK2 and GSK-3β. (**B**) PD analysis using the modified Snail1 described in (A). The PD was carried out with HEK293T cell extracts transfected for 48h with Myc-FBXL5. (**C**) GST-Snail1 purified from Sf9 cells was de-phosphorylated using Calf Intestinal Phosphatase (CIP). GST-Snail1 (Sf9) was used as positive control for phosphorylated Snail1 and GST-Snail1 (EC) as negative control. The PY20 antibody recognizes phosphorylated threonines. Despite the fact that the amino acids we needed to be de-phosphorylated were serines this is a good control since the CIP employed in this experiment is able, as indicated by the manufacturer, to de-phosphorylate threonines and serines with the same affinity. (**D**) PD analysis using phosphorylated and unphosphorylated GST-Snail1 purified from baculovirus. The PD was carried out with HEK293T cell extracts transfected for 48h with Myc-FBXL5. The bands observed under the main GST-Snail1 band are degradation bands that resulted from the treatment of the protein with CIP (30°C for 20min).

assays (*Figure R.28D*). CK2 phosphorylation was not enough to enhance the binding of Snail1 to FBXL5 or its ubiquitination.

Despite the negative results obtained with CK2 phosphorylation we thought that the differences in ubiquitination efficiency of FBXL5 upon Snail1 might be due to the posttranscriptional modifications of baculovirus-purified protein. We thus phosphorylated bacteria-purified Snail1 with GSK-3β and simultaneously with CK2 and GSK-3β (*Figure R.29A*). Once again the protein was efficiently phosphorylated as seen in the *in vitro* kinase assays yet when we tried to pull down FBXL5 we did not obtain an increase in binding (*Figure R.29B*). We therefore decided to carry out the reverse strategy and remove the phosphorylation marks on the Sf9-purified protein (*Figure R.29C*). We successively accomplished this aim and used the purified unphosphorylated GST-Snail1 for pulldown analysis. Again there were no differences in the binding to FBXL5 (*Figure R.29D*), to which we concluded that phosphorylation by CK2 and GSK-3β does not affect the *in vitro* affinity of Snail1 towards FBXL5.

R.2.6. Snail1 ubiquitination by FBXL5 decreases its binding to DNA

Since the binding of FBXL5 to Snail1 is through its C-terminal part and we know from MS analysis that K234 is ubiquitinated in this same half of the protein we wondered if the interaction, ubiquitination or both could be affecting Snail1 binding to DNA. We first analyzed the subcellular distribution of Snail1 in RWP-1 Snail1-HA cells after a 48h transfection with Myc-FBXL5 or a control vector in conditions where the proteasome was blocked. To ensure that the total levels of Snail1 were the same in both conditions we obtained total cell extracts and analyzed the expression of Snail1-HA. As expected, the protein levels detected were the same in the two

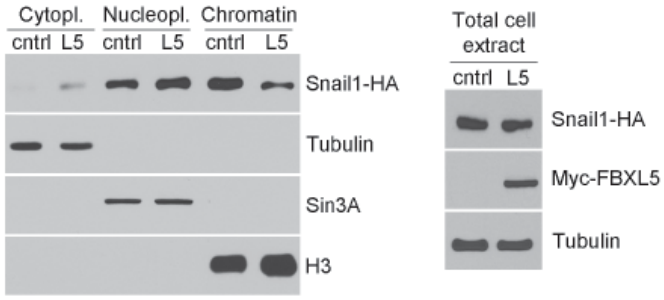

Figure R.30. FBXL5 decreases the chromatin pool of Snail1. RWP-1 Snail1-HA cells were transiently transfected with Myc-FBXL5 or a control vector for 48h and treated with 100 μM and 10 μM MG132 for 4h. Lysis was carried out using sub-fractionation of the lysates (left panel) or total cell extracts with SDS buffer (right panel). Snail1-HA levels were analyzed by Western blot. Myc-FBXL5 protein was detected as control of transfection and Tubulin, Sin3A and H3 were used as control for cytoplasmic or total, nucleoplasmic and chromatin fractions, respectively.

samples (*Figure R.30*, right panel). The analysis of the subcellular distribution of Snail1 by sub-fractionation showed that there was a significant reduction in Snail1 levels in the chromatin fraction and an increase in the cytoplasmic and nucleoplasmic compartments (*Figure R.30*, left panel). This suggests

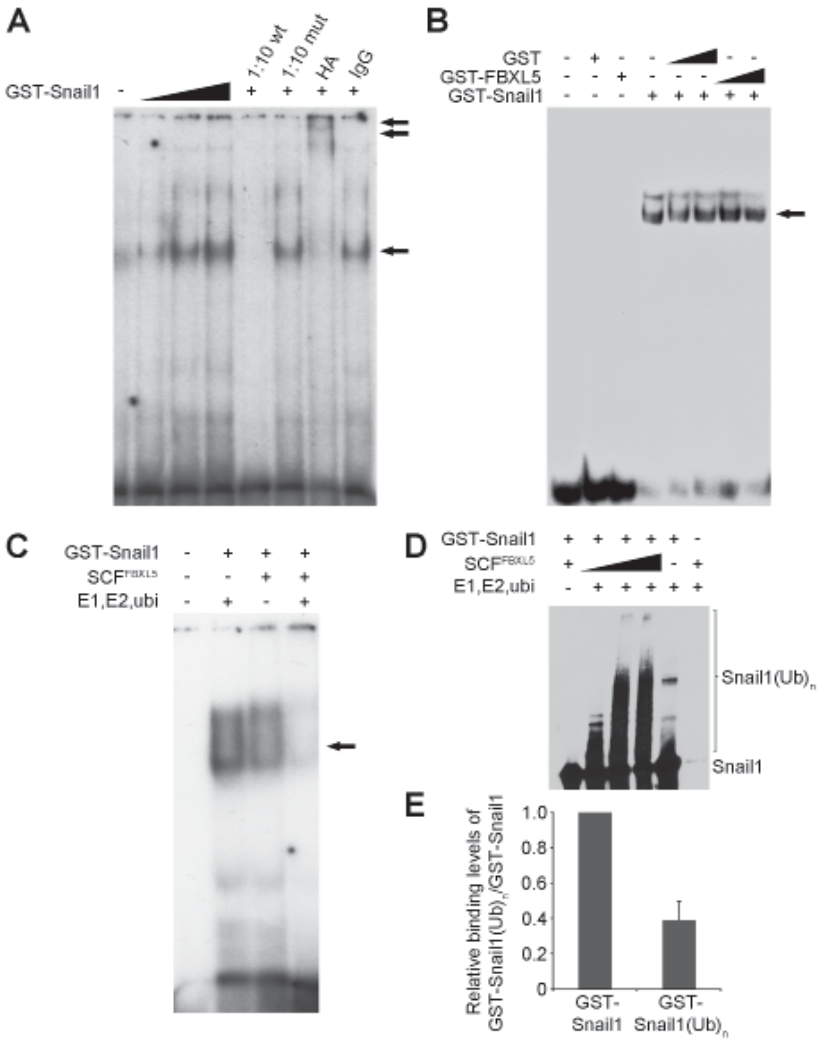

Figure R.31. DNA binding is impaired when Snail1 is ubiquitinated by FBXL5. (**A**) EMSA assay to test Sf9-purified protein for this application. Increasing amounts of GST-Snail1 bound to the labeled DNA probe were loaded in a non-denaturing polyacrylamide gel (single arrow). The maximum amount was competed with 10-fold cold wt or mutated (mut) probe compared to labeled probe. Retardation of the band (marked with two arrows) was achieved with anti-HA antibody (the GST-Snail1 retains the HA tag) and not with unspecific IgGs. (**B**) Competition assay using bacteria-purified GST-FBXL5 and GST-Snail1. The binding of FBXL5 to Snail1 was carried out previous to incubation with the probe to check if this impaired the Snail1 binding to DNA. (**C**) EMSA in which GST-Snail1 from baculovirus was ubiquitinated *in vitro* and then allowed to bind to the DNA probe. (**D**) Western blot analysis of the samples loaded in the EMSA prior to DNA binding to check ubiquitination. (**E**) Desitometric quantification of five independent EMSA experiments using GST-Snail1 or ubiquitinated GST-Snail1. Bars show the mean relative binding to the probe ± s.d.

that FBXL5 is able to either prevent the binding or displace Snail1 from the DNA when degradation by the ligase is impaired.

To determine if it was the binding of Snail1 to FBXL5 or the resulting ubiquitination of the protein what was important for Snail1 being released or not able to attach to DNA we carried out a series of Electrophoretic Mobility Shift Assays (EMSA). These experiments were done with GST-Snail1 and not with HIS-Snail1, since the latter was unable to effectively bind DNA, probably due to its histidine tail impairing the correct folding of Snail1 for this type of assays. We used a DNA probe containing the first E-box in the E-cadherin promoter [41]. The system was verified by testing increasing concentrations of Snail1, competing the probe with 10-fold more wt but not mutated (mut) probe or by retarding the band with anti-HA antibody that binds Snail1, an effect not achieved with unspecific IgGs (*Figure R.31A*). We then used the experimental set-up to check if FBXL5 binding to Snail1 impairs or competes its interaction with DNA. We found there was no difference in binding despite the fact that we repeated this experiment with GST-FBXL5 purified from bacteria (*Figure R.31B*), Flag-FBXL5 and SCF^{FBXL5}, both purified from Sf9 cells (not shown). Moreover, it was not possible to obtain a super-shift in the presence of DNA with FBXL5 and Snail1 which indicates that Snail1 has greater affinity for DNA than for FBXL5 in these *in vitro* conditions so we cannot appreciate the Snail1-FBXL5 interaction in the EMSA. In general, ubiquitin ligases only interact with their substrates for short periods of time. We think that the FBXL5-Snail1 destruction complex is dissembled *in vitro* when a third component such as DNA, to which Snail1 has higher affinity, is introduced in the reaction.

Having ruled out the fact that Snail1 and FBXL5 compete for the binding to DNA, we wanted to find out if the ubiquitination of Snail1 by FBXL5 stopped Snail1 from being able to bind DNA (*Figure R.31C*). For this purpose *in vitro* ubiquitinated Snail1 was used to carry out EMSA assays (*Figure R.31D*). As expected, we found that the ubiquitination by FBXL5 impaired Snail1 DNA binding, probably due to a conformational change of the protein, especially in its C-terminal part (*Figure R.31C*). When we quantified various independent experiments the binding was always lower with ubiquitinated Snail1, with on average around 30% of Snail1 still being able to bind the probe (*Figure R.31E*). The pool of Snail1 still capable of binding the probe was probably that which remained unmodified due to saturation of the *in vitro* reaction (*Figure R.31C*).

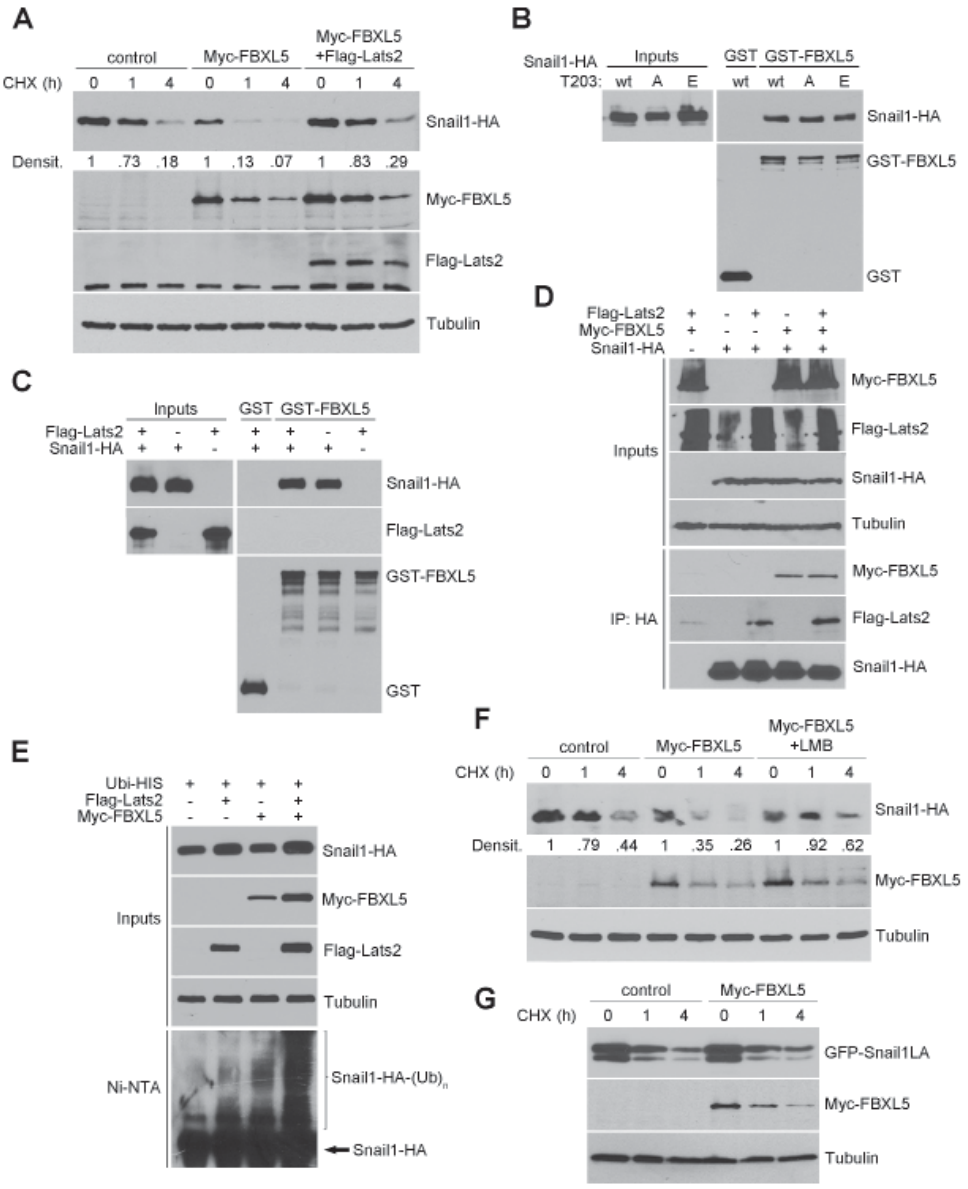

Figure R.32. Snail1 ubiquitinated by FBXL5 must exit the nucleus to be degraded. (**A**) HEK293T cells were transfected with the indicated plasmids and protein stability analyzed using CHX. (**B**) PD analysis using GST-FBXL5 and HEK293T cells transfected with Snail1 wt, T203A (unphosphorylated) or T203E (mimics phosphorylation) for 48h. GST was used as unspecific control. (**C**) PD analysis similar to (B) but cells were transfected with Snail1 or Snail1 and Lats2 for 48h. (**D**) IP using HEK293T cells transfected with the indicated vectors for 24h and treated with 10 μM MG132 for 4h. IP was carried out using rabbit anti-HA pAb and Western blot using mouse anti-Myc, anti-Flag and rat anti-HA antibodies as control. (**E**) *In vivo* ubiquitination assay using RWP-1 cells transfected for 24h with the indicated plasmids. Cells were treated with 10 μM MG132 prior to lysis and the result was analyzed with anti-HA antibodies to visualize ubiquitinated Snail1. (**F**) HEK293T cells were transfected with the indicated plasmids and treated with 5 ng/ml LMB for 1h prior to CHX treatment. (**G**) The GFP-Snail1LA-HA mutant which has impaired export to the cytoplasm due to point mutations in the NES was transfected with Myc-FBXL5 or the ΔF mutant for 24h in HEK293T cells and Snail1 protein levels analyzed by Western blot. Densitometry of the bands relative to Tubulin was performed.

R.2.7. Snail1 retention in the nucleus impairs its degradation by FBXL5

The FBXL5 binding site to Snail1 is closely located to a threonine residue, T203, phosphorylated by the Lats2 kinase [93]. T203 phosphorylation retains Snail1 in the nucleus and stabilizes the protein. We decided to study if this phosphorylation or the retention of Snail1 in the nucleus could block its degradation by FBXL5. *Figure R.32A* shows a degradation assay in which Lats2 was co-transfected with Snail1 and FBXL5. The addition of the kinase impaired the degradation of the protein and increased the half-life to similar levels as to that of cells without FBXL5. To study the binding of FBXL5 to Snail1 phosphorylated by Lats2 we used T203 mutants of Snail1 for pulldown analysis with GST-FBXL5 (*Figure R.32B*). Snail1 T203A, which cannot be phosphorylated, and Snail1 T203E, which mimics phosphorylation, equally bind the ubiquitin ligase. The co-transfection of Lats2 with Snail1 compared to Snail1 alone did not show any difference in Snail1 affinity for FBXL5 (*Figure R.32C*). Moreover, a co-immunoprecipitation of Snail1 and FBXL5 in the presence or absence of Lats2 showed that this protein is capable of binding both the ubiquitin ligase and the kinase simultaneously (*Figure R.32D*).

We thought that Lats2 could be impairing the degradation of FBXL5 by affecting its export and thus retaining ubiquitinated Snail1 in the nucleus. *In vivo* ubiquitination of Snail1 co-transfected with FBXL5 and Lats2 confirmed that despite the strong ubiquitination experienced by Snail1 in the presence of Lats2 its degradation was impaired (*Figure R.32E*). If the effect of Lats2 inhibiting the degradation of Snail1 by FBXL5 is indeed due to the retention of the protein in the nucleus a similar result should be obtained by simply blocking Snail1 export using Leptomycin B (LMB) (*Figure R.32F*) or using a Snail1 mutant that cannot be exported to the cytoplasm (*Figure R.32G*). In both cases the degradation of Snail1 by FBXL5 was blocked, demonstrating Snail1 must exit to the cytoplasm to be degraded.

R.2.8. Snail1 is stabilized by γ-irradiation in an FBXL5-dependent manner

Snail1 expression increases apoptotic resistance; moreover, different apoptotic insults affecting DNA integrity such as doxorubicin, etoposide or ionizing γ-irradiation achieved a good stabilization of exogenous Snail1 and induced the phosphorylation of histone H2AX on serine S139 (γ-H2AX) (*Figure R.33A*). When looking at which of these insults down-regulate FBXL5 protein we found that only γ-irradiation decreases FBXL5 to levels comparable to DFX treatment. We further confirmed this effect by using RWP-1 and MCF7 cell lines and analyzing the endogenous levels of both Snail1 and FBXL5 proteins. We found they were inversely modulated in

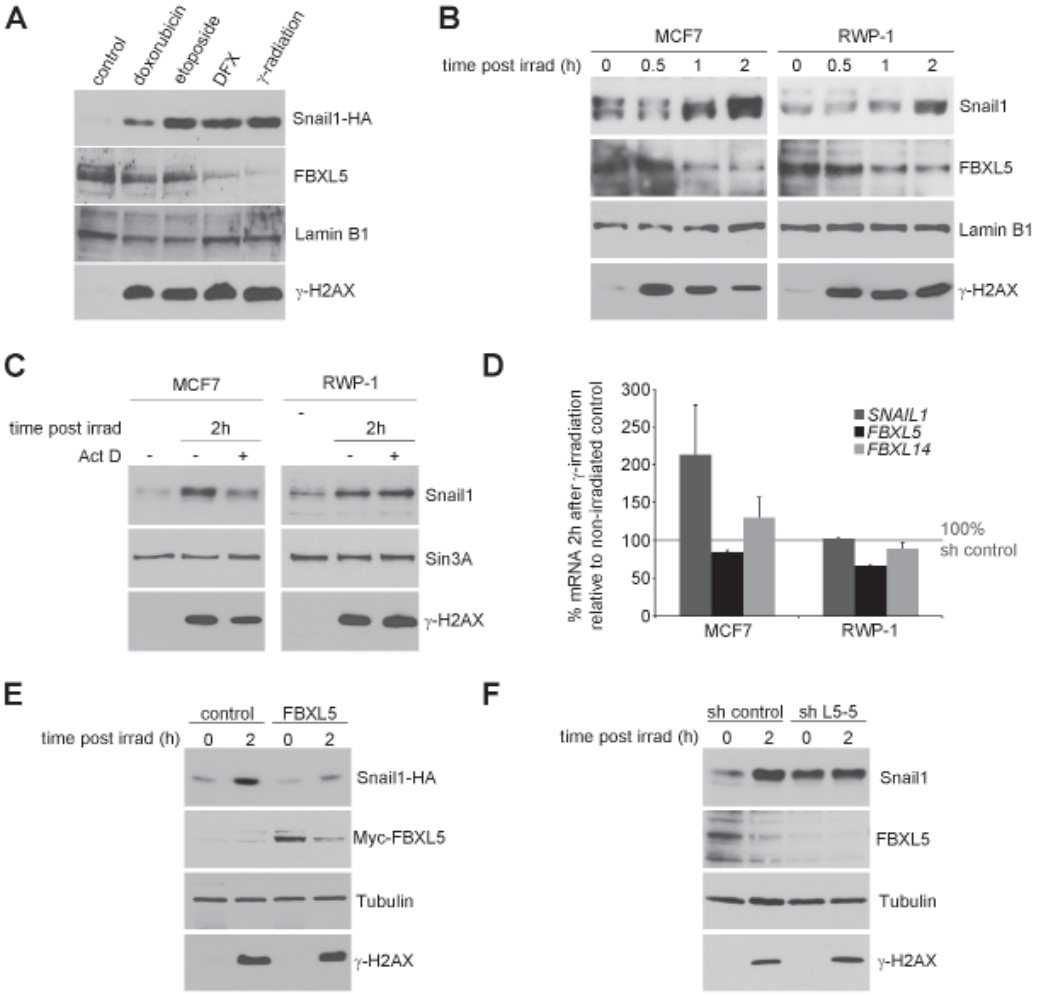

Figure R.33. Ionizing radiation causes degradation of FBXL5 and posttranslational stabilization of Snail1. (**A**) RWP-1 Snail1-HA cells were treated for 4h with 10 μM doxorubicin, 10 μM etoposide, overnight with 100 μM DFX or irradiated at 20 Gy and lysed 2h later. Cells were lysed by sub-fractionation and the nucleoplasmic fraction analyzed by Western blot for Snail1 and endogenous FBXL5 levels. The chromatin γ-H2AX levels were determined as control for DNA damage in cells. Lamin B1 was used as nucleoplasmic loading control. (**B**) Sub-fractionation of MCF7 and RWP-1 cells after 20 Gy irradiation was carried out at the indicated times. Nucleoplasmic extracts were analyzed by Western blot. (**C**) MCF7 and RWP-1 cells were treated with 2.5 μg/ml Actinomycin D (Act D) for 1h prior to irradiation with 20 Gy. Immunoblotting of the nucleoplasmic extracts was carried out. Sin3A was used as nucleoplasmic loading control. (**D**) mRNA levels of *SNAIL1*, *FBXL5* and *FBXL14* in irradiated MCF7 and RWP-1 cells were analyzed by quantitative RT-PCR. Results are shown as percentage mRNA compared to non-irradiated control and are the mean of three independent experiments ± s.d. (**E**) RWP-1 Snail1-HA cells were stably infected with pBabe control or Myc-FBXL5 vectors and irradiated with 20 Gy. Analysis of total cell extracts was performed by Western blot. (**F**) RWP-1 cells stably expressing pLKO-GFP-sh control or sh FBXL5-5 vectors were submitted to irradiation with 20 Gy and lysed after 2h. Protein levels of total cell extracts were analyzed by immunoblotting.

a post-irradiation time-dependent manner (*Figure R.33B*). While Snail1 was progressively up-regulated in both cell lines in response to irradiation FBXL5 levels were reduced.

To determine the nature of the γ-irradiation effect on Snail1 we inhibited transcription in cells using Actinomycin D (Act D) prior to irradiation. We found that while in MCF7 cells the stabilization of Snail1 was both at transcriptional and protein level, it was mainly posttranslational in RWP-1 cells (*Figure R.33C*). Accordingly, *SNAIL1* mRNA levels were increased in MCF7 cells and remained unchanged in RWP-1 cells after irradiation. *FBXL5* levels were only slightly down-regulated and no significant changes were observed in *FBXL14* (*Figure R.33D*), which was used as control of specificity of the pathway with regards to Snail1 stabilization.

When cells overexpressing Myc-FBXL5 were submitted to γ-irradiation the exogenous protein was destabilized. Moreover, Snail1-HA up-regulation was prevented in the presence of Myc-FBXL5 (*Figure R.33E*). We carried out the reverse experiment in which we knocked down FBXL5 in RWP-1 cells and found that the stabilization of Snail1 protein was similar to that obtained in irradiated control cells. The depletion of FBXL5 also inhibited the strong up-regulation of Snail1 by γ-irradiation (*Figure R.33F*). These experiments suggest that FBXL5 levels are decreased by γ-irradiation causing strong stabilization of Snail1 protein levels in many tumor cell lines.

DISCUSSION

Snail1 is known to be one of the earliest and most important EMT inducers. However, little is known about its protein regulation. A great deal of effort is focused on the RNA levels of this transcription factor that has a half-life of only around 20 minutes [83]. When the mRNA levels of Snail1 are analyzed its importance is frequently not reflected in the results since Snail1 mRNA levels do not always correlate to protein stabilization. In fact, prior to starting the work described herein, only β-Trcp1 had been related to Snail1 protein regulation through proteosomal degradation. The action of β-Trcp1 requires the previous phosphorylation of the P-S rich domain of Snail1 by the kinase GSK-3β, first in the nucleus to induce the export of the protein and then in the cytoplasm, where Snail1 is degraded [83].

In this work we have demonstrated two alternative mechanisms of Snail1 protein degradation through the action of the E3 ubiquitin ligases FBXL14 and FBXL5. While the characterization of these two Snail1 F-box ligases was being carried out another group found the RING ligase Mdm2 can also degrade Snail1 [99] although additional experimental work is required to definitively conclude that Snail1 is an Mdm2 substrate.

D.1. FBXL14

We have shown that FBXL14 degrades and ubiquitinates Snail1. Our work was originated by the observation that the inhibition of GSK-3β did not yield the same Snail1 protein stabilization as proteasome inhibition. This led us to think there might be alternative degradation pathways for Snail1. After determining that a Snail1 mutant unable to be phosphorylated by GSK-3β at the P-S rich domain could be ubiquitinated we looked for possible candidate ubiquitin ligases capable of causing such a modification on Snail1 protein. One of the proteins that behaves and has some degree of homology to Snail1 is its family member Snail2, which had been described by Vernon and coworkers to be degraded by the *Xenopus* F-box protein Ppa, the human orthologue of which is FBXL14 [100]. We obtained the necessary tools to carry out a biochemical analysis of Snail1 and FBXL14 in mammalian cell lines. FBXL14 was found to bind both the wt and a GSK-3β-independent mutant of Snail1, as well as being capable of degrading the two forms of Snail1. *In vitro* and *in vivo* ubiquitination assays determined the specific effect the ligase has on Snail1.

The site of interaction of both FBXL14 and β-Trcp1 with Snail1 is through the N-terminal part. The P-S rich region, within which we find the β-Trcp1 consensus degron sequence, is also located there. In depth determination of the minimal region of Snail1 sensitive to FBXL14 degradation showed that the degron region spans through a hydrophobic part of Snail1 found in its N-terminal part (amino acids 120–151). This information is in accordance to what has been described in *Xenopus* for Snail2, since the ubiquitin ligase and the target protein also bind through a hydrophobic region of the N-terminus (amino acids 38–64) [100]. The three lysines that when mutated inhibited the ubiquitination both by FBXL14 and β-Trcp1 were also located at the N-terminal part of the protein, and were K98, K137 and K146. The mutation of the lysines led to a Snail1 protein that was highly stable and was significantly less ubiquitinated than the wt protein. However, there was some residual ubiquitination that suggests there may be other lysines of Snail1 that can be ubiquitinated, although to a lesser extent.

The fact that the inhibition of FBXL14 in cell lines produces a strong up-regulation of Snail1 protein levels indicated its relevance in the basal control of Snail1 stability. β-Trcp1 differs in this observation as its knockdown does not produce such a relevant effect on basal levels of Snail1 protein, as seen in the screening for F-box ubiquitin ligases targeting Snail1 (see FBXW1), an observation supported by findings in other laboratories [188]. The reason for the difference is most probably due to the need of β-Trcp1 for the phosphorylation event caused by kinases like GSK-3β. Therefore the mere expression of the ubiquitin ligase does not suffice to target Snail1 for

proteosomal degradation. In fact, it has been published that when β-Trcp1 is knocked out in mice these only present minor abnormalities such as impairment in spermatogenesis and reduced fertility [189]. It was necessary to generate mice knockdown for β-Trcp2 in all the tissues in a β-Trcp1-null background to see a severe testicular phenotype related to a great increase in Snail1 protein in the tissue, blocking the process of spermatogenesis [188]. This indicates that, with respect to Snail1, β-Trcp1 is only essential in very particular tissues, supporting the idea that this F-box ligase does not have a role in the maintenance of Snail1 basal levels but generally responds to previous stimulation of other pathways activating GSK-3β (and possibly other kinases not yet described) that induce Snail1 instability through phosphorylation. Moreover, it suggests there may be some degree of redundancy between the two ligases β-Trcp1 and β-Trcp2. Although there is no available information on the knockout of Ppa/FBXL14 we think that since it regulates Snail1 and Snail2 among other EMT factors [190] it is possible that embryos cannot progress at the time of gastrulation due to aberrant and uncontrolled EMT.

To find a physiological model where FBXL14 down-regulation is associated with Snail1 protein stabilization we used two EMT systems already established in the lab and found there was great down-regulation of *FBXL14* mRNA in low oxygen conditions and not with TGF-β treatment. Hypoxia is linked to tumor progression since it is a mechanism of adaptation of the tumor to the environment. It promotes cell survival, drug resistance, increased cell migration and invasion, characteristics shared with Snail1 stabilization [191]. It was very interesting not only to find that in hypoxia *FBXL14* levels inversely correlated to HIF-1α but also to Snail1 protein levels, as expected. The observation that *FBXL14* mRNA was down-modulated by a physiological program such as hypoxia causing the disruption of the homeostasis of Snail1 protein expression by increasing its stabilization was in agreement with our hypothesis that Snail1 protein levels are controlled by multiple ligases in normal conditions.

While we were studying the regulation of FBXL14 it was published that HIF-1α, the transcription factor that senses oxygen depletion, binds the Twist1 promoter through a HRE, increasing both its mRNA and protein [117]. Therefore we thought there was a possibility of a crosstalk between Twist1 and Snail1 through the regulation of FBXL14. As shown in the results when we knocked down Twist1 and submitted cells to low oxygen conditions *FBXL14* mRNA remained unchanged and Snail1 protein was no longer stabilized. Moreover, the simple overexpression of exogenous Twist1 in cells caused a marked down-regulation of *FBXL14*. Altogether these results suggest that there is a direct link between Twist1 transcription

factor expression and FBXL14 mRNA regulation. We think that the fact that *FBXL14* contains a Twist1 consensus box in its promoter reveals the possible transcriptional mechanism of *FBXL14* down-regulation by Twist1 in hypoxia (*Figure D.1*). Nonetheless, we think there may be a direct link between the stabilization of Snail1 through Twist1 independent of FBXL14. We found that transfection of Twist1 stabilized Snail1 exogenous protein, providing another link between Twist1 and Snail1 protein expression (data not shown). It is possible that Twist1 can directly regulate Snail1 protein, a hypothesis that has been reinforced by the publication of a work showing that Twist1 physically interacts with Snail1 and Snail2 through its C-terminal WR domain when the transcription factors are phosphorylated by GSK-3β, possibly preventing degradation by β-Trcp1 [192]. There are other studies supporting our findings of increased Snail1 protein levels in hypoxia in breast cancer cell lines and tumor samples [193]. An alternative mechanism that has also been described is hypoxia-activated Notch signaling that up-regulates Snail1 by two mechanisms: the translocation of the Notch intracellular domain to the Snail1 promoter increasing the expression of the transcription factor and to the Notch-dependent recruitment of HIF-1α to the LOX promoter, which increases LOX protein levels and stabilizes Snail1 protein [145]. Both mechanisms show no change in mRNA levels of Snail1.

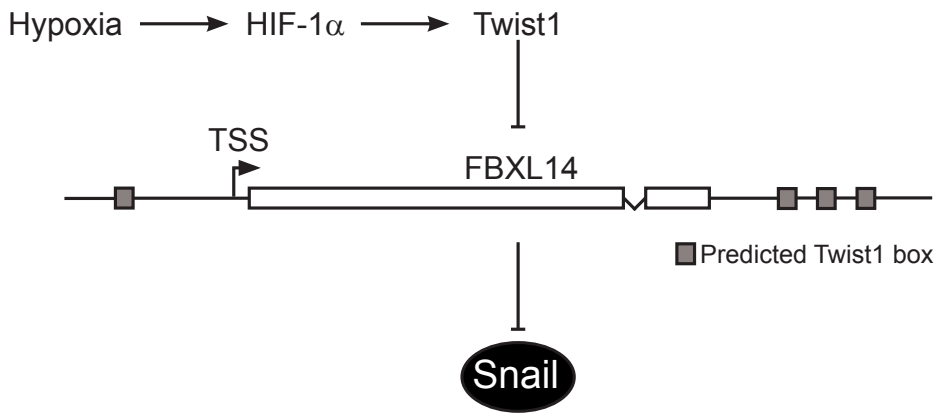

Figure D.1. FBXL14 regulation in hypoxia. Hypoxia stabilizes HIF-1α protein levels which, in turn, binds the HRE in the Twist1promoter, up-regulating this gene. Twist1 causes a down-modulation of *FBXL14* that we speculate could be due the repression of the mRNA expression through predicted Twist1 boxes found in the promoter and the 3'-UTR of *FBXL14*. TSS: transcription start site.

Based on this we wanted to study the down-modulation of *FBXL14* by *TWIST1* in hypoxia and did so using RNA from hypoxic human tumor samples and surrounding healthy tissue as control. Hypoxia was verified in the tumors by the up-regulation of *CA9*, which was strongly correlated to a down-regulation in *FBXL14* levels. The association of *TWIST1* with these

two factors was done on a presence-absence basis. When *CA9* levels are high *TWIST1* is present and *FBXL14* mRNA is down-regulated. We carried out an mRNA analysis of the tumors since there is no reliable antibody for detecting the FBXL14 endogenous protein, not allowing us to establish a relationship between Snail1 and FBXL14 levels in the study. However, other studies have linked the co-expression of HIF-1α, Snail1 and Twist1 to bad prognosis in cancer patients [194].

We thought there could exist a possible co-operation of the transcriptional down-regulation of *FBXL14* and the inactivation of GSK-3β in the stabilization of Snail1 protein. When we studied both pathways we found that in NMuMG cells only down-regulation of *FBXL14* explained the rise in Snail1 protein levels in hypoxia; however, in SW620 cells, phosphorylation of serine S9 on GSK-3β indicated that this enzyme is inactivated in low oxygen conditions. This means that in some cell lines the mechanism by which Snail1 protein is stabilized in hypoxia is dependent on the shutdown of both the FBXL14 and β-Trcp1 degradation pathways. The inactivation of GSK-3β related to the stabilization of Snail1 has been already described to usually happen due to growth factors and Wnt signaling [195]. We have found hypoxia to be another relevant mechanism through which some tissues may adapt to cellular stress and inhibit GSK-3β causing Snail1 up-regulation; although it is FBXL14 that is widely down-regulated in response to this stress pathway.

The localization of FBXL14 protein is cytoplasmic, as determined by immunofluorescence studies in NIH3T3 (see Results section) and RWP-1 cells (not shown). Cytoplasmic FBXL14 can easily target Snail1 when it exits the nucleus through phosphorylation events. The study carried out to determine the degron sequence or minimal region of Snail1 that is necessary to be degraded by FBXL14 showed that this area is comprised between aa 120–151, a region that spans from the end of the P-S rich domain to the end of the NES, and that both phosphorylated and unphosphorylated Snail1 are degraded by FBXL14 (the Snail1 duplet observed by Western blot with transfected GFP-Snail1 fusion proteins is similarly affected). The question that remains open is how this E3 ligase targets the nuclear and unmodified pool of Snail1. We think that the levels of the transcription factor are probably maintained low through the degradation of newly synthesized protein by FBXL14, when Snail1 is being translated and still present in the cytoplasm. The fact that the degron is located within a region that is not necessarily modified by phosphorylation is not surprising since many SCF^{FBXL} proteins have been described to have unmodified substrates. For example, FBXL12 mediates Ku80 ubiquitination in response to DNA damage [196] and FBXL7 degrades Aurora A in the centrosome during spindle formation, causing

mitotic arrest [197]. We hypothesize this is due to the hydrophobic nature of LRRs, which allow for strong protein interactions.

Few reports about FBXL14 can be found in the literature. In *Drosophila* it is thought that Ppa can be located in the nucleus since it contains a putative nuclear localization sequence (NLS) which is found between the F-box domain and the LRRs [198]. Moreover, the F-box protein is seen to degrade the transcription factor called Pax transcription factor Paired (Prd) in this organism [100]. The segmented pattern of expression of the transcription factor was in both cases contrary to that of the ubiquitin ligase and was determined to be important in the development of the embryos. A more recent study shows that, in *Drosophila*, Ppa can regulate the stability of the Centromeric Histone H3, protein that is, like Snail1, found in the nucleus [199]. This gives an indication that in some organisms this ubiquitin ligase could be located in the nucleus. It has been found that some species like zebrafish have two FBXL14 isoforms: FBXL14a and FBXL14b [200]. The authors of this study suggest they act as differential regulators of the dorsoventral patterning through the modulation of MAP kinase phosphatase-3 (Mkp3). They find that the murine FBXL14 is evolutionary conserved from the zebrafish isoform FBXL14b. The differences observed between various species leads us to think that the localization of the protein is not conserved and that it is cytoplasmic in mammals and nuclear in *Drosophila*.

The distinct RNA patterning of Ppa has motivated different investigations to determine if this is a common feature of this family of genes [201]. However, it has been found that it is only Ppa that shows an unusual patterned transcript localization. After the publication of our work characterizing the mechanisms through which FBXL14 acts on Snail1 in tumor cells [202] the same group that had described the degradation of Snail2 by Ppa in *Xenopus* published an interesting new study [190]. Lander and coworkers' article shows that Ppa is a common regulator of EMT transcription factors since it can degrade Snail2, Twist1 and Zeb2 as well as Snail1. These results indicate that the transcript patterning of Ppa possibly is an indicator of the regulation of a group of different proteins involved in the process of EMT.

Regarding the transcriptional regulation of *FBXL14* by the action of its target substrate Snail1 it is a new field that remains to be fully characterized. It was very surprising for us to find through ChIP that Snail1 is bound to the exonic region of the *FBXL14* gene. It is known that Snail1 represses genes such as E-cadherin by binding to their promoter; however, this is the first time that we see it directs the expression of a NAT. This possibility is easier to explain that the binding of a transcription factor to exonic regions. We think that the binding of Snail1 occurs in the promoter region of the

non-coding antisense transcript (NAT), although more work needs to be done to elucidate the exact mechanism of action (*Figure D.2*). Snail1 itself is modulated by long non-coding RNAs as shown by a high throughput study in which these transcripts were depleted, also demonstrating that their action can be both repressive and activating, like in the FBXL14 case [203]. As discussed before, we know that *FBXL14* is a gene that controls the stability of an important subset of transcription factors involved in EMT. Therefore, it is plausible that it may be tightly regulated at transcriptional level through a feed-back mechanism by the proteins it affects. Snail1 regulates the levels of the *FBXL14* NAT which may stabilize the *FBXL14* mRNA. When Snail1 is depleted the NAT is down-regulated and so is *FBXL14* (*Figure D.2*).

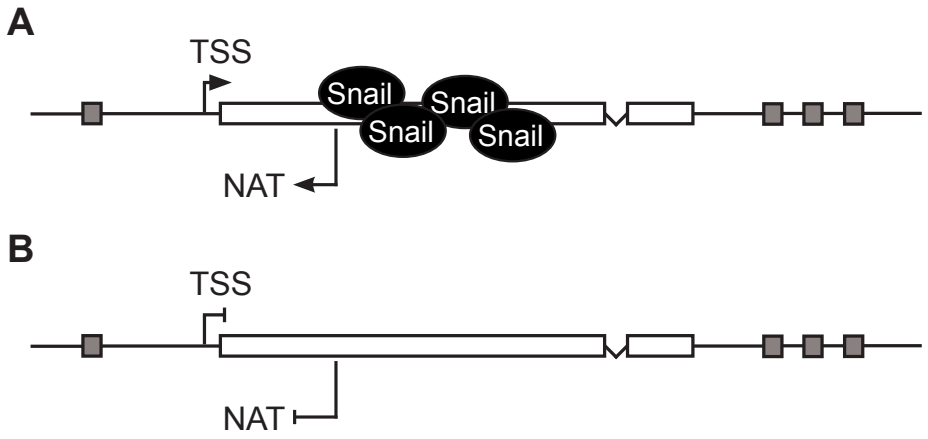

Figure D.2. Snail1 regulation of a NAT of *FBXL14* through binding to the chromatin region of the first exon of the protein-coding transcript. Model of the putative regulation loop by Snail1 binding to the chromatin of the region mapping for exon 1 of the *FBXL14* gene. (**A**) Snail1 binds to the DNA in the first exon of *FBXL14* gene, probably controlling the expression of the *FBXL14 NAT*, resulting in the stabilization of the *FBXL14* mRNA. (**B**) When Snail1 is not present there is a decrease or inhibition of the expression of the *FBXL14 NAT*.

D.2. FBXL5

The second half of this work presents the degradation and ubiquitination of Snail1 by FBXL5. Due to the complex posttranslational regulation of Snail1 we decided to look for more candidate ubiquitin ligases targeting this transcription factor. To do this we carried out a screening using shRNAs targeting all the known ubiquitin ligases and picked FBXL5 as the most promising F-box protein. The knock down of FBXL5 stabilized both endogenous and exogenous Snail1, indicating that the effect exerted by FBXL5 is reflected on the posttranslational stability of its target. Differing from the results obtained with FBXL14 and β-Trcp1, the two known ligases for Snail1, FBXL5 binding to the transcription factor was through the ZnF domains found in the C-terminal part of the protein. This fact caught our interest since this region is the one that allows for Snail1 binding to DNA. Moreover, in contrast to what has been described for Ppa/FBXL14, FBXL5 did not act as a general EMT ubiquitin ligase since it only interacted and degraded Snail1 and Snail2. Twist1 and Zeb1 were not affected by FBXL5.

FBXL5 has the particularity of being a nuclear ubiquitin ligase. When we were characterizing this protein we used both exogenous and endogenous expression in Western blot and immunofluorescence (IF) analysis. In both types of studies we found that FBXL5 is strongly localized in the nucleus with some protein expressed in the cytoplasm. This characteristic greatly enhanced our interest for the study of this F-box protein with regards to Snail1 since it is the first time a nuclear ubiquitin ligase is described to target it. We saw that FBXL5 is expressed in a quite ubiquitous manner in tumor cell lines. The verification of endogenous antibodies was a task that was carried out in a very thorough manner since it was very important for us to demonstrate the localization of FBXL5. In the results we showed that the shRNA down-regulates FBXL5 in two cell lines, causing a strong increase in Snail1 levels both in the nucleoplasm and the chromatin. Moreover, we demonstrated the interaction between FBXL5 and Snail1 in this compartment. Other FBXL type E3 ligases have also been described to be nuclear. FBXL3, an F-box E3 ligase that regulates Cry proteins, which are involved in the control of circadian processes, has also been characterized to be predominantly, but not exclusively, nuclear, and expressed ubiquitously in cells [204].

To find out the distribution of FBXL5 within cells we submitted them to various treatments. The addition of iron caused FBXL5 to be stabilized and expressed in the nucleus with augmented accumulation in the cytoplasm. We think that the pool of FBXL5 that is modulated by iron levels is especially the cytoplasmic one; however, nuclear stabilization cannot be neglected. Therefore, the ligase can be localized both in the nucleus and in

the cytoplasm. As expected, FBXL5 was totally nuclear when treated with LMB. In fact, analysis of the FBXL5 sequence shows that it contains several putative nuclear export sequences (NES). One of them is located in aa 354–364 with the consensus sequence LXXXLXXLXL, and its putative binding to CRM1 inducing the export of FBXL5 is in agreement with the results obtained with LMB. Our surprise came when we treated cells both with iron and MG132 as FBXL5 was only nuclear. Indeed, we were expecting the protein to be expressed in the whole cell but saw it clearly localized in the nucleus. It is possible that the ubiquitin ligase that targets it for degradation, which remains to be studied, is localized in the nucleus and since FBXL5 is mainly found in this compartment blocking the proteasome causes it to accumulate there.

The degradation of FBXL5 is thought to be through a putative degron sequence that is masked in the presence of iron [205]. The exact sequence has not yet been mapped but a study has shown that in the absence of iron the hemerythrin (iron-binding) domain is ubiquitinated. FBXL5 cannot ubiquitinate itself as it occurs for many members of the F-box family, for instance with FBXL14 [205]. Hemerythrin domains have an α-helical bundle fold that commonly contains a diiron center. The iron atoms are redox-active and can switch between a fully oxidized diferric (met) state, a partially reduced semi-met state and a fully reduced diferrous (dioxy) state. One of the iron atoms is coordinated by the imidazole side chains from three histidines and the other iron by two histidines, and can also bind to oxygen. The bridge between the two iron atoms is provided by a glutamate and an aspartate [205, 206]. The mammalian FBXL5 hemerythrin domain differs from the consensus hemerythrin domain described in other organisms in that it has an additional glutamic acid instead of a third histidine binding the first iron atom. Mammalian FBXL5 is not able to directly bind oxygen, although some studies suggest that hydrogen bonds may be formed from the iron to the oxygen atoms, an observation that is controversial in the field [205-207]. FBXL5 is an iron-sensing protein; however, it is not as dynamic as it was originally thought. The protein can sense the cytosolic iron of cells and is more stable in the presence of the metal. However, this only holds true when the protein is being newly synthesized. Findings by other groups show that the stability of FBXL5 is only modulated by the presence of iron when the protein is produced *de novo* [206], influencing the state of the synthesized protein. When oxygen and iron levels are high FBXL5 is presented as a highly stable, oxidized and properly folded protein that can bind to the SCF complex [206]. However, even if iron levels are high, if oxygen is low the protein will exist in its reduced form (similar to low iron conditions) and will be partially unfolded due to the dissociation of the iron atoms. This FBXL5 will be degraded by the proteasome [208]. Therefore the

E3 ligase, although not directly binding oxygen, is sensitive to its levels at the time of synthesis.

The modification of the general levels of iron by the addition of FAC or DFX directly modulated Snail1 endogenous and exogenous levels. The results shown indicate that there is an inverse correlation between the levels of iron and those of Snail1 protein. Accordingly, when FBXL5 levels go up those of Snail1 go down. The physiological meaning of these conditions translated to tumor progression is yet to be found. We have observed that the depletion of iron in cells strongly increases the expression of Snail1 protein and thus promotes EMT, at least *in vitro*. The contrary action maintains low Snail1 protein levels. The chelation of iron has been studied as a chemotherapeutic cancer treatment [209, 210] since neoplastic cells show increased requirements for iron than normal cells as they have higher numbers of transferrin receptors [211]. These drugs also inhibit enzymes that provide the precursors for DNA synthesis that facilitate DNA replication and division of cancer cells [212]. However, despite the fact that some studies are being carried out with these drugs, the chelation of iron is not one of the standard procedures for cancer treatment [213]. One of the main side effects of removing iron from cells is that HIF-1α, the protein stabilized during hypoxia, is greatly up-regulated. This is due to the fact that the von Hippel-Lindau tumor suppressor gene (VHL), the E3 ligase that degrades HIF-1α in normoxic conditions, can only recognize its target when prolyl hydroxylases act on it. Iron facilitates the binding and activation of the oxygen substrate consumed during hydroxylation, and its chelation inhibits the role of prolyl hydrolases [207, 213, 214]. Regarding EMT, a study has shown that iron chelation can inhibit the shift of cells towards a mesenchymal phenotype when it is already induced by TGF-β [215]. In our hands, chelation of iron has highly increased Snail1 levels, and we think this is due, at the early stage, to the decrease in FBXL5 levels, and later on due to the effect the stabilization of HIF-1α has on *FBXL14* mRNA. It is possible that these therapies work at the start of a cancer treatment when intracellular iron levels are high, but eventually they will lead to disturbed iron and oxygen homeostasis, inducing EMT. It is probable that the use of these drugs is not widely extended due to the side effects after the primary target, iron, is depleted from cells.

We have thoroughly demonstrated the ubiquitination of Snail1 by FBXL5 both *in vivo* and *in vitro*. The results showed that FBXL5 acts in the nucleus ubiquitinating Snail1. A C-terminal mutant of Snail1 was able to be ubiquitinated *in vivo*, although to a lower extent than the wt construct. This was the first indication that the C-terminal part of the protein could contain putative lysines ubiquitinated by FBXL5. Indeed, mass spectrometry analysis

later demonstrated that K234 is modified by FBXL5. The direct effect of FBXL5 on Snail1 was confirmed in the *in vitro* assays which also helped to establish that FBXL5 can ubiquitinate at least thee lysines (experiment with me-Ubi) and that it targets the protein for proteosomal degradation by elongating homotypic K48-linked chains. The other two Snail1 lysines modified by FBXL5 were either the same (K146) or located very close to the other lysines found to be modified by FBXL14 and β-Trcp1. We think that this region of the N-terminal is highly susceptible to being ubiquitinated to target the protein for degradation.

We used GST-Snail1 expressed in Sf9 cells and used it to bind DNA. The binding was not competed by FBXL5 addition. Western blot analysis showed that no endogenous FBXL5 protein is found strongly bound to chromatin (at least it cannot be detected), observation that is in accordance with competition experiments demonstrating that Snail1 has a much higher affinity for DNA than for FBXL5. We found that Snail1 ubiquitinated by FBXL5 was less able to bind the DNA probe, suggesting that polyubiquitination of Snail1 by FBXL5 is not compatible with its binding to DNA. This experiment does not prove that FBXL5 causes Snail1 to be detached from DNA; however, it complements the results obtained in cells transfected with the E3 and treated with the proteasome inhibitor MG132. We observed that there was substantially less Snail1 in the chromatin of cells, despite the maintenance of overall Snail1 levels in cells due to the blocking of the proteasome. The cytoplasmic and nucleoplasmic fractions were enriched in Snail1, evidencing a change in the localization of the protein in the presence of FBXL5. Other proteins such as FBXL10 have been found to have a function in chromatin, FBXL10 acts as a transcriptional repressor of c-Jun and c-Fos by binding to their promoter through its JmjC DNA-binding domain [216, 217].

The inhibition of degradation of Snail1 by FBXL5 in the presence of Lats2 shows that the phosphorylation of T203 prevents the action of the FBXL5 ubiquitin ligase. The modification induced by Lats2 on Snail1 does not allow the protein to change its cellular compartment for reasons that remain to be elucidated [93]. We speculate that Snail1 phosphorylation on T203 may recruit chaperone-binding proteins that prevent CMR1 binding and thus Snail1 export. In fact there are two chaperones that have been reported to increase Snail1 protein stability, HSP27 and HSP90, which binds to Snail1 when S100 is phosphorylated by ATM [97, 218]. We have demonstrated *in vivo* and *in vitro* that the interaction of FBXL5 with Snail1 is not blocked by the presence of Lats2, a study complemented with the use of mutants T203A and T203E that mimic the Snail1 protein modified or unchanged by Lats2, respectively. These mutants presented similar binding to FBXL5 as the wt

form of Snail1. Lats2 inhibited the degradation by FBXL5; however, the ubiquitination of Snail1 was maintained and even increased when the two proteins were overexpressed. Therefore, despite the close location of the Lats2 modification to the binding region of Snail1 and FBXL5, ubiquitination was not impaired. There was actually more ubiquitination observed than only in the presence of FBXL5 since the ubiquitinated protein was possibly retained in the nucleus due to the phosphorylation of T203, preventing the exit and thus proteosomal degradation of Snail1. This fact was confirmed with the observation that FBXL5 cannot degrade Snail1 in the presence of the nuclear export inhibitor LMB. Similarly, the Snail1 mutant Snail1LA, unable to bind CRM1 due to its amino acid changes in the NES (leucines L139 and L142 to alanines), was not degraded by FBXL5. The addition of LMB or the use of the Snail1LA mutant *in vivo* did not prevent ubiquitination, similarly to what happened in the presence of Lats2. All together these results indicate that Snail1 cannot be efficiently degraded in the nucleus by FBXL5 and that it is when the modified protein exits this compartment that it can be depleted from the cell. We think that we would obtain similar results in the presence of molecules enhancing the stability of Snail1 such as other kinases like PKA or CK2α and even in the presence of OGT or PARP1 enzymes, which add an O-GlcNAc modification and ADP(ribosyl)ate Snail1, respectively. Although it is possible that one or more of these molecules could work in an alternative pathway by blocking the interaction or the ubiquitination of Snail1 by FBXL5, presenting a different mechanism to Snail1 retention in the nucleus by Lats2.

To determine the importance of FBXL5 modulation in physiological conditions we compared the levels of exogenous Snail1 and endogenous FBXL5 in cells under different conditions of stress. The down-regulation of FBXL5 protein post γ-irradiation was comparable to that of iron depletion, and Snail1 levels were significantly up-regulated. The series of experiments carried out to verify this effect clearly show that the down-regulation of FBXL5 after irradiation induces, at least in part, the stabilization of Snail1 protein. It has been previously described that Snail1 is stabilized due to DNA damage by phosphorylation of S100 by activated ATM [97]. This type of insult has also been linked to an increase in overall TGF-β levels, although the increase in this cytokine is found at longer times than 2h, the time at which we detect a notable down-regulation of FBXL5 [219]. This means that there may be a complimentary effect which leads to long-term Snail1 stabilization post γ-irradiation: first a rapidly induced down-regulation of FBXL5 levels and phosphorylation events by ATM and CHK1, and maintained stability by the expression of TGF-β as a consequence of the up-regulation of ATM. In fact, this model would be in agreement with a recently published study that demonstrates that Snail1 is required for

TGF-β synthesis, a pathway that may need the stabilization of Snail1 due to lack of FBXL5 after irradiation before being activated to maintain high Snail1 levels [126].

In studies carried out in bacteria it was shown that radio-resistance may be acquired by low intracellular iron levels due to the fact that there is less generation of ROS, offering protein protection upon this stress condition [220]. A more recent study shows that some cancer cells with low IRP1 levels and thus lower intracellular iron are also more radio-resistant [221]. Consistently, reduced levels of ROS have been attributed to increased survival of cancer stem cells (CSCs) and of stem cells in general in response to radiation [222]. These results show that there is a possible link between low iron levels in cells leading to down-regulated FBXL5 and increased Snail1 protein stability after irradiation. Apart from down-regulation of FBXL5 and phosphorylation on S100 by ATM it has been suggested by Nagarajan and coworkers that some degree of inactivation of GSK-3β may also help in the stabilization of Snail1 after γ-irradiation of lung cells [223], which may well be a characteristic of this type of cells as observed for hypoxia and SW620 cell line.

D.3. Tight regulation of Snail1 levels by ubiquitin ligases

β-Trcp1 was the first ligase to be described targeting Snail1 degradation in response to GSK-3β-mediated phosphorylation [83]. We have described FBXL14 and FBXL5 as potent Snail1 E3 ubiquitin ligases. Therefore there are three ubiquitin ligases that degrade Snail1, raising the question as to why a protein needs so many alternative posttranslational control pathways. Snail1 is a transcription factor important in development, mainly during gastrulation. Normally it should only be re-expressed in adulthood during wound healing; however, in fibrosis and cancer its role has negative implications. The down-regulation of Snail1 protein in adult tissues is through complicated mechanisms and pathways. We think that the involvement of so many E3 ligases in Snail1 protein turnover regulation is linked to the consequences its re-expression has in adult tissues and, in general, due to its importance.

FBXL14 and FBXL5 are ubiquitin ligases expressed throughout panels of cell lines, showing no correlation at basal levels with Snail1 expression. It seems these two ligases are involved in the constant down-modulation of the transcription factor, always keeping its levels to a minimum. These ligases are dis-regulated by stresses that have been associated to tumor progression, such as hypoxia and cell survival after irradiation. The two ligases probably complement each other due to their sub-cellular localization and to the inability of FBXL5 to degrade Snail1 in the nucleus. In fact it is quite possible that both FBXL14 and β-Trcp1 complement the action of FBXL5: β-Trcp1 may be more active in aiding phosphorylated Snail1 be proteolysed in the proteasome while FBXL14 probably deals with the remaining pool of Snail1. However, the possibility that the FBXL5-ubiquitinated Snail1 is directly degraded by the proteasome as it exits the nucleus has to be kept in mind; it may not require further action by other ligases before degradation. Experiments blocking β-Trcp1 and/or FBXL14 would confirm the complete sequence of events of the degradation pathway of Snail1 ubiquitinated in the nucleus.

The regulation of the two ligases that maintain a basal control of Snail1 protein levels differs in many aspects. FBXL14 levels are maintained through complex transcriptional management. We know that *FBXL14* mRNA levels are probably governed by the presence of the NAT. The function of the other two sense transcripts, if any, is yet to be determined. In turn these levels are regulated by Snail1 protein through binding to the chromatin. It is not strange to find that the degradation target of a ligase can modulate its levels. In fact, Mdm2 and its substrate p53 are in a self-regulatory loop that ensures there is never an overload of Mdm2 nor of p53 [224]; this is comparable to Snail1 and FBXL14 that also seem to form an auto-regulatory loop

(*Figure D.2*). Regarding FBXL5, the regulation is at protein level, since iron affects its stability and determines the integrity of the protein as it is being synthesized, and irradiation somehow causes it to be rapidly degraded. p53 is also an example of a transcription factor that is regulated by more than one ubiquitin ligase: Mdm2 and Mdmx, among 15 other described ligases [225]. The cooperation of the two proteins is thought to be essential for maintaining tissue homeostasis. Mdm2 and Mdmx regulate p53 in a differential manner, similarly to what happens with FBXL14 and FBXL5. Mdm2 degrades p53 directly but Mdmx inhibits p53 by binding to and masking its transcriptional domain, not necessarily causing its degradation [224, 226]. The need for different ligases to modulate transcription factors seems to be a general mechanism that remains to be fully understood.

To sum up we think that FBXL14 and FBXL5 are the ligases that mediate the control of the basal levels of Snail1 expression. This is supported by the fact that when we knock down the ligases Snail1 protein is highly stabilized and cells acquire a mesenchymal phenotype. However, when the third ligase, β-Trcp1, is down-regulated, there are no changes in Snail1 levels. No information is available regarding the knock down of Mdm2 on Snail1 levels. We think that the action of β-Trcp1 upon Snail1 may have been overestimated since it is always determined by the inhibition of the GSK-3β by LiCl. LiCl inhibition does not only affect the kinase in its role of exposing the phospho-degron for β-Trcp1 but also blocks the exit of Snail1 due to phosphorylation of the P-S rich domain [83]. This blockade inhibits the degradation by the cytoplasmic E3 ligase FBXL14 and makes us think that the overall effect on the β-Trcp1-dependent degradation of Snail1 is less than currently thought.

Regarding the specificity of the ubiquitin ligases it is known that FBXL14 acts as a master regulator of many transcription factors including Snail1/2, Zeb2 and Twist1. The β-Trcp1 pathway is known to affect Snail1 after phosphorylation by GSK-3β and, while this report was being written, Twist1 was published to be also regulated by this ligase after phosphorylation and export by the action of inhibitor of κB kinase-β (IKK-β) [227]. We have seen that FBXL5 targets both Snail1 and Snail2, although only the action of FBXL5 on Snail1 has been studied in depth. The gathering of this information indicates there is some degree of overlapping in the action of the ubiquitin ligases upon EMT transcription factors. While FBXL5 keeps nuclear Snail1 and Snail2 levels down FBXL14 ensures the action in the cytoplasm while also down-regulating Twist1 and Zeb2. β-Trcp1 degrades Snail1 and Twist1 in response to stimuli. The multiple pathways and mechanisms that lead to Snail1 protein stabilization confirms that this fine tuning is associated to the negative consequences increased Snail1 has in pathological processes.

D.4. Summary of the thesis: Snail1 regulation by proteasome degradation

Snail1 degradation is tightly regulated by different E3 ubiquitin ligases. Previous to our work it was described that β-Trcp1 degrades the transcription factor when it is phosphorylated in the nucleus by GSK-3β, exported to the cytoplasm, phosphorylated by the same kinase, recognized by β-Trcp1 through the phospho-degron, ubiquitinated and degraded [83]. This pathway of degradation can be blocked by growth factors and Wnt signaling (see **A** in the overview scheme).

The observation that Snail1 does not need to be previously phosphorylated to be degraded led us to look for a novel ligase targeting the transcription factor. We found that the cytoplasmic ligase FBXL14 targets a Snail1 mutant that cannot be phosphorylated in its P-S rich domain as well as phosphorylated Snail1. This ligase is down-regulated at transcriptional level by Twist1 expression, which is stabilized by the HIF-1α protein, a marker of hypoxia (see **B** in the overview scheme).

A sh RNA screening to investigate the existence of other E3 ligases regulating Snail1 showed that FBXL5 also controls Snail1 protein stability. This nuclear ubiquitin ligase can modify Snail1 when bound to DNA, ubiquitinate it in the same compartment and degrade it in the cytoplasm. The degradation by FBXL5 can be blocked by factors such as Lats2 affecting the export of Snail1 to the cytoplasm. The protein stability of the ligase is reduced when cells are submitted to γ-irradiation or when iron levels are depleted, causing Snail1 protein stabilization (see **C** in the overview scheme).

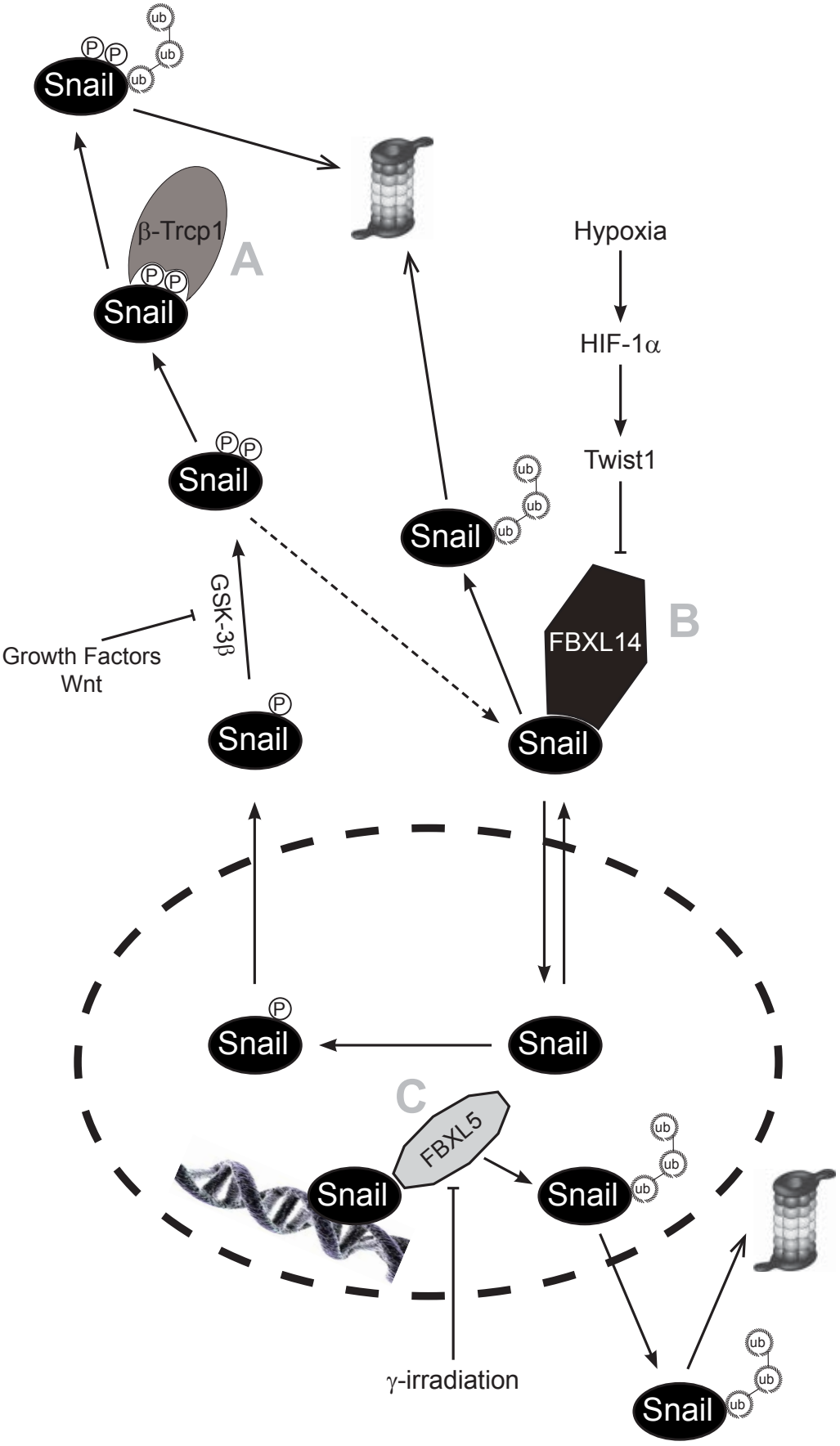
Snail
ub
P
β-Trcp1
A
Hypoxia
HIF-1α
Twist1
GSK-3β
Growth Factors
Wnt
B
FBXL14
C
FBXL5
γ-irradiation

CONCLUSIONS

The following conclusions can be drawn from the results presented in this PhD thesis:

1. Snail1 stability is regulated by the FBXL14 ubiquitin ligase, a mechanism alternative to the GSK-3β/β-Trcp1 pathway.

2. The N-terminal part of Snail1 is needed for degradation by FBXL14 which requires lysines 98, 137 and 148 for ubiquitination.

3. FBXL14 is down-regulated in hypoxia, correlating with Twist1 stabilization through increased HIF-1α levels, both in cell lines and in human tumor samples.

4. FBXL14 transcript regulation is complex as it has two sense and an antisense transcript (NAT) that are modulated by Snail1 protein levels.

5. FBXL5 is a nuclear ubiquitin ligase that degrades Snail1 and binds its C-terminal part, ubiquitinating lysines in the N-terminus (K85 and K146) and in the C-terminus (K234).

6. The ubiquitination of Snail1 by FBXL5 decreases its binding to DNA and occurs in the nuclear compartment although degradation is carried out in the cytoplasm.

7. FBXL5 levels are modulated by intracellular iron concentrations and reduced in response to γ-irradiation, correlating with stabilization of Snail1 in these conditions.

MATERIALS & METHODS

MM.1. Cell Culture

Cells were obtained from the Cancer Cell Line Repository (IMIM) and grown in Dulbecco's modified Eagle's medium (DMEM, Invitrogen) supplemented with 4.5 g/L glucose (Life Technologies), 2 mM glutamine, 56 U/ml penicillin, 56 µg/L streptomycin and 10% fetal bovine serum (FBS; all from GIBCO). Cells were maintained at 37°C in a humid atmosphere containing 5% CO_2 unless otherwise specified. NMuMG cell line was always supplemented with 10 µg/ml insulin (Invitrogen).

Cell line	Origin	Characteristics
SW620	Human colorectal adenocarcinoma	Epithelial cells mainly consisting of individual small spherical and bipolar cells lacking microvilli
MiaPaca-2	Human pancreatic carcinoma	Attached epithelial cells with floating rounded cells
RWP-1	Human pancreatic carcinoma	Epithelial morphology growing in colonies with well-formed intercellular junctions
NIH3T3	Mouse embryonic fibroblasts	Mesenchymal morphology with no expression of E-cadherin
HEK293T	Human embryonic kidney	Contains the SV40 large T-antigen that allows for episomal replication of transfected plasmids with the SV40 origin of replication
HT29-M6	Human colon adenocarcinoma	Epithelial morphology with high levels of E-cadherin
MDA-MB-231	Human breast carcinoma	Epithelial cells with low levels of E-cadherin
NMuMG	Mouse mammary cells	Epithelial morphology with high levels of E-cadherin
MCF7	Human breast adenocarcinoma	Epithelial morphology with high levels of E-cadherin

Table MM.1. Cell lines. Description of the characteristics of the different cell lines used during this study.

Stable HT29-M6 expressing pcDNA3-Snail1-HA were generated and maintained in our laboratory [228] through the addition of the G418 antibiotic (GIBCO) to the medium at 500 µg/ml. Stable RWP-1 cells expressing pcDNA3-Snail1-HA were also generated in our laboratory [64] and maintained in the same conditions as the HT29-M6 Snail1-HA clone, using 500 µg/ml G418 in the cell culture.

MM.1.1. Cell treatments

To carry out various experiments cells were treated with different molecules for the indicated times at the concentrations shown in *Table MM.2*. Hypoxic conditions were set up by placing the cells into a 1% O_2, 5% CO_2 and 96% N_2 atmosphere for the indicated time and γ-irradiation of cells was carried out at the indicated specific energy (gray; Gy) using the radioactive source Radionucleid Cs 137 and the IBL 437c version H irradiation apparatus.

Molecule	Effect	Supplier	Concentration for use
TGF-β	EMT inducer	PeproTec	5 ng/ml
LiCl	GSK-3β inhibitor	Sigma	50 mM
MG132 (Z-Leu-Leu-Leu-al)	Proteasome inhibitor	Sigma	10-50 μM
Cycloheximide (CHX)	Protein synthesis inhibitor	Sigma	20 μg/ml
Leptomycin B (LMB)	Nuclear export inhibitor (binds CRM1)	Sigma	5 ng/ml
Actinomycin D (ActD)	Transcription inhibitor	Sigma	2.5 μg/ml
Ferric Ammonium Citrate (III) (FAC)	Increase in iron levels	Sigma	100 μM
Deferoxamine mesylate (DFX)	Iron chelator	Sigma	100 μM
Doxorubicin	DNA damage by intercalating DNA	Sigma	10 μM
Etoposide	Topoisomerase I inhibitor	Calbiochem	10 μM

Table MM.2. Cell treatments. Detailed description of the cell treatments used in this work.

MM.2. Plasmid construction

The general cloning protocol for all the constructs was by (a) producing a linear insert containing the desired DNA sequence obtained by PCR amplification (Platinum Pfx DNA polymerase, Invitrogen) from genomic DNA or from a plasmid containing the insert; (b) by amplification from mRNA by RT-PCR; or (c) by excising the DNA sequence of interest from a plasmid by means of restriction enzymes. The recipient vector and insert were digested using endonucleases purchased from New England Biolabs (NEB) when needed and the linearized vector de-phosphorylated for 1h at 37°C with Calf Intestinal Phosphatase (CIP). After each step the DNA of interest was purified from solution or from an agarose gel through the Illustra GFX PCR DNA and Gel Band Purification kit (GE Healthcare) and eluted using H_2O. Ligation was carried out overnight at room temperature using a 1:5 ratio vector:insert and T4 DNA ligase (NEB). The resulting ligation was transformed in heat shock-activated DH5α *E. coli* competent cells and colonies screened by endonuclease digestion and sequencing.

In the case that blunt edges were needed in the cloning strategy DNA ends were filled in using Klenow fragment (3'→ 5', NEB) for 15min at room temperature. PCR inserts cloned blunt were phosphorylated using T4 polynucleotide kinase (NEB) and Forward buffer (Invitrogen) for 15min at room temperature.

MM.2.1. Snail1 constructs

The pcDNA3-Snail1-HA, Snail1SA-HA, Snail1SD-HA, Snail1LA-HA and GFP-Snail1 (including the wt construct, the N-terminal and C-terminal deletion mutants, all the GFP-Snail1NT mutants: Δ90-120, 82-151, 82-138 and 1-138, and the GFP-Snail1CT-ΔZnF4 construct) were cloned in our lab and have been previously described [41, 65]. Snail1 point mutants were obtained by using the QuickChange site-directed mutagenesis kit (Stratagene) and the pcDNA3-Snail1-HA vector as template. To make the Snail1 C-terminal deletion constructs we removed a BglII/EcoRV Snail1 C-terminal fragment from the GFP-Snail1-HA leaving the HA tag and cloned the different ZnF domains amplifying them with specific primers containing BglII and EcoRV restriction sites (primers ΔZnF1-F, ΔZnF1F2-F and ΔZnF-R). The primers used are listed in *Table MM.3*.

The pGEX-GST-Snail1-HA construct was previously cloned in our lab in pGEX-6P-2 (GE Healthcare) using BamHI/NotI digestion sites [41]. The human pcDNA3-Snail1-HA wt, T203A and T203E mutants were kindly provided by Dr. Gregory D. Longmore (The BRIGHT Institute, Washington, USA) and were previously described [93]. The baculovirus expression

vector pFastBac1-6xHIS-TEV-Snail1-HA was obtained by subcloning of the pcDNA3-Snail1-HA insert by digestion with BamHI/NotI. The pEBG-2T-GST-Snail1-HA construct for expression in eukaryotic cells was obtained after subcloning a BamHI/NotI insert from pcDNA3-Snail1-HA expression vector and this vector was used to subclone the GST-Snail1-HA insert by digestion with EcoRI/NotI into the pFastBac1 vector. The Snail1-HA insert from pcDNA3 was cloned into pFastBacHT B vector with the 6xHIS tag (6xHIS-TEV-Snail1-HA). pBabe-Snail1-HA was cloned using blunt ends by excising the Snail1-HA from the pcDNA3-Snail1-HA vector with XhoI/BamHI and cloned into pBabe digested with EcoRI.

Primer	Sequence
K9R-1F	5'-CCTTCCTGGTCAGGAGGCCGTCCGAC-3'
K9R-1R	5'-GTCGGACGGCCTCCTGACCAGGAAGG-3'
K16R-1F	5'-CGACCCCCGCCGGAGGCCCAACTATAGC-3'
K16R-1R	5'-GCTATAGTTGGGCCTCCGGCGGGGGTCG-3'
K98R-1F	5'-CCGATGAGGACAGTG GCAGAAGCTCCAGCCGCCCAGC-3'
K98R-1R	5'-GCTGGGCGGCTGGGAGCTTCTGCCACTGTCCTCATCGG-3'
K137R-1F	5'-GGGCCAACTTCCCAGGCAGCTG-3'
K137R-1R	5'-CAGCTGCCTGGGAAGTTGGCCC-3'
K146R-1F	5'-CTCTCGGTGGCCAGGGACCCCCAGTCG-3'
K146R-1R	5'-CGACTGGGGGTCCCTGGCCACCGAGAG-3'
ΔZnF1-F	5'-GCAATAGATCTGCACGACCTGTGGAAAGG-3'
ΔZnF1F2-F	5'-GCAATAGATCTCCTGCTCCCACTGCAAC-3'
ΔZnF-R	5'-CAAGATATCCGCGAGGGCCTC-3'

Table MM.3. Snail1 cloning primers. Primers used to obtain point mutants of the pcDNA3-Snail1-HA construct and ZnF deletion mutants of the GFP-Snail1-HA.

MM.2.2. FBXL14 constructs

The FBXL14 cDNA was amplified by RT-PCR from 1 μg RNA of RWP-1 cells (SuperScript One Step RT-PCR, Invitrogen) with primers FB-1F and FB-1R which contain a Kozak start site and BamHI and EcoRV restriction sites, respectively. It was cloned into BamHI/EcoRV-digested pcDNA3 (Invitrogen) carrying a HA epitope and into pcDNA3.1-Myc-HisA. The F-box deletion mutant of FBXL14 (ΔF) was obtained using the forward primer FB-2F(ΔF) which included a BamHI restriction site and the FB-1R primer. The BamHI/NotI FBXL14-HA insert was subcloned into pGEX-6P-1 (GE Healthcare) to produce recombinant GST-FBXL14 and into pFastBac1 for the baculovirus expression system.

To carry out RNA interference experiments the short hairpin RNAs (shRNAs) against the human FBXL14 mRNA were designed using a small interfering RNA selection program [229]. Selected oligonucleotides containing target sequences were cloned into pSUPER-Neo-IRES-GFP (Oligoengine) using

5'-BglII and 3'-XhoI as restriction sites. The sequence of the four specific shRNAs and a non-specific scrambled shRNA are shown in *Table MM.4* (FB-si-1F to FB-si-4R).

Primer	Sequence
FB-1F	5'-AACGGATCCACCATGGAGACCCACATCTCATGC-3'
FB-1R	5'-CAAGATATCCCCTTCTGGAGCTTCCC-3'
FB-2F(ΔF)	5'-AACGGATCCACCATGGAGGCCAAGCTGCACCTGCGC-3'
FB-si-1F (637-659)	5'-GATCCCCGAAGCTCACAGATCTTTCTTTCAAGAGAAGAA AGATCTGTGAGCTTCTTTTTC-3'
FB-si-1R (637-659)	5'-TCGAGAAAAAGAAGCTCACAGATCTTTCTTCTCTTGAAA GAAAGATCTGTGAGCTTCGGG-3'
FB-si-2F (880-902)	5'-GATCCCCCCAGAGTCTGGCTTACATATTCAAGAGATATG TAAGCCAGACTCTGGTTTTTC-3'
FB-si-2R (880-902)	5'-TCGAGAAAAACCAGAGTCTGGCTTACATATCTCTTGAATA TGTAAGCCAGACTCTGGGGG-3'
FB-si-3F (999-1021)	5'-GATCCCCCGCTCAACATTGGACAGTGTTCAAGAGACACT GTCCAATGTTGAGCGTTTTTC-3'
FB-si-3R (999-1021)	5'-TCGAGAAAAACGCTCAACATTGGACAGTGTCTCTTGAACA CTGTCCAATGTTGAGCGGGG-3'
FB-si-4F (scrambled)	5'-GATCCCCGCCAGCTGGAGCACTGTAATTCAAGAGATTACA GTGCTCCAGCTGGCTTTTTC-3'
FB-si-4R (scrambled)	5'-TCGAGAAAAAAGCCAGCTGGAGCACTGTAATCTCTTGAAT TACAGTGCTCCAGCTGGCGGG-3'

Table MM.4. FBXL14 cloning primers. Primers used in the cloning of FBXL14-related constructs.

MM.2.3. FBXL5 constructs

The pcDNA3-6xMyc-FBXL5 and 6xMyc-ΔF-FBXL5 were a kind gift by Dr. James A. Wohlschlegel (University of Texas, USA) and were previously reported in [186]. The baculovirus expression vector pFastBac1-3xFlag-FBXL5 was a kind gift from Dr. Richard K. Bruick (University of Texas, USA) and was previously reported in [185]. A BamHI/XhoI FBXL5 insert was subcloned from pFastBac1-3xFlag-FBXL5 into pGEX-6P-1 to produce recombinant GST-FBXL5 protein.

GFP-FBXL5 construct was obtained by PCR amplification of the sequence from a pcDNA3-6xMyc-FBXL5 construct using the following primers: FW (XhoI restriction site) 5'-ATATCTCGAGATGCGCAAGGGGG-3', RV (BamHI restriction site) 5'-TATGGATCCTTCGCCAGAGCGGCAG-3', and cloned into peGFP-C1. For subcloning of 6xMyc-FBXL5 insert into pBabe for retroviral infection pBabe vector [230] was digested with EcoRI and pcDNA3-6xMyc-FBXL5 with EcoRV/BamHI. The plasmid was generated using blunt-end ligation after Klenow treatment. For cloning of pLKO-GFP-shRNA constructs pLKO.1 vectors containing the shRNAs for FBXL5 (Sigma) were digested with BamHI and then with ScaI to recover the plasmid. pGSCW [231] was digested with PvuI/BamHI and then with

ScaI for the GFP insert. The two parts were ligated together and tested for expression.

MM.2.4. Other plasmids

The pMT107 containing human ubiquitin (6xHIS) was a kind gift from Dr. Gabriel Gil-Gómez (IMIM, Barcelona). HIS-Ubiquitin-K7R plasmid was provided by Dr. Boudewijn M.T. Burgerin and the pcDNA3-Flag-β-Trcp1/Trcp2 were provided by Dr. Ger Strous (both from the University Medical Center Utrecht, The Netherlands). pcDNA3-Twist1-V5-HIS was a kind gift from Dr. Anthony O. Gramolini (Charles H. Best Institute, Toronto, Canada). pcDNA3-Zeb1 was cloned in our lab and was previously described [68]. pcDNA3-Flag-Lats2 was provided by Dr. Gregory D. Longmore (The BRIGHT Institute, Washington, USA). pcDNA3-Snail2-HA was cloned by cDNA amplification using the forward primer 5'-CCGGATCCACCATGCCGCGCTCCTTCC-3' and reverse primer 5'-CAAGATATCCGTGTGCCACACAGC-3' with BamHI and EcoRV restriction sites, respectively, and inserted in the pcDNA3-HA vector.

The pFastBac1 vectors used for baculovirus protein expression were pFastBac1-HA-Cullin1, pFastBac1-6xHIS-T7-Skp1, pFastBac1-Roc1/Rbx1 that were obtained after subcloning the BamHI/NotI (Cullin1 and Skp1) or BamHI/XhoI (Roc1/Rbx1) inserts from pBacPAK8 vectors kindly provided by Dr. Michele Pagano (New York University, USA) and Dr. Masaki Matsumoto (Kyushu University, Japan).

MM.3. Cell transfection and infection

MM.3.1. Degradation and overexpression assays

For degradation assays HEK293T cells were seeded in 6-well plates for 14h or until they reached 90–100% confluence and transfected with 200 ng Snail1-HA and 0.5–1.2 μg FBXL14-Myc, ΔF-FBXL14-Myc, Flag-β-Trcp1, Flag-β-Trcp1 or 6xMyc-FBXL5. When indicated GFP was used as an internal control. In experiments involving Flag-Lats2 the same amount of Snail1-HA was transfected, 0.5 μg 6xMyc-FBXL5 and 1 μg Lats2. For Twist1 and Snail2 degradation assays the quantity of these vectors transfected per well was 0.4 μg instead of the 0.2 μg employed for Snail1. Cells were harvested 24h after transfection. The transfection mix was as follows: 200 μl sterile 150 mM NaCl was placed in a micro-centrifuge tube and the required DNA was pipetted into the solution. 12 μl of 1 mg/ml polyethylenimine (PEI, Polysciences, Inc.) were added and the mixture was kept at room temperature for 15min. The solution was added drop-wise to the cells containing 3 ml cell culture medium.

Stable transfection of pSUPER-Neo-IRES-GFP-sh FBXL14 plasmids in SW620 cells was carried out with 4 μg of DNA using Lipofectamine®-PLUS™ reagent (Invitrogen) for 6h following manufacturer's instructions. Cells were selected with G418 (1 mg/ml for SW620) until the non-transfected controls were dead, GFP-expressing cells sorted and analyzed by Western blot and RT-PCR.

When overexpression experiments were carried out in RWP-1 Snail1-HA cells were seeded in p100 plates and transfected with 4 μg of the indicated plasmid with Lipofectamine™ 2000 (Invitrogen) during 6h following manufacturer's instructions and grown for 48h prior to cell lysis. Where indicated cells were treated with 10 μM MG132 and 100 μM FAC for 6h.

MM.3.2. Lentiviral infection

Lentiviral expression in different cell lines was used to stably knock down or down-regulate genes using shRNAs cloned in pLKO.1-puro vector (Sigma). The different shRNAs used in this work were from the Mission® shRNA library from Sigma, and unless otherwise indicated, a mix of four or five different shRNAs was simultaneously infected. Note that in the FBXL5 section when shRNAs are numbered their reference is the following, from one to five: TRCN4290, TRCN4291, TRC4292, TRCN4293 and TRC4294. All of them target the coding region of FBXL5 except shL5-4 (reference TRC4293) which targets the 3' UTR.

For viral infection HEK293T cells were seeded in p100 plates with 10 ml medium at high confluence and transfected using PEI (1.5 ml 150 mM NaCl, DNA and 78 µl PEI mixture incubated for 15min at room temperature) with a total of 20 µg DNA of which 50% was the indicated shRNA or an equally distributed quantity of different sequences targeting the same gene, 10% was the pCMV-VSV-G vector (codes for the viral envelope), 30% was the pMDLg/pRRE vector and 10% the pRSV rev vector, the last two being involved in the packaging of the virus. The medium was changed 24h after transfection and 5.5 ml fresh medium were added. The supernatant was used for transduction of cells at 24 and 48h after the medium change by filtering it through 45 µm membrane filters (Millipore) and addition of 0.8 µg/ml of polybrene to the viral supernatant, which was used to replace the medium of target cells. After the second round of infection the medium of the target cells was changed and puromycin added when indicated to select infected cells for 72h (*Table MM.5*). Cells expressing the shRNA were then expanded and their protein and mRNA levels analyzed.

Cell line	Puromycin selection (µg/ml)
NMuMG	2
SW620	4
MCF7	2
RWP-1	2.5

Table MM.5. Puromycin selection of cell lines. In order to generate stable cell lines puromycin was used after infection at the indicated concentrations for 72h.

MM.3.4. Retroviral infection

The procedure used for retroviral infection is similar to that of lentiviral infection. In this case the vector used was pBabe-puro for overexpression of proteins. The cells used for viral production were HEK293 Phoenix GagPol, which stably express the HIV-1 *GAG* and *POL* gene products [232]. Cells were seeded in p100 plates at high confluence and transfected using PEI as previously described with a total of 10 µg DNA of which 80% was the indicated pBabe vector and 20% was the pCMV-VSV-G vector, coding for the viral envelope. The rest of the procedure was the same as for lentiviral infection of cells.

MM.4. Protein analysis

Before analysis of protein extracts quantification in duplicates using the *DC* Protein Assay kit (Lowry method; Bio-Rad) was carried out. Unless indicated, prior to addition of the desired buffer for lysis cells were washed three times with cold PBS and scraped in the plate with the buffer.

MM.4.1. Total cell extracts

Total cell extracts were obtained with two different buffers. In FBXL14 experiments Total lysis buffer was used, and in FBXL5-related work 2% SDS (sodium dodecyl sulfate) lysis buffer was employed.

To obtain extracts with Total lysis buffer cell extracts were rotated at 4°C for 30min and centrifuged for 15min at 13,200 rpm. The supernatant was collected in a new tube and stored at -20°C. Cell extracts obtained with 2% SDS lysis buffer were kept at room temperature to avoid precipitation of the SDS, syringed five times, centrifuged at 13,200 rpm for 10min and boiled at 95°C for 3min.

Total lysis buffer	**2% SDS lysis buffer**
20 mM HEPES-KOH pH 7.8	2% SDS
25% glycerol	50 mM Tris-HCl pH 7.5
1% Triton X-100	10% glycerol
420 mM NaCl	
1.5 mM $MgCl_2$	
0.2 mM EDTA	
Protease inhibitors	

MM.4.2. Sub-fractionated cell extracts

To obtain cell extracts with differentiated cytoplasmic, nucleoplasmic and chromatin fractions cells were scrapped in cold Buffer A and the lysate pipetted up and down five times in order to break cell aggregates and kept on ice for 10min. A volume equal to 1/30th of the lysate of 10% Triton X-100 was added and the tube vortexed for 20s. Centrifugation of the sample for 1min at 11,000 was used to separate the cytoplasmic extract which was stored in a new tube. The remaining pellet (nucleus) was washed twice in Buffer A to avoid cross-contamination of sub-cellular compartments and then resuspended in Buffer C. It was rotated at 4°C for 20min and centrifuged at 13,200 rpm for 15min. The supernatant was stored as nucleoplasmic fraction. The pellet was again washed twice in Buffer C and then resuspended

in 2% SDS lysis buffer, following the same protocol as for total cell extracts to obtain a homogeneous chromatin fraction. This protocol was modified from [233].

Buffer A
10 mM HEPES-KOH pH 7.8
1.5 mM $MgCl_2$
10 mM KCl
Protease inhibitors

Buffer C
20 mM HEPES-KOH pH 7.8
25% glycerol
420 mM NaCl
1.5 mM $MgCl_2$
0.2 mM EDTA
Protease inhibitors

MM.4.3. Western blot

Protein was analyzed by SDS polyacrylamide gel electrophoresis (SDS-PAGE) by loading the samples previously mixed with 5x Loading buffer and boiled at 95°C for 3min. Gels had a 7.5–15% polyacrylamide concentration. The Mini-Protean System (Bio-Rad) was used to run gels in TGS buffer that were then transferred to Protran nitrocellulose membranes (Whatman) during 60–90 min depending on the molecular weight of the protein using Transfer buffer.

5x Loading buffer
250 mM Tris-HCl pH 6.8
10% SDS
0.02% Bromophenol blue
50% glycerol
20% β-mercaptoethanol

Transfer buffer
50 mM Tris-OH
386 mM glycine
0.1% SDS
20% methanol

TGS buffer
25 mM Tris-OH pH 8.3
192 mM glycine
5% SDS

TBS-T
25 mM Tris-HCl pH 7.5
137 mM NaCl
0.1% Tween-20

Ponceau S stain
0.5% Ponceau S
1% acetic acid

Prior to blocking, and to ensure that protein was loaded and transferred correctly onto the membrane, Ponceau S staining was performed to each membrane. Membranes were placed directly from the Transfer buffer to Ponceau S staining and rocked for 5min. The solution was removed and

various washes were performed to remove excess stain with distilled water. When needed the stained membrane was scanned.

Membranes were blocked in 5% skimmed milk or 3% BSA (phospho antibodies) in TBS-T for 1h and incubated in the desired antibody for another hour at room temperature or overnight at 4°C. After three 10min washes with TBS-T Horseradish peroxidase (HRP)-combined secondary antibody (Dako) was diluted in 5% skimmed milk and the membrane was incubated for 1h at room temperature. Prior to developing three more 10min washes with TBS-T were performed. Membranes were developed using Luminata Western HRP Substrates (Millipore) and exposed on Agfa-Curix or Hyperfilms ECL (Amersham) for proteins that were more difficult to detect.

MM.4.4. Coomassie staining

In order to stain polyacrylamide gels to visualize and quantify proteins Coomassie staining was used. Once the protein was separated in the polyacrylamide gel it was submerged in Coomassie solution for 1h or until the gel appeared completely blue. The Coomassie solution was then removed, Coomassie destaining solution added to the gel and several washes performed until the desired staining was obtained.

Coomassie solution	**Coomassie destaining solution**
0.1% Coomassie brilliant blue R250	40% methanol
20% methanol	10% acetic acid
10% acetic acid	
Filter prior to use	

MM.4.5. Immunoprecipitation (IP)

MM.4.5.1. IP of exogenous proteins

Immunoprecipitation of exogenous proteins was carried out using HEK293T cells seeded in p100 plates. When cells were at 90% confluence they were transfected using PEI with 4 μg of the indicated plasmids (in total 8 μg DNA per plate). Transfection was carried out by placing 1.5 ml sterile 150 mM NaCl in a micro-centrifuge tube and pipetting the desired DNA in each tube. Then 78 μl PEI were added and the solution was incubated at room temperature for 15min. The transfection solution was added to the plates containing 10 ml medium drop-wise and 24h after transfection cells were treated with 50 μM MG132 for 6h (FBXL14 experiments) or 100 μM FAC for

1h and then 10 μM MG132 for 4h (FBXL5 experiments). Cells were washed with cold PBS and lysed with 500 μl IP buffer A (FBXL14 experiments) or IP buffer B (FBXL5 experiments). The lysates were syringed five times, vortexed for 5s, rotated at 4°C for 15min and centrifuged at 13,200 rpm for 10min. The supernatant was placed in a new tube and one tenth of the volume stored as input.

For FBXL14 experiments protein A sepharose beads (Roche) were used and pre-clearing of the lysate for 1h at 4°C was performed. In FBXL5 experiments magnetic protein A beads were used (Thermo scientific) and pre-clearing was not required. The antibody for the IP was added to the lysate and rotated for 90min at 4°C and beads were added for 1h. Three 10min washes were performed with the used IP buffer, except for FBXL5 experiments in which the first wash was carried out with IP buffer B with a final NaCl concentration of 300 mM. Elution was carried out with 2x Loading buffer and boiling for 3min at 95°C.

MM.4.5.2. IP of endogenous proteins

To co-IP transfected FBXL14-Myc using the Snail1 antibody NIH3T3 cells were transiently transfected with 8 μg of FBXL14-Myc, treated for 6h with 50 μM MG132 and lysed in IP Buffer A following the same protocol for lysis as for IP of exogenous proteins. Extracts were pre-cleared using protein A sepharose (Roche) for 1h and rabbit anti-Snail1 pAb used for 2h at 4°C. Protein A sepharose was added overnight and then washed three times for 10min with IP buffer A. Elution was carried out with 2x Loading buffer and boiling for 3min at 95°C.

IP buffer A	**IP buffer B**
50 mM Tris-HCl pH 8.0	50 mM Tris-HCl pH 7.5
150 mM NaCl	150 mM NaCl
0.5% Triton X-100	5% glycerol
Protease inhibitors	1% Nonidet P-40
	Protease inhibitors

To achieve the endogenous co-IP of FBXL5 and Snail1 RWP-1 cells were grown to 80% confluence in p150 plates and treated with 100 μM FAC and 10 μM MG132 for 6h, lysed in 500 μl IP buffer B and processed as for IP with exogenous proteins. The indicated antibody was used overnight at 4°C and protein A magnetic beads (Thermo Scientific) added for 1h at 4°C. Five 10min washes were carried out prior to elution with 2x Loading buffer and boiling for 3min at 95°C.

When Immunoglobulin G (IgG) is indicated a quantity of IgGs (Sigma) equivalent to the quantity of antibody used in the specific conditions was added and the sample was treated equally as the one containing the specific antibody.

MM.4.6. Immunofluorescence (IF)

Cells were grown at low confluence on sterile coverslips in 24-well plates, transfected with the indicated plasmids for 24h and fixed with 4% paraformaldehyde for 15min at room temperature. After washing with PBS, cells were permeabilized with PBS-0.5% Triton X-100 for 5min and blocked with PBS-1% BSA for 1h for FBXL14 experiments or permeabilized and blocked simultaneously in PBS-5% BSA-0.5% Triton X-100 for 1h. Coverslips were incubated with the indicated antibodies in blocking buffer (PBS-1% BSA-0.02% Triton X-100) at 27°C, rinsed with PBS and incubated with purified Alexa-Fluor 488, Alexa-Fluor 555 or Alexa-Fluor 647-conjugated anti-mouse, rabbit or goat IgGs (depending on the primary antibody and the combination needed; all from Invitrogen) in blocking buffer for 1h at room temperature. The cover-slips were rinsed with PBS, stained with DAPI (Sigma) dissolved 1:20,000 in PBS for 5min and mounted with Fluoromount G (Electron Microscopy Sciences). Fluorescence was visualized using the inverted fluorescence microscope DM IRBE (Leica, Wetzlar, Germany) and captured in a TCS-NT Argon/Kripton confocal laser microscope for FBXL14 experiments or the Confocal TCS SPE (Leica) system with 630x amplification for FBXL5 experiments.

MM.4.7. Pulldown (PD) assays

HEK293T cells seeded in p100 plates were transfected with 5 µg of the indicated plasmids using PEI (as in IP procedure) and lysed in 500 µl pulldown (PD) lysis buffer (20 mM Tris-HCl pH 8.0, 150 mM NaCl, 1 mM EDTA, 0.5% Nonidet P-40 and protease inhibitors) 48h after transfection, rotated at 4°C for 30min, and centrifuged at 13,200 rpm for 10min. Lysates were pre-cleared using 2 µg GST protein and 30 µl bead volume of Glutathione Sepharose 4B. PD was performed with 2 µg GST, GST-Snail1-HA, GST-FBXL14 or GST-FBXL5 for 1h at 4°C and thoroughly washed three times for 10min in PD lysis buffer. Elution was carried out with 2x Loading buffer and boiling for 3min at 95°C. Standard Western blot procedure was used to analyze the samples.

For PD assays using *in vitro* purified proteins 0.2 pmol 3xFlag-FBXL5 were incubated with 2.5 pmol GST or GST-Snail1 (all from baculovirus) in 200 µl binding buffer (50 mM Tris-HCl pH 7.5, 1% Triton X-100, 1 mM EDTA and 1 mM DTT) for 25min at room temperature. Incubation with 20 µl bead

volume of Glutathione Sepharose 4B was carried out for 25min at room temperature to recover proteins bound to GST and beads were washed three times for 5min with 750 µl binding buffer. Elution was carried out with 2x Loading buffer and boiling for 3min at 95°C. Standard Western blot procedure was used to analyze the samples.

MM.4.8. Antibodies used

Protein	Species	Provider	Ref.	Dilution
Snail1	mouse mAb	hybridoma F9	[76]	WB 1:10 IF 1:1
Myc	mouse mAb	hybridoma 9E10		WB 1:200 IF 1:50
HA	rabbit pAb	Sigma	H6908	WB 1:2000 IP/IF 1:250
Tubulin	mouse mAb	Sigma	T9026	WB 1:10000
Flag	mouse mAb	Sigma	F3165	WB 1:10000
Flag	rabbit pAb	Sigma	F7425	WB 1:2000
Snail1	rabbit pAb	Abcam	ab82846	IP 1:200
γ-H2AX (P-Ser139)	mouse mAb	Abcam	ab22551	WB 1:2000
GFP	rabbit pAb	Abcam	ab6556	WB 1:5000
HIF-1α	mouse mAb	Abcam	ab1	WB 1:200
Twist1	rabbit pAb	Abcam	ab50581	WB 1:200
Skp1	rabbit mAb	Abcam	ab10546	WB 1:2000
H3	rabbit pAb	Abcam	ab1791	WB 1:40000
PK	mouse mAb	Chemicon	AB1235	WB 1:4000
FBXL5	rabbit pAb	Santa Cruz	sc-134984	IP/IF 1:50
FBXL5	goat pAb	Santa Cruz	sc-54364	WB 1:200 (BSA) IF 1:50
CtBP1	goat pAb	Santa Cruz	sc-5963	IF 1:100
Ubiquitin	goat pAb	Santa Cruz	sc-6085	WB 1:500
β-Trcp1	rabbit pAb	Santa Cruz	sc-33213	WB 1:500
Lamin B1	rabbit pAb	Santa Cruz	sc-20682	WB 1:1000
Sin3A	rabbit pAb	Santa Cruz	sc-994	WB 1:5000
Zeb1	goat pAb	Santa Cruz	sc-10572	WB 1:1000
β-catenin	mouse mAb	BD TD	610154	WB 1:2000
E-cadherin	mouse mAb	BD TD	610182	WB 1:4000
p120 catenin	mouse mAb	BD TD	610134	WB:1:2000
P-Ser9-GSK-3β	rabbit pAb	Cell Signalling	9336	WB 1:1000 (BSA)
GSK-3β	rabbit pAb	Cell Signalling	9332	WB 1:2000
HA	rat pAb	Roche	65850900	WB 1:2000
GST	goat pAb	GE Health-care	27-457701	WB 1:5000
V5	mouse mAb	Invitrogen	46-0705	WB 1:5000
PY20	mouse mAb	Millipore	05-947	WB 1:500 (BSA)
FK2	mouse mAb	Millipore	04-263	IP 1:1000
FBXW5	rabbit pAb		[226]	WB 1:2000

Table MM.6. Antibodies and their applications. The antibodies used in this study, their commercial information and dilution for use are described in detail (BD TD: BD Transduction Labs; Santa Cruz: Santa Cruz Biotechnology).

Due to the lack of information regarding endogenous detection of FBXL5 we decided to test different antibodies against this protein. *Figure MM.1* shows how transiently transfected Myc-FBXL5 can be detected with the goat anti-FBXL5 pAb (sc-54364, Santa Cruz Biotechnology) as well as with the Myc tag antibody (hybridoma 9E10). In this report, unless otherwise specified, this antibody is used for all the Western blot applications as well as for some IF experiments.

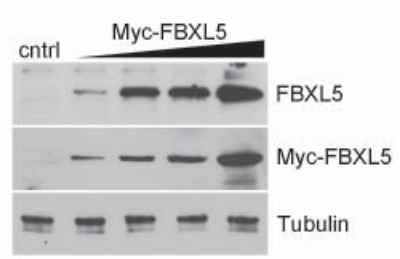

Figure MM.1. FBXL5 antibody test. The antibody used for FBXL5 detection was carefully selected for Western blot applications. In this case, HEK293T cells were transfected with increasing Myc-FBXL5 quantities and lysed after 24h. The levels of FBXL5 were analyzed in two independent membranes with goat anti-FBXL5 pAb and mouse anti-Myc mAb. Tubulin is shown as loading control.

MM.5. Ubiquitination assays

MM.5.1. *In vivo* ubiquitination assays

For *in vivo* ubiquitination assays in which the IP was carried out with rabbit anti-Snail1 pAb HEK293T cells seeded in p100 plates and transfected for 24h with 1 μg Snail1-HA and 5 μg FBXL14-Myc where indicated following the same PEI transfection protocol as for IPs. Prior to lysis cells were treated with 50 μM MG132 for 5h where indicated and lysed using an SDS denaturing buffer (IP buffer A containing 1% SDS). Cleared lysates were diluted 10-fold prior to IP which was carried out in the same conditions as the IP for endogenous proteins using the rabbit anti-Snail1 pAb.

For *in vivo* ubiquitination assays in which the IP was carried out with the mouse anti-FK2 mAb (which recognizes mono- and polyubiquitinated proteins) HEK293T cells were transfected as indicated for exogenous protein IP procedure and treated with 100 μM FAC and 10 μM MG132 for 4h. The cytoplasmic fraction was washed out when indicated using Buffer A and the pellet resuspended in RIPA buffer (50 mM Tris-HCl pH 7.5, 150 mM NaCl, 1% sodium deoxycholate, 0.1% SDS, 1 mM EDTA, 1% Triton X-100, NEM and protease inhibitors), rotated at 4°C for 10min and centrifuged at 13,200 rpm for 10min. For the IP 2 μg mouse anti-FK2 mAb antibody were used for 1h at 4°C, then 20 μl protein G magnetic beads (Thermo Scientific) were added and incubated at 4°C for 1h. Beads were washed three times in 1 ml RIPA buffer, and eluted with 2x Loading buffer and boiling for 3min at 95°C. Standard Western blot procedure was used to analyze the samples.

When the *in vivo* ubiquitination assays were carried out using overexpressed HIS-tagged ubiquitin (wt or K7R mutant) HEK293T or RWP-1 cells were seeded in 6-well plates and transfected for 24h with 200 ng Snail1-HA, 0.5 μg Ubi-HIS or UbiK7R-HIS and 0.5 μg 6xMyc-FBXL5 or control vector, using PEI in HEK293T cells or Lipofectamine™ 2000 (Invitrogen) for 6h in RWP-1 cells following manufacturer's instructions. In experiments involving Flag-Lats2 the transfection proportions were slightly changed, using 200 ng Snail1-HA, 0.8 μg Ubi-HIS or UbiK7R-HIS, 0.5 μg 6xMyc-FBXL5 or control vector and 1 μg Flag-Lats2. Only when the HIS-Ubi plasmid was used cells were treated with 25 μM MG132 for 4h prior to lysis. Cells were lysed in 500 μl of Buffer I (6 M guanidinium-HCl, 100 mM phosphate buffer at pH 8.0, 10 mM Tris-HCl pH 8.0, 0.2% Triton X-100, 5 mM imidazole and 10 mM β-mercaptoethanol), sonicated twice at 15% for 10s and incubated with 30 μl bead volume of equilibrated Nickel nitrilotriacetic acid (Ni-NTA) agarose beads (Qiagen) for 3h at room temperature. Beads were washed once in 1 ml Buffer I, once in 1 ml Buffer II (8 M urea, 100 mM phosphate buffer at pH 8.0, 10 mM Tris-HCl pH 8.0, 0.2% Triton X-100, 5 mM imidazole and

10 mM β-mercaptoethanol) and three times in 1 ml Buffer III (8 M urea, 100 mM phosphate buffer at pH 6.3, 10 mM Tris-HCl pH 6.3, 0.2% Triton X-100, 5 mM imidazole and 10 mM β-mercaptoethanol) [235]. A final wash was carried out using PBS before elution with 2x Loading buffer and boiling for 3min at 95°C. Standard Western blot procedure was used to analyze the samples.

MM.5.2. *In vitro* ubiquitination assays

For *in vitro* ubiquitination typical reactions were composed of 10–40 ng 6xHIS-Snail1-HA or GST-Snail1-HA, 0.5 –2 μg SCF^{FBXL14} or SCF^{FBXL5} (all purified from Sf9 insect cells unless otherwise indicated), 10 μg ubiquitin (wt, methylated ubiquitin which cannot elongate chains or the mutant ubiquitin K48 which is only able to elongate polyubiquitin chains through lysine 48), 40 ng E1 (6xHis-UBE1, Boston Biochem), 200 ng E3 (UbcH5c, Boston Biochem) in 20 μl reaction buffer containing 10 mM HEPES pH 7.5, 10 mM KCl, 100 mM NaCl, 1.5 mM $MgCl_2$, 1 mM DTT and 25 mM ATP for 1–2.5h at 30°C [185]. Reactions were stopped with 5x Loading buffer and boiled for 3min at 95°C. Standard Western blot procedure was used to analyze the samples unless otherwise indicated.

MM.6. Recombinant protein purification

MM.6.1. Recombinant proteins from *E. coli*

For purification of protein from *E. coli* (GST, GST-Snail1-HA, GST-FBXL14 and GST-FBXL5) the pGEX-6P-1 vectors were transformed in the BL21 *E. coli* strain and grown to saturation in 5 ml Luria-Beltrani (LB) broth supplemented with Ampicillin (50 μg/ml). The saturated culture was grown in 500 ml LB with Ampicillin until an OD_{600} of 0.6–0.8 was reached. Protein expression was induced using 0.1 M IPTG for 2h. All this procedure was carried out at 37°C. The bacterial pellet was collected after centrifugation of the culture at 4°C for 15min at 15,000xg. The pellet was resuspended in STE buffer containing 0.1 mg/ml lysozyme at 4°C for 15min. Protease and phosphatase inhibitors and 5 mM dithiothreitol (DTT) were added at this point. Sarcosyl detergent was added to 1% final concentration and mixed by pipetting. The lysate was sonicated five times at 15% for 15s on ice. A final concentration of 1% Triton X-100 was added, the lysate was vortexed for 20s and centrifuged at 15,000xg for 20min, and the supernatant was collected. Triton X-100 was added to a final concentration of 2% and vortexed for 20s.

The supernatant was incubated with 100 μl bead volume Gluthatione Sepharose 4E (GE Healthcare) per 250 ml of LB culture for 3h at 4°C and washed twice in cold PBS for 30min. Sepharose was equilibrated in Glutathione elution buffer (GEB) for 5min at room temperature and sequential elutions were carried out in 100 mM glutathione peptide (L-glutathione reduced, Sigma) in GEB at pH 8.0 for 10min at room temperature, all containing 5 mM DTT. Buffer exchange was performed using chromatography columns (Micro Bio-Spin® 6, Bio-Rad) and protein stored in aliquots at -80°C. Protein quantification was carried out using Coomassie staining of polyacrylamide gels and analysis of the bands using image software analysis (Image Quant, GE Healthcare LifeSciences).

STE buffer

10 mM Tris-HCl pH 8.0

150 mM NaCl

1 mM EDTA

Glutathione elution buffer

100 mM Tris-HCl pH 8.0

120 mM NaCl

10% glycerol

0.1% Triton X-100

HEGN buffer

25 mM HEPES-KOH pH 7.6

10% glycerol

0.02% Nonidet P-40

MM.6.2. Recombinant proteins from infected Sf9 cells

pFastBac1 baculovirus vectors coding for HA-Cullin1, 6xHIS-Skp1, Roc/Rbx1, FBXL14-HA, 3xFlag-FBXL5, 6xHIS-Snail1-HA and GST-Snail1-HA were used to generate recombinant bacmids using the Bac-to-Bac® system (Invitrogen). Isolated bacmids were transfected in Sf9 insect cells using the Cell Fectin II reagent (Invitrogen) to generate high titer baculoviruses. Infection of Sf9 cells was performed during 2–3 days and cell pellets were snap frozen and stored at -80°C.

Purification of the SCF^{FBXL5} or SCF^{FBXL14} complexes was done after infection for 48–72h of 6xHIS-Skp1, HA-Cullin1, Rbx1 and 3xFlag-FBXL5 or FBXL14-HA baculovirus at ratio 1:2:1:1, respectively. Lysis was carried out in HEGN buffer with 400 mM KCl (HEGN 400) and clarified cell extracts were diluted to 200 mM KCl with 10 mM Imidazole and incubated with 100-200 µl bead volume of Ni-NTA agarose beads for 3h, washed three times in HEGN 400 with 20 mM imidazole, once with HEGN 100 with 20 mM imidazole and eluted using HEGN 100 with 500 mM imidazole. Purified 6xHIS-Snail1-HA and SCF complexes were analyzed by SDS-PAGE and Coomassie staining, and quantified using a BSA standard and image software analysis (Image Quant, GE Healthcare LifeSciences).

For GST-Snail1-HA purification from infected Sf9 cells the pellet was resuspended in STE buffer with 1% Triton X-100, syringed 5 times and sonicated twice at 15% for 10s. The lysate was kept on ice for 10min and centrifuged at 15,000 rpm for 20min. Binding to Gluthatione Sepharose 4E beads, washing and elution was as for *E. coli* protein purification. Purification of 3xFlag-FBXL5 was carried out following the same protocol as for GST-Snail1 but using anti-Flag M2 affinity gel (A2220) and elution using the 3xFlag peptide (F4799, both from Sigma) following manufacturer's instructions. Again the proteins were analyzed by SDS-PAGE and Coomassie staining and quantified using a BSA standard and image software analysis (Image Quant, GE Healthcare LifeSciences).

MM.6.2.i. De-phosphorylation of GST-Snail1 from Sf9 cells

During the purification process of GST-Snail1 from Sf9 cells washed Gluthatione Sepharose beads with the bound protein were incubated with Calf Intestinal Phosphatase (CIP) in buffer NEB3 (100 mM NaCl, 50 mM Tris-HCl pH 7.9, 10 mM $MgCl_2$ and 1 mM DTT) for 20min at 30°C. The de-phosphorylated protein, which was still bound to the beads, was washed three times for 5min with 1 ml cold PBS and eluted as described for unmodified GST-Snail1.

MM.7. RNA analysis

MM.7.1. RNA extraction and semi-quantitative RT-PCR

Total RNA was extracted from cells with the RNeasy mini kit (Qiagen). For Snail1 amplification, 0.5 μg of total RNA were used with the Qiagen OneStep RT-PCR kit using specific primers. RNA was quantified using either a quartz cuvette and a Cary 50 UV-Vis spectrophotometer (Varian) or a NanoDrop™ Spectrophotometer (Thermo Scientific). For *FBXL14* and *HPRT* amplification 0.5 μg of total RNA were reverse-transcribed with the SuperScript™ First-Strand kit using Oligo dT (Invitrogen) according to the manufacturer's instructions and cDNA was used in semi-quantitative RT-PCR. The primers used were: L14-1, for human and murine *FBXL14* (200 ng cDNA, 34 cycles); SN-1, for murine *SNAIL1* (37 cycles); SN-2, for human *SNAIL1* (37 cycles); TW-1, for human and murine *TWIST1* (37 cycles); and HP-1, for human and murine *Hypoxanthine phosphoribosyltransferase* (*HPRT*; 100 ng; 34 cycles). For transcript analysis of *FBXL14* the indicated primers were used with 100 ng RNA and 37 cycles, with previous treatment of RNA with DNAse to avoid cross-contamination. For analysis of NAT the RT was carried out using the specific reverse primer and, before the PCR step, the forward primer was added to amplify the transcript in a strand-specific manner (*Table MM.7*).

MM.7.2. Phenol-chloroform RNA extraction

To extract RNA cells were washed three times with PBS and lysed in 800 μl TRIzol® reagent (phenol; Invitrogen). The lysate was vortexed, 200 μl chloroform added, mixed and incubated at room temperature for 2min. The solution was centrifuged at 13,200 rpm at 4°C for 15min and the clear supernatant was removed and mixed with 500 μl isopropanol. Incubation for 10min at room temperature precipitated the RNA which was pelleted at 13,200 rpm at 4°C for 15min. The pellet was washed with 1 ml 75% ethanol and centrifuged at 7,500 rpm at 4°C for 5min. After evaporation of all ethanol traces in a bath at 60°C the RNA pellet was resuspended in water and dissolved for 10min at 60°C prior to quantification.

MM.7.3. Quantitative RT-PCR

RNA was retrotranscribed using oligo dT and the Transcriptor First Strand cDNA Synthesis Kit (Roche) following manufacturer's instructions. Analyses were carried out in triplicates with 100–150 ng of cDNA using the LightCycler 480 Real Time PCR System (Roche). The primers used for quantitative RT-PCR are indicated in *Table MM.7* and can be identified since the primer name starts with a lower case *q*.

MM.7.4. Transcript analysis of tumor samples

Thirty-three samples of colon adenocarcinomas and their matched normal colon mucosa (taken, at least, 3 cm from the outer tumor margin) were obtained immediately after surgery, immersed in RNA *later*™ (Ambion Inc, Austin, Texas), snap-frozen in liquid nitrogen and stored at -80°C until processing. The use of these samples for the study was approved by the Research Ethics Board of the Hospital Universitario Puerta de Hierro (Madrid, Spain). RNA was extracted from tumor cell lines and from about 30 mg of tumor and normal tissues using RNeasy Mini Kit (Qiagen). RNA samples were treated with an RNase-free DNase, DNA-free™ (Ambion), as specified in the manufacturer's protocol and nucleic acids were quantified spectrophotometrically with the NanoDrop ND-1000 Spectrophotometer (NanoDrop Technologies, Inc, Wilmington, Delaware, USA).

The analysis of these samples was carried out as previously described [110]. 400 ng of RNA were retro-transcribed using the Gold RNA PCR Core Kit (PE Biosystems, Foster City, CA) and random hexamers. Real-time PCR was performed in a Light-Cycler apparatus (Roche Diagnostics, Mannheim, Germany) using the LightCycler-FastStart^{PLUS} DNA Master SYBR Green I Kit (Roche Diagnostics, Mannheim, Germany) and oligonucleotides corresponding to human *TWIST1* (TW-1), *FBXL14* (L14-2) and *Carbonic Anhydrase 9* (*CA9*; CA-1; *Table MM.7*). Expression of *TWIST1* RNA was only detected in 23 tumor samples and never in normal tissues. *FBXL14* RNA levels were calculated in the tumor and in normal tissues by a relative quantification approach. *CA9* was not detected in normal tissues; therefore, its expression was only determined in tumor tissues. An arbitrary value (0.001), corresponding to half the minimum value detected in the series, was assigned to three tumors in which *CA9* expression was not detected. The amounts in the target genes were expressed in relation to the expression of succinate dehydrogenase complex subunit A (SDHA; primers SDHA-1) [110]. The relative concentrations of targets and reference genes were calculated by interpolation, using a standard curve of each gene generated with a serial dilution of a cDNA prepared from RNA extracted from SW480-ADH cells. The expression levels of *FBXL14* for each patient were calculated as the ratio of its expression in tumor (T) versus its expression in normal tissue (N) (T/N).

As the gene expression values were not normally distributed (according to Kolmogorov-Smirnov test), to carry out the statistical analysis we normalized data distribution by using $\log_{10}$. Expression levels of *CA9* and *FBXL14* were contrasted with presence or absence of *TWIST1* expression in different tumor samples by ANOVA. *CA9* and *FBXL14* expression levels were studied by the Pearson test. Two-tailed p values ≤ 0.05 were considered

statistically significant. Statistical analysis was carried out using the SPSS statistical package, version 13.0.

MM.7.5. Primers used

Primer	Sequence
L14-1	5'-ATGGCATCAACCGCATGGTGC-3' and 5'-CCTTCTCACTGTCCGTCATCTGCC-3'
L14-2	5'-GGCTGCACCCGAATCACCAAG-3' and 5'-TCCCCTCGTGCCTCCTTCTCAC-3'
SN-1	5'-GCGCCCGTCGTCCTTCTCGTC-3' and 5'-CTTCCGCGACTGGGGGTCCT-3'
SN-2	5'-TTCCAGCGCCCTACGACCAG-3' and 5'-GCCTTTCCCACTGTCCTCATC-3
HP-1	5'-GGCCAGACTTTGTTGGATTTG-3' and 5'-TGCGCTCATCTTAGGCTTTGT-3'
TW-1	5'-CATGTCCGCGTCCCACTAG-3' and 5'-TGTCCATTTTCTCCTTCTCTGG-3'
CA-1	5'-ATCCACGTGGTTCACCTCAG-3' and 5'-CGATTTCTTCCAAGCGAGAC-3'
SDHA	5'-TGGGAACAAGAGGGCATCTG-3' and 5'-CCACCACTGCATCAAATTCATG-3'
L14-t2A	5'-GTGAGAAGGTCAGGGATTGCTCT-3' and 5'-CCACTCTGGTGCTGCTCAG-3'
L14-t2B	5'-GTGCCTCAAGGGATTGCTCT-3' and 5'-CCACTCTGGTGCTGCTCAG-3'
L14-NAT	5'-CCTTCTCACTGTCCGTCATCTGCC-3' and 5'-ATGGCATCAACCGCATGGTGC-3'
qSNAIL1	5'-GCCTTTCCCACTGTCCTCATC-3' and 5'-TTCCAGCAGCCCTACGACCAG-3'
qFBXL14	5'-TGCCTGTTCCCGGAGCTGCT-3' and 5'-CTTGTGGTAGGCGGCGTCCC-3'
qFBXL5	5'-CTTACCCAGACTGACATTTCAGATTC-3' and 5'-GAAGACTCTGGCAGCAACCAA-3'
qHPRT	5'-GGCCAGACTTTGTTGGATTTG-3' and 5'-TGCGCTCATCTTAGGCTTTGT-3'
qFBXW5	5'-CGCAGTGCCACAGGCGCCAA-3' and 5'-ACGGGCCCTGCCGTGGTCAT-3'
qFBXO3	5'-AGCCCGATTGGAAATGGGTCCTGATG-3' and 5'-AGGCGTGAGCAGCGGCGTCT-3'
qFBXO4	5'-TTCAGCGACTGGGGCCGCCT-3' and 5'-CAGCCGCGTCAGGGTGCTGG-3'
qFBXO5	5'-GCCGGTCCAGAAGACGGCGG-3' and 5'-TTACAACCGGCTCCCCACGTCCG-3'
qFBXO24	5'-GCCTAGGCTGGGGACATGGTGAA-3' and 5'-AGCGGCAGGTCTGGCCGAGG-3'
qFBXO25	5'-ACAGAAGATGGCTGGAAGAGATGT-3' and 5'-TAGCCATGCCTTTTGAGTATTTGTGT-3'
qFBXO27	5'-AGCTGCCAGTCTCCCGCCCG-3' and 5'-TCGGAGGCCTTCTTGGCCGCA-3'

Table MM.7. Primers used for mRNA analysis. The sequences of the different primers used in this study are listed. The first primer is forward and the second primer reverse; q: quantitative RT-PCR.

MM.8. Chromatin immunoprecipitation (ChIP)

Chromatin immunoprecipitation (ChIP) assays were performed using p150 plates of the indicated cells at 80% confluence. Cells were crosslinked with 1% formaldehyde in serum-free DMEM at 37°C for 10min. Crosslinking was stopped using a final concentration of 125 mM glycine for 2min at room temperature. From this point on all the processes were at 4°C. Cells were collected in 1 ml Soft lysis buffer, centrifuged at 3,000 rpm for 15min and the pellet resuspended in 0.5 ml SDS lysis buffer and sonicated 10 times for 10s at 40% (Branson) to generate DNA fragments of around 500 bp. Incubation of 20min on ice and centrifugation was used to verify lack of sedimentation of the chromatin. For IP 0.5–1 μg of chromatin was diluted 10 times in dilution buffer (final SDS concentration of 0.1%), incubated overnight with rabbit anti-HA pAb (1:250) or mouse hybridoma anti-Snail1 mAb (1:10), and immunocomplexes were recovered for 1h with blocked (BSA and sheared salmon sperm DNA) 20 μl protein A or protein G magnetic beads (Invitrogen), respectively. Beads were washed five times with 1 ml of each of the following buffers: Low salt, High salt, LiCl and TE and eluted for 30min at 37°C in 100 μl Elution buffer.

To de-crosslink proteins from DNA 200 mM final concentration of NaCl was added to each sample and incubated at 65°C for at least 4h. Proteinase K treatment was carried out by adding 10 μl 0.5 M EDTA, 20 μl 1 M Tris pH 6.5 and 2 μl Proteinase K (Sigma) for 1 h at 55°C. DNA was purified using the Illustra GFX PCR DNA and Gel Band Purification kit (GE Healthcare) and eluted using 50 μl of water. Bound DNA was detected by quantitative RT-PCR as for RNA analysis with the following primers: prom forward (FW) 5'-GCTTAGGGGAAGGCTGTTCC-3' and reverse (RV) 5'- CCCTCCAGTCGGTGTTCTAGAA-3'; primer 1 FW 5'-AGGCCAAGCTGCACCTG-3' and RV 5'-TTGTAGCAGCCGCTGAG GTT-3'; primer 2 FW 5'-TTCTGCTCATTGCCTGGG-3' and RV 5'-GTGAGTTTCTG GCAGTCCTGAA-3'; primer 3 FW 5'-AGGCTCCTCAACCTCAGCTT-3' and RV 5'-CATGGCCAGATGCATGATG-3'; and primer 4 FW 5'-CTGTGACA AGGTGGGAGATCA-3' and RV 5'-TGCATCTGCCGCACCAT-3'.

Soft lysis buffer

50 mM Tris-HCl pH 8.0
2 mM EDTA
0.1% Nonidet P-40
10% glycerol
Protease inhibitors

Dilution buffer

0.01% SDS
1.1% Triton X-100
1.2 mM EDTA
167 mM NaCl
16.7 mM Tris-HCl pH 8.0

High salt buffer

0.1% SDS
1% Triton X-100
2 mM EDTA
20 mM Tris-HCl pH 8.0
500 mM NaCl

TE buffer

10 mM Tris-HCl pH 8.0
1 mM EDTA pH 8.0

SDS lysis buffer

50 mM Tris-HCl pH 8.0
10 mM EDTA
1% SDS

Low salt buffer

0.1% SDS
1% Triton X-100
2 mM EDTA
20 mM Tris pH 8.0
150 mM NaCl

LiCl buffer

250 mM LiCl
1% Nonidet P-40
1% Sodium deoxycholate
1 mM EDTA
10 mM Tris-HCl pH 8.0

Elution buffer

1% SDS
100 mM Na_2CO_3

MM.9. Electrophoretic Mobility Shift Assay (EMSA)

The DNA probes were obtained by annealing the forward and reverse oligonucleotides in TEN buffer, placed at 95°C for 5min and allowed to cool down to room temperature in a dry heating block. The sequences corresponded to E-box 1 in the E-cadherin promoter (positions –64 to –92) with the following sequence: 5'-GGCTGAGGGTTCACCTGCCGCCACAGCC-3'. The mutated E-box 1 version was 5'-GGCTGAGGGTTAACCTACCGCCACAGCC-3' (mutated bases are underlined) [41]. The probe was labeled with ^{32}P using T4 polynucleotide kinase (Invitrogen) and Forward Reaction Buffer according to manufacturer's instructions. Excess unincorporated radioactive $\gamma^{32}P$-ATP was removed using Illustra MicroSpin G-50 Columns (GE Healthcare). The counts per minute (cpm) of the labeled probe were determined using the liquid scintillation analyzer Tri-Carb 2800TR (Perkin-Elmer). When used, the probe was diluted to 10,000 cpm/µl in TE buffer.

TEN Buffer
10 mM Tris-HCl pH 7.5
50 mM NaCl
1 mM EDTA

TBE buffer
45 mM Tris
45 mM boric acid
1 mM EDTA pH 8.0

EMSA loading buffer
20% Ficoll 400
0.25% Bromophenol blue
0.25% Cyanol xylene

Binding buffer
20 mM HEPES-KOH pH 7.9
100 mM KCl
3 mM $MgCl_2$
0.1% Nonidet P-40
1 mM DTT
1.5 µM $ZnCl_2$

6% non-denaturing gel (30 ml)
4.7 ml acrylamide:bisacrylamide 40% (19:1)
3 ml TBE 10x
400 µl 10% APS
40 µl TEMED

Recombinant proteins (in 10 mM Tris-HCl pH 7.4) were incubated in 20 µl Binding buffer on ice for 30min unless otherwise stated. 500 ng of poly dI-dC (Sigma) and 0.2 pmol of ^{32}P-labelled probe ($5x10^4$ cpm) were added to the reactions and incubated on ice for an additional 30min. For super-shift reactions 250 ng of rabbit IgG or rabbit pAb HA were added and incubated at room temperature for 15min. When competition was carried out with the wt or mutated probe 10-fold cold probe were used when compared to the labeled probe. In the case of binding of DNA to the product of a

ubiquitination reaction, the Binding buffer, the labeled probe and the poly dI-dC were added after the reaction time in a total volume of 30 µl and incubated on ice for 30min. Protein-bound DNA complexes were resolved in a 6% non-denaturing TBE-polyacrylamide gel and run at constant intensity of 10 mA in TBE buffer in the Protean® ii xi Cell System (Bio-Rad) previously pre-run for at least 1h at 10 mA. Before loading the samples the first sample (control) was mixed with EMSA loading buffer containing two dies that allowed for the tracking of the radioactive free probe in the gel as it was running. After running the gel was dried using 80°C heat in vacuum conditions for 1h and different expositions were made using Hyperfilms ECL (Amersham).

MM.10. Mass Spectrometry (MS) analysis

The protein bands excised from a Colloidal blue stained (Invitrogen) 4-20% Mini-Protean® TGX™ Precast polyacrylamide gel (Bio-Rad) were obtained from *in vitro* ubiquitination assays carried out as described in section *MM.5.2* using 4-fold more HIS-Snail1 than indicated. The reaction time was 2.5h and all the procedure was carried out avoiding keratin contamination of the samples. The two sections below describing the MS analysis included below were written and the procedures carried out by Drs. E. Sabidó and G. Espadas-García in the CRG/UPF Proteomics Unit (PRBB, Barcelona).

MM.10.1. Sample preparation

Gel bands were destained with 40 % acetonitrile in a 100 mM ammonium bicarbonate buffer, reduced with DTT (2 µM, 30min, 56°C) and alkylated in the dark with iodoacetamide (10 µM, 30 min, 25°C). Gel bands were then dehydrated with acetonitrile and digested with 0.3 µg of trypsin (Promega) overnight at 37˚C. After digestion, tryptic peptides were extracted and cleaned up on a homemade Empore C18 column (3M, St. Paul, MN, USA) [236].

The peptide mixes were analyzed using a LTQ-Orbitrap Velos mass spectrometer (Thermo Fisher Scientific, San Jose, CA, USA) coupled to an EasyLC (Thermo Fisher Scientific (Proxeon), Odense, Denmark). Peptides were loaded directly onto the analytical column at a flow rate of 1.5–2 µl/min using a wash-volume of four times the injection volume, and were separated by reversed-phase chromatography using a 12 cm column with an inner diameter of 75 µm, packed with 5 µm C18 particles (Nikkyo Technos Co., Ltd. Japan). Chromatographic gradients started at 97% buffer A and 3% buffer B with a flow rate of 300 nl/min, and gradually increased to 93% buffer A and 7% buffer B in 1min, and to 65% buffer A and 35% buffer B in 60min. After each analysis, the column was washed for 10min with 10% buffer A and 90% buffer B. Buffer A: 0.1% formic acid in water. Buffer B: 0.1% formic acid in acetonitrile.

The mass spectrometer was operated in positive ionization mode with nanospray voltage set at 2.2 kV and source temperature at 250°C. Ultramark 1621 for the FT mass analyzer was used for external calibration prior the analyses. Moreover, an internal calibration was also performed using the background polysiloxane ion signal at m/z 445.1200. The instrument was operated in DDA mode and full MS scans with one micro scan at resolution of 60,000 were used over a mass range of m/z 250-2,000 with detection in the Orbitrap. Auto gain control (AGC) was set to 1e6, dynamic exclusion (60 seconds) and the charge state filter disqualifying singly charged peptides was

activated. Following each survey scan the top twenty most intense ions with multiple charged ions above a threshold ion count of 5,000 were selected for fragmentation at normalized collision energy of 35%. Fragment ion spectra produced via collision-induced dissociation (CID) were acquired in the linear ion trap, AGC was set to 5e4, isolation window of 2.0 m/z, activation time of 0.1ms and maximum injection time of 100ms was used. All data were acquired with Xcalibur software v2.2.

MM.10.2. Data analysis

Proteome Discoverer software suite (v1.3.0.339, Thermo Fisher Scientific) and the Mascot search engine (v2.3, Matrix Science [237]) were used for peptide identification. Data were searched against an in-house generated database containing all proteins corresponding to mouse in the SwissProt database plus the most common contaminants as previously described [238]. A precursor ion mass tolerance of 7 ppm at the MS1 level was used, and up to three miscleavages for trypsin were allowed. The fragment ion mass tolerance was set to 0.5 Da. Oxidation of methionine, protein acetylation at the N-terminal, phosphorylation at serine, threonine and tyrosine and ubiquitination (glycine-glycine) at lysines were defined as variable modification. Carbamidomethylation on cysteines was set as a fix modification. The identified peptides were filtered using a Mascot Ion Score of 20.

MM.11. *In vitro* kinase assays

To phosphorylate recombinant Snail1 4 pmol of the purified protein were incubated with 100 ng CK2 (α and β subunits; Biaffin GmbH & Co KG) or 50 units GSK-3β (NEB) for 30min at 30°C and stopped with 2x Loading buffer and boiling at 95°C for 3min. The reaction was carried out in a total volume of 10 µl containing 20 mM Tris-HCl pH 8.0, 100 mM NaCl, 125 µg/ml BSA, 20 mM $MgCl_2$, 0.75 mM DTT and 125 µM ATP. When using radioactive ATP 2 µCi were added to the 125 µM ATP. Radioactive reactions were employed as positive control of the activity of the kinase upon the target protein, and one third of the reaction was loaded and separated in a 10% polyacrylamide gel. After running, the gel was dried using 80°C heat in vacuum conditions for 1h and different expositions were made using Hyperfilms ECL (Amersham). The non-radioactive reactions performed in parallel were used for pulldown and *in vitro* ubiquitination assays as described in the corresponding sections.

REFERENCES

1. Lodish, H., A. Berk, S.L. Zipursky, P. Matsudaira, D. Baltimore, and J. Darnell, *Molecular Cell Biology*. 4th ed. 2000, New York: W. H. Freeman.

2. Evan, G. and T. Littlewood, *A matter of life and cell death.* Science, 1998. **281**(5381): p. 1317-22.

3. Luo, J., N.L. Solimini, and S.J. Elledge, *Principles of cancer therapy: oncogene and non-oncogene addiction.* Cell, 2009. **136**(5): p. 823-37.

4. Hanahan, D. and R.A. Weinberg, *Hallmarks of cancer: the next generation.* Cell, 2011. **144**(5): p. 646-74.

5. Hanahan, D. and R.A. Weinberg, *The hallmarks of cancer.* Cell, 2000. **100**(1): p. 57-70.

6. Shankaran, V., H. Ikeda, A.T. Bruce, J.M. White, P.E. Swanson, L.J. Old, and R.D. Schreiber, *IFNgamma and lymphocytes prevent primary tumour development and shape tumour immunogenicity.* Nature, 2001. **410**(6832): p. 1107-11.

7. Kroemer, G. and J. Pouyssegur, *Tumor cell metabolism: cancer's Achilles' heel.* Cancer Cell, 2008. **13**(6): p. 472-82.

8. Thiery, J.P., H. Acloque, R.Y. Huang, and M.A. Nieto, *Epithelial-mesenchymal transitions in development and disease.* Cell, 2009. **139**(5): p. 871-90.

9. Yang, J. and R.A. Weinberg, *Epithelial-mesenchymal transition: at the crossroads of development and tumor metastasis.* Dev Cell, 2008. **14**(6): p. 818-29.

10. Lee, J.M., S. Dedhar, R. Kalluri, and E.W. Thompson, *The epithelial-mesenchymal transition: new insights in signaling, development, and disease.* J Cell Biol, 2006. **172**(7): p. 973-81.

11. Gros, J., M. Manceau, V. Thome, and C. Marcelle, *A common somitic origin for embryonic muscle progenitors and satellite cells.* Nature, 2005. **435**(7044): p. 954-8.

12. Monsoro-Burq, A.H., *Sclerotome development and morphogenesis: when experimental embryology meets genetics.* Int J Dev Biol, 2005. **49**(2-3): p. 301-8.

13. Johansson, K.A. and A. Grapin-Botton, *Development and diseases of the pancreas.* Clin Genet, 2002. **62**(1): p. 14-23.

14. Nakajima, Y., T. Yamagishi, S. Hokari, and H. Nakamura, *Mechanisms involved in valvuloseptal endocardial cushion formation in early cardiogenesis: roles of transforming growth factor (TGF)-beta and bone morphogenetic protein (BMP).* Anat Rec, 2000. **258**(2): p. 119-27.

15. Arnoux, V., M. Nassour, A. L'Helgoualc'h, R.A. Hipskind, and P. Savagner, *Erk5 controls Slug expression and keratinocyte activation during wound healing.* Mol Biol Cell, 2008. **19**(11): p. 4738-49.

16. Ahmed, N., S. Maines-Bandiera, M.A. Quinn, W.G. Unger, S. Dedhar, and N. Auersperg, *Molecular pathways regulating EGF-induced epithelio-mesenchymal transition in human ovarian surface epithelium.* Am J Physiol Cell Physiol, 2006. **290**(6): p. C1532-42.

17. Iwano, M., D. Plieth, T.M. Danoff, C. Xue, H. Okada, and E.G. Neilson, *Evidence that fibroblasts derive from epithelium during tissue fibrosis.* J Clin Invest, 2002. **110**(3): p. 341-50.

18. Kim, K.K., M.C. Kugler, P.J. Wolters, L. Robillard, M.G. Galvez, A.N. Brumwell, D. Sheppard, and H.A. Chapman, *Alveolar epithelial cell mesenchymal transition develops in vivo during pulmonary fibrosis and is regulated by the extracellular matrix.* Proc Natl Acad Sci U S A, 2006. **103**(35): p. 13180-5.

19. Boutet, A., C.A. De Frutos, P.H. Maxwell, M.J. Mayol, J. Romero, and M.A. Nieto, *Snail activation disrupts tissue homeostasis and induces fibrosis in the adult kidney.* EMBO J, 2006. **25**(23): p. 5603-13.

20. Acloque, H., M.S. Adams, K. Fishwick, M. Bronner-Fraser, and M.A. Nieto, *Epithelial-mesenchymal transitions: the importance of changing cell state in development and disease.* J Clin Invest, 2009. **119**(6): p. 1438-49.

21. Thiery, J.P., *Epithelial-mesenchymal transitions in tumour progression.* Nat Rev Cancer, 2002. **2**(6): p. 442-54.

22. Tarin, D., E.W. Thompson, and D.F. Newgreen, *The fallacy of epithelial mesenchymal transition in neoplasia.* Cancer Res, 2005. **65**(14): p. 5996-6000; discussion 6000-1.

23. Friedl, P. and S. Alexander, *Cancer invasion and the microenvironment: plasticity and reciprocity.* Cell, 2011. **147**(5): p. 992-1009.

24. Hanahan, D. and L.M. Coussens, *Accessories to the crime: functions of cells recruited to the tumor microenvironment.* Cancer Cell, 2012. **21**(3): p. 309-22.

25. Peinado, H., D. Olmeda, and A. Cano, *Snail, Zeb and bHLH factors in tumour progression: an alliance against the epithelial phenotype?* Nat Rev Cancer, 2007. **7**(6): p. 415-28.

26. Gupta, G.P. and J. Massague, *Cancer metastasis: building a framework.* Cell, 2006. **127**(4): p. 679-95.

27. Magee, J.A., E. Piskounova, and S.J. Morrison, *Cancer stem cells: impact, heterogeneity, and uncertainty.* Cancer Cell, 2012. **21**(3): p. 283-96.

28. Rhim, A.D., E.T. Mirek, N.M. Aiello, A. Maitra, J.M. Bailey, F. McAllister, M. Reichert, G.L. Beatty, A.K. Rustgi, R.H. Vonderheide, S.D. Leach, and B.Z. Stanger, *EMT and dissemination precede pancreatic tumor formation.* Cell, 2012. **148**(1-2): p. 349-61.

29. Sanchez-Tillo, E., Y. Liu, O. de Barrios, L. Siles, L. Fanlo, M. Cuatrecasas, D.S. Darling, D.C. Dean, A. Castells, and A. Postigo, *EMT-activating transcription factors in cancer: beyond EMT and tumor invasiveness.* Cell Mol Life Sci, 2012. **69**(20): p. 3429-56.

30. Brabletz, T., A. Jung, S. Spaderna, F. Hlubek, and T. Kirchner, *Opinion: migrating cancer stem cells - an integrated concept of malignant tumour progression.* Nat Rev Cancer, 2005. **5**(9): p. 744-9.

31. Fialkow, P.J., *Clonal origin of human tumors.* Biochim Biophys Acta, 1976. **458**(3): p. 283-321.

32. Hollier, B.G., K. Evans, and S.A. Mani, *The epithelial-to-mesenchymal transition and cancer stem cells: a coalition against cancer therapies.* J Mammary Gland Biol Neoplasia, 2009. **14**(1): p. 29-43.

33. de Herreros, A.G., S. Peiro, M. Nassour, and P. Savagner, *Snail family regulation and epithelial mesenchymal transitions in breast cancer progression.* J Mammary Gland Biol Neoplasia, 2010. **15**(2): p. 135-47.

34. Brabletz, T., *EMT and MET in metastasis: where are the cancer stem cells?* Cancer Cell, 2012. **22**(6): p. 699-701.

35. Tsai, J.H., J.L. Donaher, D.A. Murphy, S. Chau, and J. Yang, *Spatiotemporal regulation of epithelial-mesenchymal transition is essential for squamous cell carcinoma metastasis.* Cancer Cell, 2012. **22**(6): p. 725-36.

36. Ocaña, O.H., R. Corcoles, A. Fabra, G. Moreno-Bueno, H. Acloque, S. Vega, A. Barrallo-Gimeno, A. Cano, and M.A. Nieto, *Metastatic colonization requires the repression of the epithelial-mesenchymal transition inducer Prrx1.* Cancer Cell, 2012. **22**(6): p. 709-24.

37. Wang, Z., Y. Li, A. Ahmad, S. Banerjee, A.S. Azmi, D. Kong, and F.H. Sarkar, *Pancreatic cancer: understanding and overcoming chemoresistance.* Nat Rev Gastroenterol Hepatol, 2011. **8**(1): p. 27-33.

38. Xu, J., S. Lamouille, and R. Derynck, *TGF-beta-induced epithelial to mesenchymal transition.* Cell Res, 2009. **19**(2): p. 156-72.

39. Tsukita, S., M. Furuse, and M. Itoh, *Multifunctional strands in tight junctions.* Nat Rev Mol Cell Biol, 2001. **2**(4): p. 285-93.

40. Niessen, C.M. and C.J. Gottardi, *Molecular components of the adherens junction.* Biochim Biophys Acta, 2008. **1778**(3): p. 562-71.

41. Batlle, E., E. Sancho, C. Franci, D. Dominguez, M. Monfar, J. Baulida, and A. Garcia De Herreros, *The transcription factor snail is a repressor of E-cadherin gene expression in epithelial tumour cells.* Nat Cell Biol, 2000. **2**(2): p. 84-9.

42. Kemler, R., *From cadherins to catenins: cytoplasmic protein interactions and regulation of cell adhesion.* Trends Genet, 1993. **9**(9): p. 317-21.

43. Wheelock, M.J. and K.R. Johnson, *Cadherins as modulators of cellular phenotype.* Annu Rev Cell Dev Biol, 2003. **19**: p. 207-35.

44. De Craene, B., B. Gilbert, C. Stove, E. Bruyneel, F. van Roy, and G. Berx, *The transcription factor snail induces tumor cell invasion through modulation of the epithelial cell differentiation program.* Cancer Res, 2005. **65**(14): p. 6237-44.

45. Savagner, P., K.M. Yamada, and J.P. Thiery, *The zinc-finger protein slug causes desmosome dissociation, an initial and necessary step for growth factor-induced epithelial-mesenchymal transition.* J Cell Biol, 1997. **137**(6): p. 1403-19.

46. Cano, A., M.A. Perez-Moreno, I. Rodrigo, A. Locascio, M.J. Blanco, M.G. del Barrio, F. Portillo, and M.A. Nieto, *The transcription factor snail controls epithelial-mesenchymal transitions by repressing E-cadherin expression.* Nat Cell Biol, 2000. **2**(2): p. 76-83.

47. Giroldi, L.A., P.P. Bringuier, M. de Weijert, C. Jansen, A. van Bokhoven, and J.A. Schalken, *Role of E boxes in the repression of E-cadherin expression.* Biochem Biophys Res Commun, 1997. **241**(2): p. 453-8.

48. Nieto, M.A., *The snail superfamily of zinc-finger transcription factors.* Nat Rev Mol Cell Biol, 2002. **3**(3): p. 155-66.

49. Sefton, M., S. Sanchez, and M.A. Nieto, *Conserved and divergent roles for members of the Snail family of transcription factors in the chick and mouse embryo.* Development, 1998. **125**(16): p. 3111-21.

50. Bolos, V., H. Peinado, M.A. Perez-Moreno, M.F. Fraga, M. Esteller, and A. Cano, *The transcription factor Slug represses E-cadherin expression and induces epithelial to mesenchymal transitions: a comparison with Snail and E47 repressors.* J Cell Sci, 2003. **116**(Pt 3): p. 499-511.

51. Manzanares, M., A. Locascio, and M.A. Nieto, *The increasing complexity of the Snail gene superfamily in metazoan evolution.* Trends Genet, 2001. **17**(4): p. 178-81.

52. Peinado, H., E. Ballestar, M. Esteller, and A. Cano, *Snail mediates E-cadherin repression by the recruitment of the Sin3A/histone deacetylase 1 (HDAC1)/HDAC2 complex.* Mol Cell Biol, 2004. **24**(1): p. 306-19.

53. Herranz, N., D. Pasini, V.M. Diaz, C. Franci, A. Gutierrez, N. Dave, M. Escriva, I. Hernandez-Munoz, L. Di Croce, K. Helin, A. Garcia de Herreros, and S. Peiro, *Polycomb complex 2 is required for E-cadherin repression by the Snail1 transcription factor.* Mol Cell Biol, 2008. **28**(15): p. 4772-81.

54. Hou, Z., H. Peng, K. Ayyanathan, K.P. Yan, E.M. Langer, G.D. Longmore, and F.J. Rauscher, 3rd, *The LIM protein AJUBA recruits protein arginine methyltransferase 5 to mediate SNAIL-dependent transcriptional repression.* Mol Cell Biol, 2008. **28**(10): p. 3198-207.

55. Lin, T., A. Ponn, X. Hu, B.K. Law, and J. Lu, *Requirement of the histone demethylase LSD1 in Snai1-mediated transcriptional repression during epithelial-mesenchymal transition.* Oncogene, 2010. **29**(35): p. 4896-904.

56. Ferrari-Amorotti, G., V. Fragliasso, R. Esteki, Z. Prudente, A.R. Soliera, S. Cattelani, G. Manzotti, G. Grisendi, M. Dominici, M. Pieraccioli, G. Raschella, C. Chiodoni, M.P.

Colombo, and B. Calabretta, *Inhibiting Interactions of Lysine Demethylase LSD1 with Snail/Slug Blocks Cancer Cell Invasion.* Cancer Res, 2012.

57. Lin, Y., Y. Wu, J. Li, C. Dong, X. Ye, Y.I. Chi, B.M. Evers, and B.P. Zhou, *The SNAG domain of Snail1 functions as a molecular hook for recruiting lysine-specific demethylase 1.* EMBO J, 2010. **29**(11): p. 1803-16.

58. Vincent, T., E.P. Neve, J.R. Johnson, A. Kukalev, F. Rojo, J. Albanell, K. Pietras, I. Virtanen, L. Philipson, P.L. Leopold, R.G. Crystal, A.G. de Herreros, A. Moustakas, R.F. Pettersson, and J. Fuxe, *A SNAIL1-SMAD3/4 transcriptional repressor complex promotes TGF-beta mediated epithelial-mesenchymal transition.* Nat Cell Biol, 2009. **11**(8): p. 943-50.

59. Peinado, H., M. Del Carmen Iglesias-de la Cruz, D. Olmeda, K. Csiszar, K.S. Fong, S. Vega, M.A. Nieto, A. Cano, and F. Portillo, *A molecular role for lysyl oxidase-like 2 enzyme in snail regulation and tumor progression.* EMBO J, 2005. **24**(19): p. 3446-58.

60. Peinado, H., F. Portillo, and A. Cano, *Switching on-off Snail: LOXL2 versus GSK3beta.* Cell Cycle, 2005. **4**(12): p. 1749-52.

61. Nibu, Y., H. Zhang, and M. Levine, *Interaction of short-range repressors with Drosophila CtBP in the embryo.* Science, 1998. **280**(5360): p. 101-4.

62. Bailey, C.K., S. Misra, M.K. Mittal, and G. Chaudhuri, *Human SLUG does not directly bind to CtBP1.* Biochem Biophys Res Commun, 2007. **353**(3): p. 661-4.

63. Villagrasa, P., V.M. Diaz, R. Viñas-Castells, S. Peiro, B. Del Valle-Perez, N. Dave, A. Rodriguez-Asiain, J.I. Casal, J.M. Lizcano, M. Duñach, and A. Garcia de Herreros, *Akt2 interacts with Snail1 in the E-cadherin promoter.* Oncogene, 2012. **31**(36): p. 4022-33.

64. Peiro, S., M. Escriva, I. Puig, M.J. Barbera, N. Dave, N. Herranz, M.J. Larriba, M. Takkunen, C. Franci, A. Munoz, I. Virtanen, J. Baulida, and A. Garcia de Herreros, *Snail1 transcriptional repressor binds to its own promoter and controls its expression.* Nucleic Acids Res, 2006. **34**(7): p. 2077-84.

65. Dominguez, D., B. Montserrat-Sentis, A. Virgos-Soler, S. Guaita, J. Grueso, M. Porta, I. Puig, J. Baulida, C. Franci, and A. Garcia de Herreros, *Phosphorylation regulates the subcellular location and activity of the snail transcriptional repressor.* Mol Cell Biol, 2003. **23**(14): p. 5078-89.

66. Mingot, J.M., S. Vega, B. Maestro, J.M. Sanz, and M.A. Nieto, *Characterization of Snail nuclear import pathways as representatives of C2H2 zinc finger transcription factors.* J Cell Sci, 2009. **122**(Pt 9): p. 1452-60.

67. Ko, H., H.S. Kim, N.H. Kim, S.H. Lee, K.H. Kim, S.H. Hong, and J.I. Yook, *Nuclear localization signals of the E-cadherin transcriptional repressor Snail.* Cells Tissues Organs, 2007. **185**(1-3): p. 66-72.

68. Guaita, S., I. Puig, C. Franci, M. Garrido, D. Dominguez, E. Batlle, E. Sancho, S. Dedhar, A.G. De Herreros, and J. Baulida, *Snail induction of epithelial to mesenchymal transition*

in tumor cells is accompanied by MUC1 repression and ZEB1 expression. J Biol Chem, 2002. **277**(42): p. 39209-16.

69. Ikenouchi, J., M. Matsuda, M. Furuse, and S. Tsukita, *Regulation of tight junctions during the epithelium-mesenchyme transition: direct repression of the gene expression of claudins/occludin by Snail.* J Cell Sci, 2003. **116**(Pt 10): p. 1959-67.

70. Palmer, H.G., M.J. Larriba, J.M. Garcia, P. Ordonez-Moran, C. Pena, S. Peiro, I. Puig, R. Rodriguez, R. de la Fuente, A. Bernad, M. Pollan, F. Bonilla, C. Gamallo, A.G. de Herreros, and A. Munoz, *The transcription factor SNAIL represses vitamin D receptor expression and responsiveness in human colon cancer.* Nat Med, 2004. **10**(9): p. 917-9.

71. Radisky, D.C., D.D. Levy, L.E. Littlepage, H. Liu, C.M. Nelson, J.E. Fata, D. Leake, E.L. Godden, D.G. Albertson, M.A. Nieto, Z. Werb, and M.J. Bissell, *Rac1b and reactive oxygen species mediate MMP-3-induced EMT and genomic instability.* Nature, 2005. **436**(7047): p. 123-7.

72. Jung, H., K.P. Lee, S.J. Park, J.H. Park, Y.S. Jang, S.Y. Choi, J.G. Jung, K. Jo, D.Y. Park, J.H. Yoon, D.S. Lim, G.R. Hong, C. Choi, Y.K. Park, J.W. Lee, H.J. Hong, S. Kim, and Y.W. Park, *TMPRSS4 promotes invasion, migration and metastasis of human tumor cells by facilitating an epithelial-mesenchymal transition.* Oncogene, 2008. **27**(18): p. 2635-47.

73. Billottet, C., M. Tuefferd, D. Gentien, A. Rapinat, J.P. Thiery, P. Broet, and J. Jouanneau, *Modulation of several waves of gene expression during FGF-1 induced epithelial-mesenchymal transition of carcinoma cells.* J Cell Biochem, 2008. **104**(3): p. 826-39.

74. Ruan, K., S. Bao, and G. Ouyang, *The multifaceted role of periostin in tumorigenesis.* Cell Mol Life Sci, 2009. **66**(14): p. 2219-30.

75. Carver, E.A., R. Jiang, Y. Lan, K.F. Oram, and T. Gridley, *The mouse snail gene encodes a key regulator of the epithelial-mesenchymal transition.* Mol Cell Biol, 2001. **21**(23): p. 8184-8.

76. Franci, C., M. Takkunen, N. Dave, F. Alameda, S. Gomez, R. Rodriguez, M. Escriva, B. Montserrat-Sentis, T. Baro, M. Garrido, F. Bonilla, I. Virtanen, and A. Garcia de Herreros, *Expression of Snail protein in tumor-stroma interface.* Oncogene, 2006. **25**(37): p. 5134-44.

77. Franci, C., M. Gallen, F. Alameda, T. Baro, M. Iglesias, I. Virtanen, and A. Garcia de Herreros, *Snail1 protein in the stroma as a new putative prognosis marker for colon tumours.* PLoS One, 2009. **4**(5): p. e5595.

78. Cobaleda, C., M. Perez-Caro, C. Vicente-Duenas, and I. Sanchez-Garcia, *Function of the zinc-finger transcription factor SNAI2 in cancer and development.* Annu Rev Genet, 2007. **41**: p. 41-61.

79. Mittal, M.K., J.N. Myers, S. Misra, C.K. Bailey, and G. Chaudhuri, *In vivo binding to and functional repression of the VDR gene promoter by SLUG in human breast cells.* Biochem Biophys Res Commun, 2008. **372**(1): p. 30-4.

80. Mittal, M.K., K. Singh, S. Misra, and G. Chaudhuri, *SLUG-induced elevation of D1 cyclin in breast cancer cells through the inhibition of its ubiquitination.* J Biol Chem, 2011. **286**(1): p. 469-79.

81. Molina-Ortiz, P., A. Villarejo, M. MacPherson, V. Santos, A. Montes, S. Souchelnytskyi, F. Portillo, and A. Cano, *Characterization of the SNAG and SLUG domains of Snail2 in the repression of E-cadherin and EMT induction: modulation by serine 4 phosphorylation.* PLoS One, 2012. **7**(5): p. e36132.

82. Jiang, R., Y. Lan, C.R. Norton, J.P. Sundberg, and T. Gridley, *The Slug gene is not essential for mesoderm or neural crest development in mice.* Dev Biol, 1998. **198**(2): p. 277-85.

83. Zhou, B.P., J. Deng, W. Xia, J. Xu, Y.M. Li, M. Gunduz, and M.C. Hung, *Dual regulation of Snail by GSK-3beta-mediated phosphorylation in control of epithelial-mesenchymal transition.* Nat Cell Biol, 2004. **6**(10): p. 931-40.

84. Yook, J.I., X.Y. Li, I. Ota, E.R. Fearon, and S.J. Weiss, *Wnt-dependent regulation of the E-cadherin repressor snail.* J Biol Chem, 2005. **280**(12): p. 11740-8.

85. Yook, J.I., X.Y. Li, I. Ota, C. Hu, H.S. Kim, N.H. Kim, S.Y. Cha, J.K. Ryu, Y.J. Choi, J. Kim, E.R. Fearon, and S.J. Weiss, *A Wnt-Axin2-GSK3beta cascade regulates Snail1 activity in breast cancer cells.* Nat Cell Biol, 2006. **8**(12): p. 1398-406.

86. Xu, Y., S.H. Lee, H.S. Kim, N.H. Kim, S. Piao, S.H. Park, Y.S. Jung, J.I. Yook, B.J. Park, and N.C. Ha, *Role of CK1 in GSK3beta-mediated phosphorylation and degradation of snail.* Oncogene, 2010. **29**(21): p. 3124-33.

87. MacPherson, M.R., P. Molina, S. Souchelnytskyi, C. Wernstedt, J. Martin-Perez, F. Portillo, and A. Cano, *Phosphorylation of serine 11 and serine 92 as new positive regulators of human Snail1 function: potential involvement of casein kinase-2 and the cAMP-activated kinase protein kinase A.* Mol Biol Cell, 2010. **21**(2): p. 244-53.

88. Deshiere, A., E. Duchemin-Pelletier, E. Spreux, D. Ciais, F. Combes, Y. Vandenbrouck, Y. Coute, I. Mikaelian, S. Giusiano, C. Charpin, C. Cochet, and O. Filhol, *Unbalanced expression of CK2 kinase subunits is sufficient to drive epithelial-to-mesenchymal transition by Snail1 induction.* Oncogene, 2012.

89. Du, C., C. Zhang, S. Hassan, M.H. Biswas, and K.C. Balaji, *Protein kinase D1 suppresses epithelial-to-mesenchymal transition through phosphorylation of snail.* Cancer Res, 2010. **70**(20): p. 7810-9.

90. Bastea, L.I., H. Doppler, B. Balogun, and P. Storz, *Protein kinase D1 maintains the epithelial phenotype by inducing a DNA-bound, inactive SNAI1 transcriptional repressor complex.* PLoS One, 2012. **7**(1): p. e30459.

91. Eiseler, T., C. Kohler, S.C. Nimmagadda, A. Jamali, N. Funk, G. Joodi, P. Storz, and T. Seufferlein, *Protein kinase D1 mediates anchorage-dependent and -independent growth of tumor cells via the zinc finger transcription factor Snail1.* J Biol Chem, 2012. **287**(39): p. 32367-80.

92. Yang, Z., S. Rayala, D. Nguyen, R.K. Vadlamudi, S. Chen, and R. Kumar, *Pak1 phosphorylation of snail, a master regulator of epithelial-to-mesenchyme transition, modulates snail's subcellular localization and functions.* Cancer Res, 2005. **65**(8): p. 3179-84.

93. Zhang, K., E. Rodriguez-Aznar, N. Yabuta, R.J. Owen, J.M. Mingot, H. Nojima, M.A. Nieto, and G.D. Longmore, *Lats2 kinase potentiates Snail1 activity by promoting nuclear retention upon phosphorylation.* EMBO J, 2012. **31**(1): p. 29-43.

94. Roig, J. and J.A. Traugh, *p21-activated protein kinase gamma-PAK is activated by ionizing radiation and other DNA-damaging agents. Similarities and differences to alpha-PAK.* J Biol Chem, 1999. **274**(44): p. 31119-22.

95. Escriva, M., S. Peiro, N. Herranz, P. Villagrasa, N. Dave, B. Montserrat-Sentis, S.A. Murray, C. Franci, T. Gridley, I. Virtanen, and A. Garcia de Herreros, *Repression of PTEN phosphatase by Snail1 transcriptional factor during gamma radiation-induced apoptosis.* Mol Cell Biol, 2008. **28**(5): p. 1528-40.

96. Escriva, M., *Characterization of Snail1 and PTEN transcriptional regulation by Snail1: new insights into epithelial-to-mesenchymal transition and cell resistance to apoptosis*, in *Departament de Ciències de la Salut i de la Vida*. 2008, Universitat Pompeu Fabra: Barcelona.

97. Sun, M., X. Guo, X. Qian, H. Wang, C. Yang, K.L. Brinkman, M. Serrano-Gonzalez, R.S. Jope, B. Zhou, D.A. Engler, M. Zhan, S.T. Wong, L. Fu, and B. Xu, *Activation of the ATM-Snail pathway promotes breast cancer metastasis.* J Mol Cell Biol, 2012. **4**(5): p. 304-15.

98. Wang, S.P., W.L. Wang, Y.L. Chang, C.T. Wu, Y.C. Chao, S.H. Kao, A. Yuan, C.W. Lin, S.C. Yang, W.K. Chan, K.C. Li, T.M. Hong, and P.C. Yang, *p53 controls cancer cell invasion by inducing the MDM2-mediated degradation of Slug.* Nat Cell Biol, 2009. **11**(6): p. 694-704.

99. Lim, S.O., H. Kim, and G. Jung, *p53 inhibits tumor cell invasion via the degradation of snail protein in hepatocellular carcinoma.* FEBS Lett, 2010. **584**(11): p. 2231-6.

100. Vernon, A.E. and C. LaBonne, *Slug stability is dynamically regulated during neural crest development by the F-box protein Ppa.* Development, 2006. **133**(17): p. 3359-70.

101. Rodriguez, M.I., A. Gonzalez-Flores, F. Dantzer, J. Collard, A.G. de Herreros, and F.J. Oliver, *Poly(ADP-ribose)-dependent regulation of Snail1 protein stability.* Oncogene, 2011. **30**(42): p. 4365-72.

102. Park, S.Y., H.S. Kim, N.H. Kim, S. Ji, S.Y. Cha, J.G. Kang, I. Ota, K. Shimada, N. Konishi, H.W. Nam, S.W. Hong, W.H. Yang, J. Roth, J.I. Yook, and J.W. Cho, *Snail1 is stabilized by O-GlcNAc modification in hyperglycaemic condition.* EMBO J, 2010. **29**(22): p. 3787-96.

103. Wu, Y., B.M. Evers, and B.P. Zhou, *Small C-terminal domain phosphatase enhances snail activity through dephosphorylation.* J Biol Chem, 2009. **284**(1): p. 640-8.

104. Gheldof, A., P. Hulpiau, F. van Roy, B. De Craene, and G. Berx, *Evolutionary functional analysis and molecular regulation of the ZEB transcription factors.* Cell Mol Life Sci, 2012. **69**(15): p. 2527-41.

105. Vandewalle, C., J. Comijn, B. De Craene, P. Vermassen, E. Bruyneel, H. Andersen, E. Tulchinsky, F. Van Roy, and G. Berx, *SIP1/ZEB2 induces EMT by repressing genes of different epithelial cell-cell junctions.* Nucleic Acids Res, 2005. **33**(20): p. 6566-78.

106. Postigo, A.A., *Opposing functions of ZEB proteins in the regulation of the TGFbeta/BMP signaling pathway.* EMBO J, 2003. **22**(10): p. 2443-52.

107. Sanchez-Tillo, E., O. de Barrios, L. Siles, M. Cuatrecasas, A. Castells, and A. Postigo, *beta-catenin/TCF4 complex induces the epithelial-to-mesenchymal transition (EMT)-activator ZEB1 to regulate tumor invasiveness.* Proc Natl Acad Sci U S A, 2011. **108**(48): p. 19204-9.

108. Dave, N., S. Guaita-Esteruelas, S. Gutarra, A. Frias, M. Beltran, S. Peiro, and A.G. de Herreros, *Functional cooperation between Snail1 and twist in the regulation of ZEB1 expression during epithelial to mesenchymal transition.* J Biol Chem, 2011. **286**(14): p. 12024-32.

109. Eger, A., K. Aigner, S. Sonderegger, B. Dampier, S. Oehler, M. Schreiber, G. Berx, A. Cano, H. Beug, and R. Foisner, *DeltaEF1 is a transcriptional repressor of E-cadherin and regulates epithelial plasticity in breast cancer cells.* Oncogene, 2005. **24**(14): p. 2375-85.

110. Beltran, M., I. Puig, C. Pena, J.M. Garcia, A.B. Alvarez, R. Pena, F. Bonilla, and A.G. de Herreros, *A natural antisense transcript regulates Zeb2/Sip1 gene expression during Snail1-induced epithelial-mesenchymal transition.* Genes Dev, 2008. **22**(6): p. 756-69.

111. Ellenberger, T., D. Fass, M. Arnaud, and S.C. Harrison, *Crystal structure of transcription factor E47: E-box recognition by a basic region helix-loop-helix dimer.* Genes Dev, 1994. **8**(8): p. 970-80.

112. Qin, Q., Y. Xu, T. He, C. Qin, and J. Xu, *Normal and disease-related biological functions of Twist1 and underlying molecular mechanisms.* Cell Res, 2012. **22**(1): p. 90-106.

113. Fu, J., L. Qin, T. He, J. Qin, J. Hong, J. Wong, L. Liao, and J. Xu, *The TWIST/Mi2/NuRD protein complex and its essential role in cancer metastasis.* Cell Res, 2011. **21**(2): p. 275-89.

114. Yang, F., L. Sun, Q. Li, X. Han, L. Lei, H. Zhang, and Y. Shang, *SET8 promotes epithelial-mesenchymal transition and confers TWIST dual transcriptional activities.* EMBO J, 2012. **31**(1): p. 110-23.

115. Alexander, N.R., N.L. Tran, H. Rekapally, C.E. Summers, C. Glackin, and R.L. Heimark, *N-cadherin gene expression in prostate carcinoma is modulated by integrin-dependent nuclear translocation of Twist1.* Cancer Res, 2006. **66**(7): p. 3365-9.

116. Franco, H.L., J. Casasnovas, J.R. Rodriguez-Medina, and C.L. Cadilla, *Redundant or separate entities?--roles of Twist1 and Twist2 as molecular switches during gene transcription.* Nucleic Acids Res, 2011. **39**(4): p. 1177-86.

117. Yang, M.H., M.Z. Wu, S.H. Chiou, P.M. Chen, S.Y. Chang, C.J. Liu, S.C. Teng, and K.J. Wu, *Direct regulation of TWIST by HIF-1alpha promotes metastasis.* Nat Cell Biol, 2008. **10**(3): p. 295-305.

118. Fuxe, J., T. Vincent, and A. Garcia de Herreros, *Transcriptional crosstalk between TGF-beta and stem cell pathways in tumor cell invasion: role of EMT promoting Smad complexes.* Cell Cycle, 2010. **9**(12): p. 2363-74.

119. Ciruna, B. and J. Rossant, *FGF signaling regulates mesoderm cell fate specification and morphogenetic movement at the primitive streak.* Dev Cell, 2001. **1**(1): p. 37-49.

120. Birchmeier, W., V. Brinkmann, C. Niemann, S. Meiners, S. DiCesare, H. Naundorf, and M. Sachs, *Role of HGF/SF and c-Met in morphogenesis and metastasis of epithelial cells.* Ciba Found Symp, 1997. **212**: p. 230-40; discussion 240-6.

121. Rosario, M. and W. Birchmeier, *How to make tubes: signaling by the Met receptor tyrosine kinase.* Trends Cell Biol, 2003. **13**(6): p. 328-35.

122. Schulte, J., M. Weidig, P. Balzer, P. Richter, M. Franz, K. Junker, M. Gajda, K. Friedrich, H. Wunderlich, A. Ostman, I. Petersen, and A. Berndt, *Expression of the E-cadherin repressors Snail, Slug and Zeb1 in urothelial carcinoma of the urinary bladder: relation to stromal fibroblast activation and invasive behaviour of carcinoma cells.* Histochem Cell Biol, 2012. **138**(6): p. 847-60.

123. Wintzell, M., E. Hjerpe, E. Avall Lundqvist, and M. Shoshan, *Protein markers of cancer-associated fibroblasts and tumor-initiating cells reveal subpopulations in freshly isolated ovarian cancer ascites.* BMC Cancer, 2012. **12**(1): p. 359.

124. Raible, D.W., *Development of the neural crest: achieving specificity in regulatory pathways.* Curr Opin Cell Biol, 2006. **18**(6): p. 698-703.

125. Grunert, S., M. Jechlinger, and H. Beug, *Diverse cellular and molecular mechanisms contribute to epithelial plasticity and metastasis.* Nat Rev Mol Cell Biol, 2003. **4**(8): p. 657-65.

126. Batlle, R., L. Alba-Castellon, J. Loubat-Casanovas, E. Armenteros, C. Franci, J. Stanisavljevic, R. Banderas, J. Martin-Caballero, F. Bonilla, J. Baulida, J.I. Casal, T. Gridley, and A.G. de Herreros, *Snail1 controls TGF-beta responsiveness and differentiation of mesenchymal stem cells.* Oncogene, 2012.

127. Wu, J., J. Yang, and P.S. Klein, *Neural crest induction by the canonical Wnt pathway can be dissociated from anterior-posterior neural patterning in Xenopus.* Dev Biol, 2005. **279**(1): p. 220-32.

128. De Calisto, J., C. Araya, L. Marchant, C.F. Riaz, and R. Mayor, *Essential role of non-canonical Wnt signalling in neural crest migration.* Development, 2005. **132**(11): p. 2587-97.

129. Barrallo-Gimeno, A. and M.A. Nieto, *The Snail genes as inducers of cell movement and survival: implications in development and cancer.* Development, 2005. **132**(14): p. 3151-61.

130. Radtke, F. and K. Raj, *The role of Notch in tumorigenesis: oncogene or tumour suppressor?* Nat Rev Cancer, 2003. **3**(10): p. 756-67.

131. Cornell, R.A. and J.S. Eisen, *Notch in the pathway: the roles of Notch signaling in neural crest development.* Semin Cell Dev Biol, 2005. **16**(6): p. 663-72.

132. Timmerman, L.A., J. Grego-Bessa, A. Raya, E. Bertran, J.M. Perez-Pomares, J. Diez, S. Aranda, S. Palomo, F. McCormick, J.C. Izpisua-Belmonte, and J.L. de la Pompa, *Notch promotes epithelial-mesenchymal transition during cardiac development and oncogenic transformation.* Genes Dev, 2004. **18**(1): p. 99-115.

133. Wang, Z., Y. Li, D. Kong, S. Banerjee, A. Ahmad, A.S. Azmi, S. Ali, J.L. Abbruzzese, G.E. Gallick, and F.H. Sarkar, *Acquisition of epithelial-mesenchymal transition phenotype of gemcitabine-resistant pancreatic cancer cells is linked with activation of the notch signaling pathway.* Cancer Res, 2009. **69**(6): p. 2400-7.

134. Rho, J.K., Y.J. Choi, J.K. Lee, B.Y. Ryoo, Na, II, S.H. Yang, C.H. Kim, and J.C. Lee, *Epithelial to mesenchymal transition derived from repeated exposure to gefitinib determines the sensitivity to EGFR inhibitors in A549, a non-small cell lung cancer cell line.* Lung Cancer, 2009. **63**(2): p. 219-26.

135. Min, C., S.F. Eddy, D.H. Sherr, and G.E. Sonenshein, *NF-kappaB and epithelial to mesenchymal transition of cancer.* J Cell Biochem, 2008. **104**(3): p. 733-44.

136. Huber, M.A., N. Azoitei, B. Baumann, S. Grunert, A. Sommer, H. Pehamberger, N. Kraut, H. Beug, and T. Wirth, *NF-kappaB is essential for epithelial-mesenchymal transition and metastasis in a model of breast cancer progression.* J Clin Invest, 2004. **114**(4): p. 569-81.

137. Kim, H.J., B.C. Litzenburger, X. Cui, D.A. Delgado, B.C. Grabiner, X. Lin, M.T. Lewis, M.M. Gottardis, T.W. Wong, R.M. Attar, J.M. Carboni, and A.V. Lee, *Constitutively active type I insulin-like growth factor receptor causes transformation and xenograft growth of immortalized mammary epithelial cells and is accompanied by an epithelial-to-mesenchymal transition mediated by NF-kappaB and snail.* Mol Cell Biol, 2007. **27**(8): p. 3165-75.

138. Stanisavljevic, J., M. Porta-de-la-Riva, R. Batlle, A.G. de Herreros, and J. Baulida, *The p65 subunit of NF-kappaB and PARP1 assist Snail1 in activating fibronectin transcription.* J Cell Sci, 2011. **124**(Pt 24): p. 4161-71.

139. Wu, Y., J. Deng, P.G. Rychahou, S. Qiu, B.M. Evers, and B.P. Zhou, *Stabilization of snail by NF-kappaB is required for inflammation-induced cell migration and invasion.* Cancer Cell, 2009. **15**(5): p. 416-28.

140. Sullivan, N.J., A.K. Sasser, A.E. Axel, F. Vesuna, V. Raman, N. Ramirez, T.M. Oberyszyn, and B.M. Hall, *Interleukin-6 induces an epithelial-mesenchymal transition phenotype in human breast cancer cells.* Oncogene, 2009. **28**(33): p. 2940-7.

141. Waerner, T., M. Alacakaptan, I. Tamir, R. Oberauer, A. Gal, T. Brabletz, M. Schreiber, M. Jechlinger, and H. Beug, *ILEI: a cytokine essential for EMT, tumor formation, and late events in metastasis in epithelial cells.* Cancer Cell, 2006. **10**(3): p. 227-39.

142. Li, X., M.T. Lewis, J. Huang, C. Gutierrez, C.K. Osborne, M.F. Wu, S.G. Hilsenbeck, A. Pavlick, X. Zhang, G.C. Chamness, H. Wong, J. Rosen, and J.C. Chang, *Intrinsic resistance of tumorigenic breast cancer cells to chemotherapy.* J Natl Cancer Inst, 2008. **100**(9): p. 672-9.

143. Lopez-Novoa, J.M. and M.A. Nieto, *Inflammation and EMT: an alliance towards organ fibrosis and cancer progression.* EMBO Mol Med, 2009. **1**(6-7): p. 303-14.

144. Evans, A.J., R.C. Russell, O. Roche, T.N. Burry, J.E. Fish, V.W. Chow, W.Y. Kim, A. Saravanan, M.A. Maynard, M.L. Gervais, R.I. Sufan, A.M. Roberts, L.A. Wilson, M. Betten, C. Vandewalle, G. Berx, P.A. Marsden, M.S. Irwin, B.T. Teh, M.A. Jewett, and M. Ohh, *VHL promotes E2 box-dependent E-cadherin transcription by HIF-mediated regulation of SIP1 and snail.* Mol Cell Biol, 2007. **27**(1): p. 157-69.

145. Sahlgren, C., M.V. Gustafsson, S. Jin, L. Poellinger, and U. Lendahl, *Notch signaling mediates hypoxia-induced tumor cell migration and invasion.* Proc Natl Acad Sci U S A, 2008. **105**(17): p. 6392-7.

146. Hudson, L.G., C. Choi, K.M. Newkirk, J. Parkhani, K.L. Cooper, P. Lu, and D.F. Kusewitt, *Ultraviolet radiation stimulates expression of Snail family transcription factors in keratinocytes.* Mol Carcinog, 2007. **46**(4): p. 257-68.

147. Inoue, A., M.G. Seidel, W. Wu, S. Kamizono, A.A. Ferrando, R.T. Bronson, H. Iwasaki, K. Akashi, A. Morimoto, J.K. Hitzler, T.I. Pestina, C.W. Jackson, R. Tanaka, M.J. Chong, P.J. McKinnon, T. Inukai, G.C. Grosveld, and A.T. Look, *Slug, a highly conserved zinc finger transcriptional repressor, protects hematopoietic progenitor cells from radiation-induced apoptosis in vivo.* Cancer Cell, 2002. **2**(4): p. 279-88.

148. Cannito, S., E. Novo, A. Compagnone, L. Valfre di Bonzo, C. Busletta, E. Zamara, C. Paternostro, D. Povero, A. Bandino, F. Bozzo, C. Cravanzola, V. Bravoco, S. Colombatto, and M. Parola, *Redox mechanisms switch on hypoxia-dependent epithelial-mesenchymal transition in cancer cells.* Carcinogenesis, 2008. **29**(12): p. 2267-78.

149. Zhang, K.H., H.Y. Tian, X. Gao, W.W. Lei, Y. Hu, D.M. Wang, X.C. Pan, M.L. Yu, G.J. Xu, F.K. Zhao, and J.G. Song, *Ferritin heavy chain-mediated iron homeostasis and subsequent increased reactive oxygen species production are essential for epithelial-mesenchymal transition.* Cancer Res, 2009. **69**(13): p. 5340-8.

150. Weissman, A.M., N. Shabek, and A. Ciechanover, *The predator becomes the prey: regulating the ubiquitin system by ubiquitylation and degradation.* Nat Rev Mol Cell Biol, 2011. **12**(9): p. 605-20.

151. Marteijn, J.A., J.H. Jansen, and B.A. van der Reijden, *Ubiquitylation in normal and malignant hematopoiesis: novel therapeutic targets.* Leukemia, 2006. **20**(9): p. 1511-8.

152. Ravid, T. and M. Hochstrasser, *Diversity of degradation signals in the ubiquitin-proteasome system.* Nat Rev Mol Cell Biol, 2008. **9**(9): p. 679-90.

153. Varshavsky, A., *Naming a targeting signal.* Cell, 1991. **64**(1): p. 13-5.

154. Ang, X.L. and J. Wade Harper, *SCF-mediated protein degradation and cell cycle control.* Oncogene, 2005. **24**(17): p. 2860-70.

155. Li, W. and Y. Ye, *Polyubiquitin chains: functions, structures, and mechanisms.* Cell Mol Life Sci, 2008. **65**(15): p. 2397-406.

156. Huibregtse, J.M., M. Scheffner, and P.M. Howley, *A cellular protein mediates association of p53 with the E6 oncoprotein of human papillomavirus types 16 or 18.* EMBO J, 1991. **10**(13): p. 4129-35.

157. Scheffner, M. and O. Staub, *HECT E3s and human disease.* BMC Biochem, 2007. **8 Suppl 1**: p. S6.

158. Bernassola, F., M. Karin, A. Ciechanover, and G. Melino, *The HECT family of E3 ubiquitin ligases: multiple players in cancer development.* Cancer Cell, 2008. **14**(1): p. 10-21.

159. Metzger, M.B., V.A. Hristova, and A.M. Weissman, *HECT and RING finger families of E3 ubiquitin ligases at a glance.* J Cell Sci, 2012. **125**(Pt 3): p. 531-7.

160. Pickart, C.M. and R.E. Cohen, *Proteasomes and their kin: proteases in the machine age.* Nat Rev Mol Cell Biol, 2004. **5**(3): p. 177-87.

161. Pan, Z.Q., A. Kentsis, D.C. Dias, K. Yamoah, and K. Wu, *Nedd8 on cullin: building an expressway to protein destruction.* Oncogene, 2004. **23**(11): p. 1985-97.

162. Merlet, J., J. Burger, J.E. Gomes, and L. Pintard, *Regulation of cullin-RING E3 ubiquitin-ligases by neddylation and dimerization.* Cell Mol Life Sci, 2009. **66**(11-12): p. 1924-38.

163. Lipkowitz, S. and A.M. Weissman, *RINGs of good and evil: RING finger ubiquitin ligases at the crossroads of tumour suppression and oncogenesis.* Nat Rev Cancer, 2011. **11**(9): p. 629-43.

164. Kipreos, E.T. and M. Pagano, *The F-box protein family.* Genome Biol, 2000. **1**(5): p. REVIEWS3002.

165. Jin, J., T. Cardozo, R.C. Lovering, S.J. Elledge, M. Pagano, and J.W. Harper, *Systematic analysis and nomenclature of mammalian F-box proteins.* Genes Dev, 2004. **18**(21): p. 2573-80.

166. Sarikas, A., T. Hartmann, and Z.Q. Pan, *The cullin protein family.* Genome Biol, 2011. **12**(4): p. 220.

167. Deshaies, R.J. and C.A. Joazeiro, *RING domain E3 ubiquitin ligases.* Annu Rev Biochem, 2009. **78**: p. 399-434.

168. Ikeda, F. and I. Dikic, *Atypical ubiquitin chains: new molecular signals. 'Protein Modifications: Beyond the Usual Suspects' review series.* EMBO Rep, 2008. **9**(6): p. 536-42.

169. Bedford, L., R. Layfield, R.J. Mayer, J. Peng, and P. Xu, *Diverse polyubiquitin chains accumulate following 26S proteasomal dysfunction in mammalian neurones.* Neurosci Lett, 2011. **491**(1): p. 44-7.

170. Xu, P., D.M. Duong, N.T. Seyfried, D. Cheng, Y. Xie, J. Robert, J. Rush, M. Hochstrasser, D. Finley, and J. Peng, *Quantitative proteomics reveals the function of unconventional ubiquitin chains in proteasomal degradation.* Cell, 2009. **137**(1): p. 133-45.

171. Williamson, A., K.E. Wickliffe, B.G. Mellone, L. Song, G.H. Karpen, and M. Rape, *Identification of a physiological E2 module for the human anaphase-promoting complex.* Proc Natl Acad Sci U S A, 2009. **106**(43): p. 18213-8.

172. Duncan, L.M., S. Piper, R.B. Dodd, M.K. Saville, C.M. Sanderson, J.P. Luzio, and P.J. Lehner, *Lysine-63-linked ubiquitination is required for endolysosomal degradation of class I molecules.* EMBO J, 2006. **25**(8): p. 1635-45.

173. Ikeda, H. and T.K. Kerppola, *Lysosomal localization of ubiquitinated Jun requires multiple determinants in a lysine-27-linked polyubiquitin conjugate.* Mol Biol Cell, 2008. **19**(11): p. 4588-601.

174. Chastagner, P., A. Israel, and C. Brou, *Itch/AIP4 mediates Deltex degradation through the formation of K29-linked polyubiquitin chains.* EMBO Rep, 2006. **7**(11): p. 1147-53.

175. Peng, J., D. Schwartz, J.E. Elias, C.C. Thoreen, D. Cheng, G. Marsischky, J. Roelofs, D. Finley, and S.P. Gygi, *A proteomics approach to understanding protein ubiquitination.* Nat Biotechnol, 2003. **21**(8): p. 921-6.

176. Trotman, L.C., X. Wang, A. Alimonti, Z. Chen, J. Teruya-Feldstein, H. Yang, N.P. Pavletich, B.S. Carver, C. Cordon-Cardo, H. Erdjument-Bromage, P. Tempst, S.G. Chi, H.J. Kim, T. Misteli, X. Jiang, and P.P. Pandolfi, *Ubiquitination regulates PTEN nuclear import and tumor suppression.* Cell, 2007. **128**(1): p. 141-56.

177. Voges, D., P. Zwickl, and W. Baumeister, *The 26S proteasome: a molecular machine designed for controlled proteolysis.* Annu Rev Biochem, 1999. **68**: p. 1015-68.

178. Kisselev, A.F., W.A. van der Linden, and H.S. Overkleeft, *Proteasome inhibitors: an expanding army attacking a unique target.* Chem Biol, 2012. **19**(1): p. 99-115.

179. Sowa, M.E., E.J. Bennett, S.P. Gygi, and J.W. Harper, *Defining the human deubiquitinating enzyme interaction landscape.* Cell, 2009. **138**(2): p. 389-403.

180. Fraile, J.M., V. Quesada, D. Rodriguez, J.M. Freije, and C. Lopez-Otin, *Deubiquitinases in cancer: new functions and therapeutic options.* Oncogene, 2012. **31**(19): p. 2373-88.

181. Clague, M.J., J.M. Coulson, and S. Urbe, *Cellular functions of the DUBs.* J Cell Sci, 2012. **125**(Pt 2): p. 277-86.

182. Li, M., C.L. Brooks, F. Wu-Baer, D. Chen, R. Baer, and W. Gu, *Mono- versus polyubiquitination: differential control of p53 fate by Mdm2.* Science, 2003. **302**(5652): p. 1972-5.

183. Wykoff, C.C., N.J. Beasley, P.H. Watson, K.J. Turner, J. Pastorek, A. Sibtain, G.D. Wilson, H. Turley, K.L. Talks, P.H. Maxwell, C.W. Pugh, P.J. Ratcliffe, and A.L. Harris, *Hypoxia-inducible expression of tumor-associated carbonic anhydrases.* Cancer Res, 2000. **60**(24): p. 7075-83.

184. Zhang, N., J. Liu, X. Ding, F. Aikhionbare, C. Jin, and X. Yao, *FBXL5 interacts with p150Glued and regulates its ubiquitination.* Biochem Biophys Res Commun, 2007. **359**(1): p. 34-9.

185. Salahudeen, A.A., J.W. Thompson, J.C. Ruiz, H.W. Ma, L.N. Kinch, Q. Li, N.V. Grishin, and R.K. Bruick, *An E3 ligase possessing an iron-responsive hemerythrin domain is a regulator of iron homeostasis.* Science, 2009. **326**(5953): p. 722-6.

186. Vashisht, A.A., K.B. Zumbrennen, X. Huang, D.N. Powers, A. Durazo, D. Sun, N. Bhaskaran, A. Persson, M. Uhlen, O. Sangfelt, C. Spruck, E.A. Leibold, and J.A. Wohlschlegel, *Control of iron homeostasis by an iron-regulated ubiquitin ligase.* Science, 2009. **326**(5953): p. 718-21.

187. O'Shaughnessy, L. and S. Doyle, *Purification of proteins from baculovirus-infected insect cells.* Methods Mol Biol, 2011. **681**: p. 295-309.

188. Kanarek, N., E. Horwitz, I. Mayan, M. Leshets, G. Cojocaru, M. Davis, B.Z. Tsuberi, E. Pikarsky, M. Pagano, and Y. Ben-Neriah, *Spermatogenesis rescue in a mouse deficient for the ubiquitin ligase SCF{beta}-TrCP by single substrate depletion.* Genes Dev, 2010. **24**(5): p. 470-7.

189. Guardavaccaro, D., Y. Kudo, J. Boulaire, M. Barchi, L. Busino, M. Donzelli, F. Margottin-Goguet, P.K. Jackson, L. Yamasaki, and M. Pagano, *Control of meiotic and mitotic progression by the F box protein beta-Trcp1 in vivo.* Dev Cell, 2003. **4**(6): p. 799-812.

190. Lander, R., K. Nordin, and C. LaBonne, *The F-box protein Ppa is a common regulator of core EMT factors Twist, Snail, Slug, and Sip1.* J Cell Biol, 2011. **194**(1): p. 17-25.

191. Salnikov, A.V., L. Liu, M. Platen, J. Gladkich, O. Salnikova, E. Ryschich, J. Mattern, G. Moldenhauer, J. Werner, P. Schemmer, M.W. Buchler, and I. Herr, *Hypoxia induces EMT in low and highly aggressive pancreatic tumor cells but only cells with cancer stem cell characteristics acquire pronounced migratory potential.* PLoS One, 2012. **7**(9): p. e46391.

192. Lander, R., T. Nasr, S.D. Ochoa, K. Nordin, M.S. Prasad, and C. Labonne, *Interactions between Twist and other core epithelial-mesenchymal transition factors are controlled by GSK3-mediated phosphorylation.* Nat Commun, 2013. **4**: p. 1542.

193. Lundgren, K., B. Nordenskjold, and G. Landberg, *Hypoxia, Snail and incomplete epithelial-mesenchymal transition in breast cancer.* Br J Cancer, 2009. **101**(10): p. 1769-81.

194. Yang, M.H. and K.J. Wu, *TWIST activation by hypoxia inducible factor-1 (HIF-1): implications in metastasis and development.* Cell Cycle, 2008. **7**(14): p. 2090-6.

195. Doble, B.W. and J.R. Woodgett, *GSK-3: tricks of the trade for a multi-tasking kinase.* J Cell Sci, 2003. **116**(Pt 7): p. 1175-86.

196. Postow, L. and H. Funabiki, *An SCF complex containing Fbxl12 mediates DNA damage-induced Ku80 ubiquitylation.* Cell Cycle, 2013. **12**(4): p. 587-95.

197. Coon, T.A., J.R. Glasser, R.K. Mallampalli, and B.B. Chen, *Novel E3 ligase component FBXL7 ubiquitinates and degrades Aurora A, causing mitotic arrest.* Cell Cycle, 2012. **11**(4): p. 721-9.

198. Raj, L., P. Vivekanand, T.K. Das, E. Badam, M. Fernandes, R.L. Finley, R. Brent, L.F. Appel, S.D. Hanes, and M. Weir, *Targeted localized degradation of Paired protein in Drosophila development.* Curr Biol, 2000. **10**(20): p. 1265-72.

199. Moreno-Moreno, O., S. Medina-Giro, M. Torras-Llort, and F. Azorin, *The F box protein partner of paired regulates stability of Drosophila centromeric histone H3, CenH3(CID).* Curr Biol, 2011. **21**(17): p. 1488-93.

200. Zheng, H., Y. Du, Y. Hua, Z. Wu, Y. Yan, and Y. Li, *Essential role of Fbxl14 ubiquitin ligase in regulation of vertebrate axis formation through modulating Mkp3 level.* Cell Res, 2012. **22**(5): p. 936-40.

201. Das, T., C. Purkayastha-Mukherjee, J. D'Angelo, and M. Weir, *A conserved F-box gene with unusual transcript localization.* Dev Genes Evol, 2002. **212**(3): p. 134-40.

202. Viñas-Castells, R., M. Beltran, G. Valls, I. Gomez, J.M. Garcia, B. Montserrat-Sentis, J. Baulida, F. Bonilla, A.G. de Herreros, and V.M. Diaz, *The hypoxia-controlled FBXL14 ubiquitin ligase targets SNAIL1 for proteasome degradation.* J Biol Chem, 2010. **285**(6): p. 3794-805.

203. Orom, U.A., T. Derrien, M. Beringer, K. Gumireddy, A. Gardini, G. Bussotti, F. Lai, M. Zytnicki, C. Notredame, Q. Huang, R. Guigo, and R. Shiekhattar, *Long noncoding RNAs with enhancer-like function in human cells.* Cell, 2010. **143**(1): p. 46-58.

204. Godinho, S.I., E.S. Maywood, L. Shaw, V. Tucci, A.R. Barnard, L. Busino, M. Pagano, R. Kendall, M.M. Quwailid, M.R. Romero, J. O'Neill, J.E. Chesham, D. Brooker, Z. Lalanne, M.H. Hastings, and P.M. Nolan, *The after-hours mutant reveals a role for Fbxl3 in determining mammalian circadian period.* Science, 2007. **316**(5826): p. 897-900.

205. Thompson, J.W., A.A. Salahudeen, S. Chollangi, J.C. Ruiz, C.A. Brautigam, T.M. Makris, J.D. Lipscomb, D.R. Tomchick, and R.K. Bruick, *Structural and molecular characterization of iron-sensing hemerythrin-like domain within F-box and leucine-rich repeat protein 5 (FBXL5).* J Biol Chem, 2012. **287**(10): p. 7357-65.

206. Shu, C., M.W. Sung, M.D. Stewart, T.I. Igumenova, X. Tan, and P. Li, *The structural basis of iron sensing by the human F-box protein FBXL5.* Chembiochem, 2012. **13**(6): p. 788-91.

207. Thompson, J.W. and R.K. Bruick, *Protein degradation and iron homeostasis.* Biochim Biophys Acta, 2012. **1823**(9): p. 1484-90.

208. Chollangi, S., J.W. Thompson, J.C. Ruiz, K.H. Gardner, and R.K. Bruick, *Hemerythrin-like domain within F-box and leucine-rich repeat protein 5 (FBXL5) communicates cellular iron and oxygen availability by distinct mechanisms.* J Biol Chem, 2012. **287**(28): p. 23710-7.

209. Yu, Y., J. Wong, D.B. Lovejoy, D.S. Kalinowski, and D.R. Richardson, *Chelators at the cancer coalface: desferrioxamine to Triapine and beyond.* Clin Cancer Res, 2006. **12**(23): p. 6876-83.

210. Kalinowski, D.S. and D.R. Richardson, *The evolution of iron chelators for the treatment of iron overload disease and cancer.* Pharmacol Rev, 2005. **57**(4): p. 547-83.

211. Le, N.T. and D.R. Richardson, *Iron chelators with high antiproliferative activity up-regulate the expression of a growth inhibitory and metastasis suppressor gene: a link between iron metabolism and proliferation.* Blood, 2004. **104**(9): p. 2967-75.

212. Richardson, D.R., *Molecular mechanisms of iron uptake by cells and the use of iron chelators for the treatment of cancer.* Curr Med Chem, 2005. **12**(23): p. 2711-29.

213. Yu, Y., E. Gutierrez, Z. Kovacevic, F. Saletta, P. Obeidy, Y. Suryo Rahmanto, and D.R. Richardson, *Iron chelators for the treatment of cancer.* Curr Med Chem, 2012. **19**(17): p. 2689-702.

214. Le, N.T. and D.R. Richardson, *The role of iron in cell cycle progression and the proliferation of neoplastic cells.* Biochim Biophys Acta, 2002. **1603**(1): p. 31-46.

215. Chen, Z., D. Zhang, F. Yue, M. Zheng, Z. Kovacevic, and D.R. Richardson, *The iron chelators Dp44mT and DFO inhibit TGF-beta-induced epithelial-mesenchymal transition via up-regulation of N-Myc downstream-regulated gene 1 (NDRG1).* J Biol Chem, 2012. **287**(21): p. 17016-28.

216. Koyama-Nasu, R., G. David, and N. Tanese, *The F-box protein Fbl10 is a novel transcriptional repressor of c-Jun.* Nat Cell Biol, 2007. **9**(9): p. 1074-80.

217. Ge, R., Z. Wang, Q. Zeng, X. Xu, and A.F. Olumi, *F-box protein 10, an NF-kappaB-dependent anti-apoptotic protein, regulates TRAIL-induced apoptosis through modulating c-Fos/c-FLIP pathway.* Cell Death Differ, 2011. **18**(7): p. 1184-95.

218. Wettstein, G., P.S. Bellaye, M. Kolb, A. Hammann, B. Crestani, P. Soler, J. Marchal-Somme, A. Hazoume, J. Gauldie, A. Gunther, O. Micheau, M. Gleave, P. Camus, C. Garrido, and P. Bonniaud, *Inhibition of HSP27 blocks fibrosis development and EMT features by promoting Snail degradation.* FASEB J, 2013.

219. Zhou, Y.C., J.Y. Liu, J. Li, J. Zhang, Y.Q. Xu, H.W. Zhang, L.B. Qiu, G.R. Ding, X.M. Su, S. Mei, and G.Z. Guo, *Ionizing radiation promotes migration and invasion of cancer cells through transforming growth factor-beta-mediated epithelial-mesenchymal transition.* Int J Radiat Oncol Biol Phys, 2011. **81**(5): p. 1530-7.

220. Daly, M.J., E.K. Gaidamakova, V.Y. Matrosova, A. Vasilenko, M. Zhai, A. Venkateswaran, M. Hess, M.V. Omelchenko, H.M. Kostandarithes, K.S. Makarova, L.P. Wackett, J.K.

Fredrickson, and D. Ghosal, *Accumulation of Mn(II) in Deinococcus radiodurans facilitates gamma-radiation resistance.* Science, 2004. **306**(5698): p. 1025-8.

221. Haro, K.J., A. Sheth, and D.A. Scheinberg, *Dysregulation of IRP1-mediated iron metabolism causes gamma ray-specific radioresistance in leukemia cells.* PLoS One, 2012. **7**(11): p. e48841.

222. Diehn, M., R.W. Cho, N.A. Lobo, T. Kalisky, M.J. Dorie, A.N. Kulp, D. Qian, J.S. Lam, L.E. Ailles, M. Wong, B. Joshua, M.J. Kaplan, I. Wapnir, F.M. Dirbas, G. Somlo, C. Garberoglio, B. Paz, J. Shen, S.K. Lau, S.R. Quake, J.M. Brown, I.L. Weissman, and M.F. Clarke, *Association of reactive oxygen species levels and radioresistance in cancer stem cells.* Nature, 2009. **458**(7239): p. 780-3.

223. Nagarajan, D., T. Melo, Z. Deng, C. Almeida, and W. Zhao, *ERK/GSK3beta/Snail signaling mediates radiation-induced alveolar epithelial-to-mesenchymal transition.* Free Radic Biol Med, 2012. **52**(6): p. 983-92.

224. Pei, D., Y. Zhang, and J. Zheng, *Regulation of p53: a collaboration between Mdm2 and Mdmx.* Oncotarget, 2012. **3**(3): p. 228-35.

225. Love, I.M. and S.R. Grossman, *It Takes 15 to Tango: Making Sense of the Many Ubiquitin Ligases of p53.* Genes Cancer, 2012. **3**(3-4): p. 249-63.

226. Wade, M., Y.C. Li, and G.M. Wahl, *MDM2, MDMX and p53 in oncogenesis and cancer therapy.* Nat Rev Cancer, 2012. **13**(2): p. 83-96.

227. Zhong, J., K. Ogura, Z. Wang, and H. Inuzuka, *Degradation of the transcription factor Twist, an oncoprotein that promotes cancer metastasis.* Discov Med, 2013. **15**(80): p. 7-15.

228. Lesuffleur, T., A. Barbat, E. Dussaulx, and A. Zweibaum, *Growth adaptation to methotrexate of HT-29 human colon carcinoma cells is associated with their ability to differentiate into columnar absorptive and mucus-secreting cells.* Cancer Res, 1990. **50**(19): p. 6334-43.

229. Yuan, B.F., Y.H. Hao, and Z. Tan, *Universal sensing strategy for the detection of nucleic acid targets by optical biosensor based on surface plasmon resonance.* Clin Chem, 2004. **50**(6): p. 1057-60.

230. Morgenstern, J.P. and H. Land, *Advanced mammalian gene transfer: high titre retroviral vectors with multiple drug selection markers and a complementary helper-free packaging cell line.* Nucleic Acids Res, 1990. **18**(12): p. 3587-96.

231. O'Connor, P.B. and C.E. Costello, *Internal calibration on adjacent samples (InCAS) with Fourier transform mass spectrometry.* Anal Chem, 2000. **72**(24): p. 5881-5.

232. Wang, C.T., J.J. Li, H.Y. Lai, and B.S. Hu, *A human cell line constitutively expressing HIV-1 Gag and Gag-Pol gene products.* J Med Virol, 1999. **57**(1): p. 17-24.

233. Dignam, J.D., R.M. Lebovitz, and R.G. Roeder, *Accurate transcription initiation by RNA polymerase II in a soluble extract from isolated mammalian nuclei.* Nucleic Acids Res, 1983. **11**(5): p. 1475-89.

234. Werner, A., A. Disanza, N. Reifenberger, G. Habeck, J. Becker, M. Calabrese, H. Urlaub, H. Lorenz, B. Schulman, G. Scita, and F. Melchior, *SCF(Fbxw5) mediates transient degradation of actin remodeller Eps8 to allow proper mitotic progression.* Nat Cell Biol, 2012. **15**(2): p. 179-88.

235. Treier, M., L.M. Staszewski, and D. Bohmann, *Ubiquitin-dependent c-Jun degradation in vivo is mediated by the delta domain.* Cell, 1994. **78**(5): p. 787-98.

236. Rappsilber, J., M. Mann, and Y. Ishihama, *Protocol for micro-purification, enrichment, pre-fractionation and storage of peptides for proteomics using StageTips.* Nat Protoc, 2007. **2**(8): p. 1896-906.

237. Perkins, D.N., D.J. Pappin, D.M. Creasy, and J.S. Cottrell, *Probability-based protein identification by searching sequence databases using mass spectrometry data.* Electrophoresis, 1999. **20**(18): p. 3551-67.

238. Bunkenborg, J., G.E. Garcia, M.I. Paz, J.S. Andersen, and H. Molina, *The minotaur proteome: avoiding cross-species identifications deriving from bovine serum in cell culture models.* Proteomics, 2010. **10**(16): p. 3040-4.

RESEARCH ARTICLES

Research articles resulting from this thesis:

The work related to **FBXL14** presented in this thesis was published in:

Viñas-Castells R, Beltran M, Valls G, Gómez I, García JM, Montserrat-Sentís B, Baulida J, Bonilla F, García de Herreros A and Díaz VM. The hypoxia-controlled FBXL14 ubiquitin ligase targets SNAIL1 for proteasome degradation. *The Journal of Biological Chemistry* (2010) 285(6): p. 3794-805.

The work related to **FBXL5** has been submitted for publication while this thesis was being written:

Viñas-Castells R, *et al*. FBXL5 ubiquitinates and controls Snail1 function: implications for Snail1 up-regulation by gamma irradiation.

Collaboration with a project to determine the role of the different **Akt isoforms** in the regulation of Snail1 was established in the lab. It yielded the following publication:

Villagrasa P, Diaz VM, **Viñas-Castells R**, Peiro S, Del Valle-Pérez B, Dave N, Rodríguez-Asiain A, Casal JI, Lizcano JM, Duñach M and García de Herreros A. Akt2 interacts with Snail1 in the E-cadherin promoter. *Oncogene* (2012) 31(36): p. 4022-33.

Rosa Viñas Castells ha cursado los estudios de doctorado con financiación de una Ayuda Predoctoral de Formación en Investigación en Salud (PFIS) otorgada por el Instituto de Salud Carlos III.

Aquesta tesi ha estat impresa amb el suport de la Fundació IMIM.